

CARBON PARTITIONING IN NITROGEN-FIXING ROOT NODULES

Dissertation

zur Erlangung des Doktorgrades

der Mathematisch-Naturwissenschaftlichen Fakultäten

der Georg-August-Universität zu Göttingen

vorgelegt von

Maria Schubert, geb. Ramenskaia

aus St. Petersburg, Russland

Göttingen 2002

D 7

Referent: Prof. Dr. Hans-Walter Heldt

Korreferentin: Prof. Dr. Christiane Gatz

Tag der mündlichen Prüfung: 30.10.2002

Content

1.	Introduction.....	1
1.1.	Degradation of sucrose in sink organs.....	1
1.1.1.	The role of sucrose in the plant cell.....	1
1.1.1.1.	Sucrose synthase	2
1.1.1.2.	Invertases	2
1.2.	Transport of sugars	4
1.2.1.	Phloem loading.....	4
1.2.2.	Phloem unloading and post-phloem transport.....	5
1.2.2.1.	Symplastic sugar transport	5
1.2.2.2.	Apoplastic phloem unloading and post-phloem transport.....	6
1.2.2.3.	Sugar transporters in apoplastic sugar transport.....	7
1.3.	The regulation of phloem unloading and sink strength in different systems ..	9
1.3.1.	Developmental sinks	9
1.3.2.	Optional sinks.....	10
1.4.	Nitrogen-fixing root nodule symbioses	10
1.4.1.	Nitrogen fixation in nodules	11
1.4.2.	Infection of plants and nodule formation.....	12
1.4.3.	Nodule structure	13
1.4.4.	Phylogenetic relationship of root nodule symbioses.....	15
1.4.5.	Carbon sources supplied by the host plant to nitrogen-fixing microsymbionts..	15
1.4.6.	Carbon transport and metabolism in nitrogen-fixing root nodules	17
1.5.	Aim of this thesis	18
2.	Materials and methods.....	20
2.1.	Materials.....	20
2.1.1.	Plant material	20
2.1.2.	Bacterial and yeast strains	20
2.1.3.	Oligonucleotides (Primers).....	21
2.1.4.	Plasmides	21
2.1.5.	Enzymes.....	22
2.1.5.1.	Restriction enzymes.....	22
2.1.5.2.	Other enzymes and kits	22
2.1.6.	Chemicals.....	23

2.1.7.	Other materials and devices.....	24
2.1.8.	Culture media	24
2.1.8.1.	Plant media.....	24
2.1.8.2.	Bacterial media	25
2.1.8.3.	Media for <i>Saccharomyces cerevisiae</i>	27
2.1.8.4.	Medium additives.....	28
2.2.	Plant culture methods and growth conditions	28
2.3.	RNA isolation from plant tissue.....	29
2.3.1.	RNA isolation from <i>Medicago truncatula</i> and <i>Datisca glomerata</i> (modified after Burgos et al., 1995).....	29
2.3.2.	RNA isolation from <i>Casuarina glauca</i>	30
2.4.	Isolation of plasmid DNA from bacteria and yeast	31
2.4.1.	Plasmid mini-preparation protocol „ Triton Boiling“	31
2.4.2.	Mini preparation of bacterial plasmid DNA for the sequence analysis	31
2.4.3.	Maxi preparation of bacterial plasmid DNA	32
2.4.4.	Preparation of plasmid DNA from yeast.....	32
2.5.	Concentration and purification of DNA or RNA solutions	32
2.5.1.	Precipitation of nucleic acids	32
2.5.2.	Phenol-chloroform extraction and precipitation of DNA.....	33
2.6.	Electrophoretic separation of DNA and RNA	33
2.6.1.	TEA-Agarose gel electrophoresis.....	33
2.6.2.	Separation of RNA on agarose gel for Northern blots.....	34
2.7.	Northern blot hybridization	34
2.7.1.	RNA transfer to nylon membranes (Northern blotting)	34
2.7.2.	DNA probe labelling with α -[³² P]-dATP.....	35
2.7.3.	Hybridization.....	35
2.8.	First strand cDNA synthesis (Reverse transcription).....	36
2.9.	Amplification of DNA fragments	36
2.9.1.	Polymerase chain reaction (PCR)	37
2.9.2.	Design of synthetic oligonucleotide primers	37
2.10.	Rapid amplification of cDNA ends (RACE): 5'-RACE	38
2.11.	DNA sequencing.....	39
2.12.	Cloning methods	40
2.12.1.	Digestion with restriction enzymes	40
2.12.2.	Phosphatase treatment	40
2.12.3.	Filling-in of 5' overhanging ends with Klenow fragment.....	41

2.12.4.	Isolation of DNA fragments from agarose gels.....	41
2.12.5.	Ligation.....	42
2.13.	Transformation of <i>Escherichia coli</i>	42
2.13.1.	Preparation of competent <i>E.coli</i> cells.....	42
2.13.2.	Transformation of competent <i>E.coli</i> cells.....	43
2.13.3.	Characterisation of transformants.....	44
2.14.	Yeast transformation	45
2.15.	Bacterial and yeast glycerol cultures	46
2.16.	Extraction of sugars	46
2.16.1.	Chloroform-methanol extraction.....	46
2.16.2.	Preparative isolation of unknown sugars / sugar derivates from <i>Datisca</i>	47
2.16.3.	Ethanol extraction.....	48
2.16.4.	Perchlorate extraction.....	49
2.16.5.	Acetone extraction.....	49
2.17.	Sugar analysis by high-performance liquid chromatography (HPLC)	49
2.18.	Sugar analysis	50
2.18.1.	Acid hydrolysis.....	50
2.18.2.	Enzymatic hydrolysis.....	51
2.19.	Sucrose synthase extraction and assay	52
2.19.1.	Extraction of sucrose synthase (SuSy).....	52
2.19.2.	Sucrose synthase activity assay.....	52
2.20.	Invertase extraction and assay	53
2.20.1.	Extraction of invertase.....	53
2.20.2.	Invertase activity assay.....	54
2.21.	<i>In situ</i> glucose and acid (apoplastic) invertase activity staining	55
2.22.	Total protein isolation from plant material	55
2.23.	Bradford protein concentration determination	56
2.24.	Sodiumdodecyl sulfate polyacrylamide gel electrophoresis (SDS-PAGE)	57
2.24.1.	Buffers and solutions for analytic SDS-PAGE.....	58
2.24.2.	Pouring the SDS-Polyacrylamide gel.....	58
2.24.3.	Probe preparation and SDS polyacrylamide gel electrophoresis (SDS-PAGE)	60
2.24.4.	Coomassie staining of SDS polyacrylamide gels.....	60
2.25.	Western blot	61

2.25.1.	Protein transfer to a nitrocellulose membrane.....	61
2.25.2.	Staining of the blot.....	61
2.25.3.	Immunological detection of transferred proteins.....	62
2.26.	Measurement of sugar uptake in yeast.....	63
2.27.	Statistic evaluation of experimental data.....	64
3.	Results.....	65
3.1.	Sugar contents in roots and nodules.....	65
3.1.1.	Sugar contents in roots and nodules of <i>Medicago truncatula</i>	65
3.1.2.	Sugar contents in <i>Casuarina glauca</i>	67
3.1.3.	Sugar contents in <i>Datisca glomerata</i>	67
3.1.3.1.	Isolation and characterization of two unknown carbohydrates from <i>Datisca glomerata</i>	67
3.1.3.2.	Sugar contents in roots, nodules and leaves of <i>Datisca</i> after determination of the molecular mass of the novel sugars	74
3.2.	Activities of sucrose cleaving enzymes in roots and root nodules	75
3.2.1.	Invertase activities.....	75
3.2.2.	Sucrose synthase activities	77
3.2.3.	<i>In situ</i> localization of acid invertase activity.....	78
3.2.3.1.	<i>In situ</i> localization of glucose in roots and nodules	79
3.2.3.2.	<i>In situ</i> localization of acid invertase in roots and nodules.....	79
3.3.	Expression levels of sucrose synthase and sugar transporters in roots and nodules.....	81
3.3.1.	Expression levels of sucrose synthase (RNA gel blot hybridization analysis).....	82
3.3.2.	Levels of sucrose synthase protein (Protein blot analysis).....	83
3.3.3.	Expression levels of sugar transporters in roots, nodules and leaves.....	84
3.4.	Isolation and characterization of hexose transporter cDNAs.....	85
3.4.1.	Full size cDNA of the <i>Medicago truncatula</i> hexose transporter (<i>MtHT</i>)	85
3.4.2.	Full size cDNA of the <i>Datisca glomerata</i> hexose transporter (<i>DgHT</i>)	88
3.4.3.	Protein sequence analysis of <i>DgHT</i> and <i>MtHT</i>	91
3.5.	Functional characterization of the hexose transporters by expression in yeast	94
3.5.1.	Construction of shuttle vectors for the heterologous expression of <i>MtHT</i> and <i>DgHT</i> in yeast.....	94
3.5.1.1.	Cloning of <i>MtHT</i> in pNEV-X.....	95
3.5.1.2.	Cloning of <i>DgHT</i> in pNEV-E	95
3.5.2.	Sugar uptake studies with yeast strains expressing <i>MtHT</i> and <i>DgHT</i>	95
3.5.2.1.	Functional characterization of <i>MtHT</i>	97
3.5.2.2.	Functional characterization of <i>DgHT</i>	97

4.	Discussion.....	101
4.1.	Cytological information on putative mechanism of carbon transport in root nodules.....	101
4.1.1.	<i>Medicago</i>	102
4.1.2.	Cytology of roots and nodules of <i>Datisca glomerata</i>	102
4.1.3.	Cytology of roots and nodules of <i>Casuarina glauca</i>	103
4.2.	Expression levels and patterns of hexose transporter genes in roots and nodules.....	104
4.2.1.	<i>Medicago</i>	104
4.2.2.	<i>Datisca</i>	105
4.2.3.	<i>Casuarina</i>	105
4.3.	Activities and localization of sucrose degrading enzymes in roots and nodules.....	106
4.3.1.	Invertases.....	106
4.3.2.	Sucrose synthase (SuSy).....	108
4.4.	The <i>Datisca</i> nodule paradox: hexose transporter expression in the absence of apoplastic invertase activity. Could hexoses be the carbon sources for symbiotic <i>Frankia</i> in <i>Datisca</i> nodules?.....	111
4.5.	Hexose transporters from nodules.....	112
4.6.	Nodule and root sugar contents.....	114
4.6.1.	Sucrose, glucose and fructose in nodules and roots.....	114
4.6.2.	<i>Datisca</i> contains novel non-structural rhamnosyl saccharides.....	116
4.6.2.1.	Free rutinose and methylrutinose are found in <i>Datisca</i> sugar extracts	116
4.6.2.2.	Possible ways of rutinose and methylrutinose synthesis.....	117
4.6.2.3.	Are rutinose and methylrutinose carbon storage or transport forms?..	118
5.	Summary.....	122
6.	Abbreviations.....	124
7.	References.....	127

1. Introduction

One of the key features of plants is their ability to reduce carbon dioxide to sugars in the presence of sunlight and water as well as the subsequent transport of assimilated carbon to non-photosynthetic tissues. Partitioning of photosynthetic assimilates among organs is a critical process in plant development. Based on their ability/need to either produce or import assimilates, plant organs are classified as sources (photosynthetically active leaves and, to a less extent, shoots) or sinks. There are two types of sink organs/tissues – developmental, such as roots, tubers, flowers, seeds and fruits, and optional, like pathogen infection sites, e.g. tumours induced by *Agrobacterium tumefaciens*, or symbiotic structures, e.g. nitrogen-fixing root nodules induced by symbiotic nitrogen-fixing bacteria. The subject of this thesis is the study of sugar partitioning mechanisms in one type of optional sinks, namely nitrogen-fixing root nodules. Phloem unloading, post-phloem transport and the utilisation of sucrose, the main transport sugar of plants, are compared in nodules (optional sinks) and roots (developmental sinks).

1.1. Degradation of sucrose in sink organs

1.1.1. The role of sucrose in the plant cell

The major part of the organic carbon produced during photosynthesis is channelled into the synthesis of sucrose. Sucrose is a highly soluble sugar which can attain considerable concentrations without an apparent inhibitory effect on most biochemical reactions in the cell. This capacity makes sucrose a useful component contributing to the regulation of osmotic pressure and flow of water between cellular compartments. Sucrose can be transported across biological membranes, such as the plasmalemma and the tonoplast (reviewed by Sauer and Tanner, 1993). Being neutral, it does not interact electrostatically with other charged molecules in the cell. As a nonreducing molecule, it is relatively inert from interactions with other functional groups, particularly primary amines and oxidizing agents encountered in the biological milieu. The free energy of hydrolysis of sucrose is close to that of the γ -phosphoryl group of ATP. Therefore, the metabolic utilisation of the α -glucosyl moiety in sucrose is much more efficient in energy conservation than most other glycosides. As a major transportable metabolite in the plant, sucrose is delivered from the photosynthetic tissues to all plant organs, there to serve as source of organic carbons for building permanent structural elements and as metabolic fuel for the energy

production. A large portion of the sucrose itself may accumulate and can be stored at high concentrations in sink organs, e.g. sugar beet (Saftner et al., 1983).

Utilization of sucrose as a source of carbon and energy depends on its cleavage into hexoses, and in plants this reaction is catalysed either by sucrose synthase (EC 2.4.1.13) or by invertase (EC 3.2.1.26).

1.1.1.1. Sucrose synthase

Sucrose synthase (SuSy) is recognized as an important enzyme of sucrose utilization in plant sink tissues (Ho, 1988). In spite of its name, SuSy is not active in sucrose biosynthesis *in vivo*, but in degradation. SuSy is a homotetrameric enzyme consisting of 92 to 93 kDa subunits and catalyses the reversible, UDP-dependent cleavage of sucrose into UDP-glucose and fructose in a variety of plant sink tissues such as tubers, developing leaves and seeds, and root nodules. The resulting UDP-glucose (or glucose-1-phosphate) and fructose are used in various important metabolic pathways, including glycolysis, starch biosynthesis, and the synthesis of cellulose and callose (Delmer and Amor, 1995; Verma and Hong, 2001).

The highest activity of SuSy often occurs during rapid growth (e.g. in elongating maize leaves; Nguyen-Quoc et al., 1990) or during storage product deposition (e.g. in developing seeds; King et al., 1997). SuSy is a globular protein and generally considered to be a soluble cytosolic enzyme. However, a certain fraction of the enzyme was found to be associated with the plasma membrane (Amor et al., 1995; Carlson and Chourey, 1996), perhaps in a specific complex with the integral membrane protein glucane synthase (Verma and Hong, 2001). There is evidence suggesting that reversible phosphorylation of SuSy at Ser-15 (Huber et al., 1996) may control the binding to the plasma membrane, with the dephosphorylated enzyme being primarily associated with the membrane (Winter et al., 1997).

1.1.1.2. Invertases

Invertases (EC 3.2.1.26; β -fructosidases) catalyse the irreversible hydrolysis of sucrose to glucose and fructose. Three different types of invertase have been identified that are characterized by their intracellular location, pH optima and isoelectric points (Avigad, 1982), namely vacuolar, apoplastic and cytosolic.

Most plant species contain at least two isoforms of vacuolar invertase, which represent soluble proteins (soluble acid invertases) in the lumen of this acidic

compartment (Sturm, 1999). Also, several isoforms of extracellular invertase (cell wall invertases, apoplastic invertases) have been detected that are ionically bound to the cell wall (Sturm, 1996; Tymowska-Lalanne and Kreis, 1998). Vacuolar and cell wall invertases share some biochemical properties, e.g. they cleave sucrose most efficiently between pH 4.5 and 5.0 and attack the disaccharide from the fructose residue. Thus, these so-called acid invertases are β -fructofuranosidases and also hydrolyze other β -fructose-containing oligosaccharides such as raffinose and stachyose. Additionally, plants have at least two isoforms of cytoplasmic invertase with pH optima for sucrose cleavage in the neutral or slightly alkaline range. Neutral and alkaline invertases are less well characterized but, in contrast to the acid invertases, these enzymes appear to be specific for sucrose (Sturm, 1999).

The following functions have been proposed for invertases:

- provision of the cells with substrates for respiration and with carbon skeletons for biosynthetic metabolism
- regulation of long-distance transport of sucrose by generating a sucrose gradient between source and sink tissues
- regulation of cell elongation, because the invertase reaction products, glucose and fructose, increase the osmotic pressure of cells

Different functions have been assigned to the different isoenzymes. High activity of an extracellular invertase is usually associated with rapidly growing tissues, and it has been suggested that this invertase is important for phloem unloading (Eschrich, 1980) and for determining sink strength (Ho, 1988). The role of extracellular invertase for sink/source regulation and sink metabolism is supported by a study on cultured cells of *Chenopodium rubrum*: the enzyme activity and mRNA levels of apoplastic invertase increased when heterotrophic metabolism was induced in photoautotrophic suspension culture cells (Roitsch et al., 1995).

The developmental functions of different invertases are reflected by their expression patterns. The analysis of isoform-specific steady-state transcript levels of five genes for acid invertases in carrot showed markedly different expression patterns specific for organ and stage of development (Sturm et al., 1995). Similar results were obtained for tomato (Godt and Roitsch, 1997). In addition to the organ- and development-specific regulation of gene expression, alterations in sugar composition and concentration markedly affect the expression of some of the acid invertases. In maize, Xu and co-workers (1996) identified two gene classes for soluble acid invertase with contrasting sugar responses. One class is up-regulated by increasing carbohydrate supply, whereas the second class in the same gene family is repressed by sugars and up-regulated by depletion of this resource. In contrast, in suspension cells of *Chenopodium rubrum*, the

expression of soluble acid invertase was not affected by sugars, whereas the expression of cell wall invertase was enhanced (Roitsch et al., 1995). Acid invertases are also regulated by plant hormones, wounding and in response to pathogen infection (Ehneß and Roitsch, 1997; Rozenkranz et al., 2001; Sturm, 1999).

Another factor that has to be taken into account regarding invertase activities is the existence of specific inhibitors. A proteinaceous inhibitor of 17 kDa, inhibiting cell wall invertase *in vitro*, was isolated from a suspension culture of tobacco (Weil et al., 1994), and related amino acid sequences were also found in other plant genomes. A purified invertase inhibitor could also inhibit vacuolar acid invertase activity *in vitro*, but since the inhibitor is located in the apoplast *in vivo*, it should only be able to interact with the cell wall enzyme (Sander et al., 1996). Binding of the inhibitor to cell wall invertase is necessary but not sufficient for inhibition of catalytic activity. Thus, even though the two proteins are associated, for example, during a 40-d culture period of tobacco cells, the inhibition of invertase activity is only apparent during the later stages of the culture (Krausgrill et al., 1998). The inhibitor protein binds to the invertase and inhibits it at very low concentrations of sucrose. Thus, it is possible that this system protects the plant cell from sucrose exhaustion during sugar starvation. A vacuolar invertase inhibitor has been identified as well (Greiner et al., 1999).

1.2. Transport of sugars

1.2.1. Phloem loading

Long-distance transport of carbohydrates occurs in the phloem and is driven by differences in solute concentrations and osmotic potentials (Ho, 1988). In most plants, the most abundant carbon compound in the phloem is the disaccharide sucrose (Zimmermann and Ziegler, 1975). However, for a minority of plant species, the main translocated sugars fall into two groups, the sugar alcohols (mannitol and sorbitol) and oligosaccharides of the raffinose family (raffinose, stachyose and verbascose; Zamski and Schaffer, 1996). When such unusual carbohydrates predominate, sucrose is present as well. In dicotyledonous plants, a correlation between sugar types transported in the phloem and the anatomy and type of companion cells in minor veins, where phloem loading takes place, was demonstrated (Gamalei, 1984). Plants transporting mainly members of the raffinose family of oligosaccharides or sugar alcohols contain abundant symplastic connections between companion cells and bundle sheath cells, while plants transporting mainly sucrose show scarce or no symplastic connections. It is concluded that sucrose is transported into the companion cell-sieve element complex apoplastically

via membrane transporters, while unusual carbohydrates are transported symplastically via plasmodesmata. Thus, based on their companion cell anatomy and their transport sugars, plants can be classified as apoplastic or symplastic phloem loaders, respectively. As a rule, phloem loading mechanisms are specific to plant families.

Interestingly, most symplastic phloem loaders represent woody plants, while amongst apoplastic phloem loaders herbaceous species dominate (Gamalei, 1984).

1.2.2. Phloem unloading and post-phloem transport

At the sink end of the phloem path, assimilates move from the sieve element-companion cell complexes to the sites of utilisation/storage of carbohydrates (phloem unloading). In most sinks, phloem unloading occurs symplastically, but in some cases this is interrupted by an apoplastic step (Patrick, 1997). The same mechanisms are applied for the transport of nutrients from cell to cell within tissues.

In contrast to phloem loading mechanisms, phloem unloading mechanisms are not specific for plant families. Unloading mechanisms can depend on the type of plant sink organ and on the developmental stage of the plant/organ. For example, during the elongation phase of potato stolon growth apoplastic sucrose unloading predominates, while during the first observable phases of tuberization a transition from apoplastic to symplastic phloem unloading occurs (Viola et al., 2001). Also during tomato fruit development, the mechanism of sucrose unloading is not constant. During the first stage of development, 0 to 35 days after anthesis, sucrose is unloaded symplastically through numerous plasmodesmata (N'tchobo et al., 1999). Later the symplastic connections are lost, and, sucrose is unloaded apoplastically (Ruan and Patrick, 1995).

1.2.2.1. Symplastic sugar transport

Sucrose can be transported symplastically via plasmodesmata (Figure 1.1; for review see Patrick, 1997). A diffusive efflux of assimilates from sieve elements to sink tissues, or from one sink tissue cell to another is driven by concentration differences of assimilates between both tissues/cells. Metabolism and intracellular compartmentation determine the cytoplasmic concentrations of sucrose in the sink cells. In sucrose-storing sinks, active vacuolar accumulation by a tonoplast sucrose/H⁺ antiporter (Greuter and Keller, 1993) could function to sustain low cytoplasmic sucrose concentrations that favour phloem unloading. Such a mechanism would depend on osmotic adjustment between the cytoplasm and vacuole to prevent vacuolar swelling. In contrast, for hexose utilizing or

starch storing sinks, sucrose metabolism appears to play a more prominent role in governing phloem unloading through regulating sucrose levels in the cytoplasm (Stitt and Sonnewald, 1995). In this case, transport into intracellular compartments by facilitated diffusion is driven by cytoplasmic levels of metabolites resulting from sucrose hydrolysis. Thus, sucrose synthase (SuSy) activity in the cytosol of sink cells can determine the sink strength (Patrick, 1997).

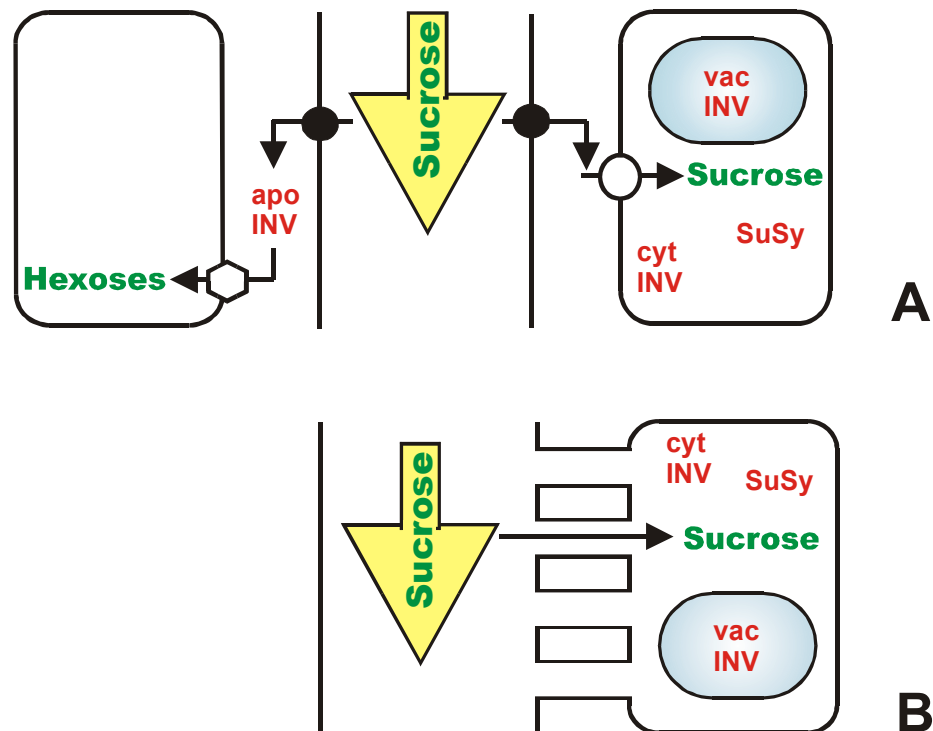


Figure 1.1. Phloem unloading mechanisms. (A) Apoplastic sugar transport. Sucrose is exported by an as yet uncharacterized sucrose efflux transporter (black circle) from the phloem into the apoplast, where it can be taken up via a sucrose transporter (open circle) directly into the sink cell, or it is hydrolysed by apoplastic invertase (apoINV) and is taken up into the sink cell in the form of hexoses via a hexose transporter (open hexagon). vacINV – vacuolar invertase; cytINV – cytosolic invertase; SuSy – sucrose synthase. (B) Symplastic phloem unloading occurs via plasmodesmata directly into the sink cell where sucrose is introduced into cell metabolism via cleavage by sucrose synthase, cytosolic or vacuolar invertase.

1.2.2.2. Apoplastic phloem unloading and post-phloem transport

According to the model proposed for apoplastic phloem unloading (Eschrich, 1980), sucrose is released from the phloem into the apoplast via sucrose efflux transporters, which have been postulated to function as facilitators or as proton antiporters (Walker et al., 1995). In the apoplast of sink tissues, sucrose can either be taken up directly into sink

cells by sucrose transporters in the plasma membrane, or hydrolysed into glucose and fructose by apoplastic invertase. The hexoses produced are taken up by the sink cells via monosaccharide transporters in the plasma membrane (Figure 1.1; Büttner and Sauer, 2000). Thus, in case of apoplastic phloem unloading, the sink strength is determined by the activity of apoplastic invertase, and the amount and activity of plasma membrane sugar transporters.

Cells that are involved in apoplastic transport can display a specific differentiation. So-called transfer cells, characterized by intensive uptake of metabolites from the apoplast, have cell wall invaginations that substantially increase the surface area of the plasma membrane. However, uptake of sugars from the apoplast also occurs in cells with smooth cell walls. Apoplastic sugar transport can also occur after phloem unloading. It is often involved in sugar transport to sinks that contain different genomes, e.g. biotrophic relationships, symbioses, host-parasite relationships and seed loading (Day et al., 2001; Smith et al., 2001; Patrick et al., 2001). However, in many organs apoplastic barriers, e.g. lignified or suberized cell walls, exist between the phloem and the sink cells (Patrick, 1997).

1.2.2.3. Sugar transporters in apoplastic sugar transport

Apoplastic transport of carbohydrates depends on the existence of specific transporters that catalyse the membrane penetration of sugars. Two types of transporters are necessary to allow apoplastic transport. First, a transport protein is needed for the export of sucrose into the apoplast. Such proteins have not been identified to date. Second, transporters are needed for the import of sucrose or hexoses into the sink cell.

The first plant hexose transporter cDNA was cloned from the lower plant *Chlorella kessleri* (Sauer and Tanner, 1989). The cDNA (*HUP1*) was used as a probe for the identification of the first monosaccharide transporter from a higher plant, *Arabidopsis* (Sauer et al., 1990). In the meantime, monosaccharide transporters have been cloned from several plants (Büttner and Sauer, 2000), e.g. a sink-specific monosaccharide transporter from *Nicotiana tabacum* (Sauer and Stadler, 1993). Monosaccharide transporters comprise a large gene family in all plants examined thus far: *Ricinus communis* (eight genes; Weig et al., 1994), *Chenopodium rubrum* (seven genes; Roitsch and Tanner, 1994), and *Arabidopsis thaliana* (14 genes; Büttner and Sauer, 2000). Transporters catalysing the uptake of monosaccharides that most likely derive from extracellular sucrose hydrolysis have been identified in pollen grains (*AtSTP2*; Truernit et al., 1999; *AtSTP4*; Truernit et al., 1996), in guard cells of various *Arabidopsis* organs (*AtSTP1*; Büttner and Sauer, 2000), in root tips (*AtSTP4*; Truernit et al., 1996) and in

leaves (*AtSTP3*; Büttner et al., 2000). The expression of plant monosaccharide transporter genes is not only developmentally regulated, but also controlled by environmental stimuli, such as pathogen infection (*AtSTP4*) or wounding (*AtSTP3* and *AtSTP4*; Truernit et al., 1996; Büttner et al., 2000).

The hydropathy profiles for all plant monosaccharide transporters are very similar and suggest 12 membrane-spanning domains, a typical feature of all members of the major facilitator superfamily (MFS; Marger and Saier, 1993). Sequence analysis indicates that they may have evolved by gene duplication from an ancestral gene coding for a six-transmembrane helix transporter (Büttner and Sauer, 2000).

The kinetic properties of monosaccharide transporters have been studied by their heterologous expression in yeast or in *Xenopus* oocytes (Bush, 1993; Büttner and Sauer, 2000). All eleven of the investigated monosaccharide transporters were shown to be sensitive to uncouplers of the transmembrane proton gradient and to accumulate their substrates inside the cells to concentrations exceeding the extracellular concentrations, indicating that they catalyse active transport. They all represent H⁺-symporters and accept pyranose monosaccharides (Büttner and Sauer, 2000).

The first sucrose transporter cDNA was isolated from spinach (*SoSUT*; Riesmeier et al., 1992). Meanwhile, sucrose transporters have been described in a wide variety of systems and termed SUT (from sucrose transporter) or SUC (from sucrose carrier). Eight sucrose transporter genes have been found in *Arabidopsis* (Williams et al., 2000; www.tigr.org). The *SUT* genes encode highly hydrophobic proteins. Like monosaccharide transporters, sucrose transporters contain twelve membrane-spanning domains. In fact, they are distantly related to the hexose transporter family (Sauer et al., 1994). In apoplastic phloem loading, sucrose transporters accumulate sucrose in the sieve element-companion cell (SE/CC) complex to drive long-distance transport. In some plants these sucrose transporters have been detected in sieve elements (Kühn et al., 1997) or in companion cells (Stadler et al., 1995). Sucrose transporters have also been found in particular root cells: *DcSUT2* is expressed in storage parenchyma cells of carrot tap-roots where it seems to import sucrose for storage (Shakya and Sturm, 1997). In *Arabidopsis* roots, strong expression was found for the sucrose transporter SUC1, and weak expression levels were shown for SUC2 (Sauer and Stolz, 1994). The latter has been detected in phloem cells all over the plant, including root and stem phloem, where it may retrieve sucrose that has leaked into the apoplast or possibly catalyses the efflux of sucrose from the phloem (Truernit and Sauer, 1995) and participates in phloem unloading (Sauer et al., 1994).

1.3. The regulation of phloem unloading and sink strength in different systems

Mechanisms of phloem unloading and sink strength regulation have been examined in several systems, including developmental sinks like seeds, storage organs and fruits, and optional sinks, like pathogen infection sites.

1.3.1. Developmental sinks

The systems best examined for phloem unloading mechanisms so far are seeds of different plants, including legumes (Weber et al., 1997). For instance, the transport mechanisms and the cellular pathways of sucrose were analyzed in detail in fava bean seeds at the filling stage (Patrick, 1997). The sieve elements of the phloem end in the seed coat and are symplastically connected with the coat cells. Phloem unloading and post-phloem transport through the seed coat occur via the symplast. From the coat cells, sugars are unloaded into the seed apoplast and must be taken up by the apoplastically isolated embryo. Active transport systems are present in different parts of the seed (Gahrtz et al., 1996). Transfer cell formation (see 1.2.2.2) is correlated with strong induction of the expression of the *Vicia faba* sucrose transporter gene *VfSUT1* (Weber et al., 1997). The sucrose uptake system changes from the invertase-mediated unloading process, which provides the sink strength during the prestorage phase, to the storage phase, which probably allows the development of the cotyledons (Weber et al., 1996).

The fava bean seed system is a good example for the different roles in sink development that were proposed for apoplastic invertase and sucrose synthase. Expression of apoplastic invertase gene expression, which is usually associated with tissues characterized by high mitotic activity, was found here during embryo development, whereas expression of sucrose synthase was found during storage product deposition in the developing cotyledons (Heim et al., 1993; King et al., 1997). Possibly, the epidermal contact of the cotyledons with the seed coat provides a signal for transfer cell differentiation. An interesting analogy can be drawn from studies of pathogen-plant interactions. The parasites *Orobancha* and *Cuscuta* retrieve sugars from their hosts, probably by establishing a sucrose uptake system involving transfer cells, which only form after contact with the host vascular tissue (Ayres et al., 1996).

1.3.2. Optional sinks

The formation of optional sinks represents a facultative event for the plant. Examples for optional sinks are sites of pathogen infection, for instance tumors induced by *Agrobacterium tumefaciens*, sites of wounding, or symbiotic structures like nitrogen-fixing root nodules. In order to understand the regulation of phloem unloading and post-phloem transport, it is important to know which sugar transport mechanisms take place in optional sinks.

The large number of additional metabolic tasks in wounded or infected tissues cannot be sufficiently energized by the endogenous resources of the respective cells. Carbohydrates have to be imported into the affected tissues, which can be achieved by the rapid and simultaneous induction of genes for extracellular invertases (Sturm and Chrispeels, 1990) and plasma membrane monosaccharide transporters (Truernit et al., 1996; Büttner et al., 2000). In case of symplastic phloem unloading and post-phloem transport to the facultative sink, the activities of cytoplasmic or vacuolar sucrose-degrading enzymes have to be increased.

An example for optional sinks displaying symplastic phloem unloading and post-phloem transport are plant tumours induced by *Agrobacterium tumefaciens* that contain a well developed vascular system (Pradel et al., 1999). The distribution of the fluorescent dye carboxyfluorescein (CF) in tumours induced on three host plants, *Nicotiana benthamiana*, *Cucurbita maxima* and *Ricinus communis*, demonstrated a clear symplastic pathway between the phloem of the host stem and the tumour parenchyma, and also a considerable capacity for subsequent cell-to-cell transport between tumor parenchyma cells (Pradel et al., 1999).

Symbiotic nitrogen-fixing root nodules represent another example of optional sinks with high metabolic activity that requires large amounts of carbohydrates. The analysis of the sink function of these nodules is the topic of this thesis.

1.4. Nitrogen-fixing root nodule symbioses

Nitrogen is the element that most commonly restricts plant growth. The biosphere nitrogen is continuously depleted by denitrification. Only some prokaryotes can form the enzyme complex nitrogenase that reduces dinitrogen to ammonia and thereby introduces it into the biosphere. Since nitrogenase is highly oxygen-sensitive, its formation has to be tightly controlled, or oxygen protection systems have to be provided. Some prokaryotes fix nitrogen in symbiosis with higher plants. In root nodule symbioses, nitrogen-fixing soil

bacteria induce the formation of special organs, the root nodules, on their plant hosts. Inside nodule cells, the bacteria fix nitrogen and deliver the products of nitrogen fixation to the plant, while being supplied with carbon sources by the plant. Two groups of soil bacteria are able to enter root nodule symbiosis with higher plants: rhizobia - unicellular, Gram-negative bacteria, and actinomycetes of the genus *Frankia* – Gram-positive bacteria that grow in hyphal form. Rhizobia enter symbioses with legumes and one non-legume, *Parasponia sp.*, a member of the Ulmaceae family (Pueppke and Broughton, 1999), whereas *Frankia* strains can interact with a diverse group of mostly woody dicotyledonous plants that are members of eight different families, collectively called actinorhizal plants (Benson and Silvester, 1993).

1.4.1. Nitrogen fixation in nodules

The biological reduction of dinitrogen to ammonia is carried out by two enzymes, dinitrogenase and dinitrogenase reductase. Together, these enzymes are often referred to as nitrogenase. Dinitrogenase is encoded by genes *nifD* and *nifK*, whereas dinitrogenase reductase is encoded by *nifH*. The name *nif* of these genes is derived from “nitrogen fixation”. Nitrogenase is very sensitive to oxygen (Shaw and Brill, 1977), while the process of nitrogen fixation requires large amounts of energy provided by respiratory processes, leading to the so-called "oxygen dilemma" of nitrogen fixation. Therefore, the expression of *nif*-genes is strongly regulated and takes place only under nitrogen-limiting conditions and at very low oxygen concentrations, which may be achieved by the formation of oxygen diffusion barriers.

In legume nodules, an oxygen-diffusion barrier in combination with the high metabolic activity of the infected cells results in a low concentration of free oxygen in the area of nitrogen-fixing infected cells (Denison and Layzell, 1991). Within infected cells high levels of oxygen-binding proteins, leghemoglobins, provide an efficient transport of oxygen to the sites of respiration (Appleby, 1984). The oxygen barrier is present in the nodule parenchyma, which surrounds the inner tissue and encloses the peripheral nodule vascular system (Figure 1.2). The nodule parenchyma consists of layers of cells more or less devoid of intercellular spaces (Minchin, 1997).

Frankia can grow on dinitrogen as sole nitrogen source in the soil (Benson and Silvester, 1993). In order to provide oxygen protection for nitrogenase, *Frankia* forms vesicles at the end of hyphae or at short side branches of hyphae. These vesicles are surrounded by a multilayered envelope containing hopanoids, bacterial steroid lipids (Berry et al., 1993), and in them nitrogenase is formed in a low-oxygen environment (Meesters et al., 1985; Parsons et al., 1987). Several diverse mechanisms have evolved for oxygen control in

actinorhizal nodules formed by different plant families. In actinorhizal nodules of *Casuarina*, *Frankia* does not form vesicles but nitrogen fixation takes place in differentiated hyphae (Berg and McDowell, 1987a), and an oxygen diffusion barrier is achieved by lignification of the walls of infected and adjacent uninfected cells (Berg and McDowell, 1987b). *Casuarina* nodules also contain high amounts of nodule-specific hemoglobin, thus facilitating oxygen transport to the sites of respiration (Fleming et al., 1987). In other actinorhizal plants, e.g. *Datisca sp.*, no hemoglobin is present in nodules, and *Frankia* forms vesicles for nitrogen fixation (Benson and Silvester, 1993).

1.4.2. Infection of plants and nodule formation

Bacteria can enter plant roots either intracellularly or intercellularly (Pawlowski and Bisseling, 1996). During intracellular infections, the bacteria are always surrounded by a membrane of plant origin, allowing the plant to control the microsymbiont's access to nutrients.

Most herbaceous legumes, including *Medicago truncatula*, are infected intracellularly via root hairs. Bacterial signal factors, the Nod factors, induce the deformation of root hairs and the induction of cortical cell divisions that ultimately lead to the formation of a nodule meristem (reviewed by Mylona et al., 1995). When a *Rhizobium* is trapped in a curled root hair, a localized hydrolysis of the root hair cell wall is induced, the plasma membrane invaginates, and new cell wall material is deposited (Kijne, 1992). This leads to the formation of a tubular structure, an infection thread, which grows to a nodule primordium, afterwards the bacteria are released into the cells by a process resembling endocytosis (Basset et al., 1977). During this process, rhizobia become enclosed by a plant-derived membrane, the peribacteroid membrane (PBM), that results in the formation of the symbiosome (Roth and Stacey, 1989). In the symbiosomes, rhizobia differentiate into their endosymbiotic form, the bacteroids, and start to fix nitrogen (Newcomb, 1981). In several other rhizobial symbioses (*Parasponia* and some primitive legumes) the bacteria are not released from the infection threads and, the infection cells are filled with the branching infection threads (reviewed by Pawlowski and Bisseling, 1996).

In intracellularly infected actinorhizal plants like *Casuarina glauca*, bacterial hyphae also enter the plant root via infection-thread like structures (Torrey, 1976), which grow toward the dividing cells in cortex and infect them by intense branching within the cells, forming the so-called pre-nodule. Nodule primordium formation in actinorhizal plants is induced in the root pericycle and not in the root cortex as in legumes, therefore infection thread-like structures grow further from the pre-nodule to the pericycle and infect primordium cells, leading to nodule formation.

During intercellular infection, rhizobia can penetrate through the gaps in the epidermis that can form where lateral roots or adventitious roots emerge from the main root or stem, respectively (Chandler et al., 1982; James et al., 1992), while *Frankia* hyphae can penetrate the roots between root epidermal cells. In actinorhizal plants *Frankia* hyphae colonize the apoplastic space of the root cortex growing through the middle lamellae while cortical cells secrete electron-dense material rich in pectin and proteins into the intercellular spaces (Miller and Baker, 1985; Racette and Torrey, 1989; Liu and Berry, 1991). Hyphal tips enter primordium cells as the host cell plasma membrane invaginates. Surrounded by the invaginated host plasma membrane and embedded in fibrillar host-derived material, the hyphae proliferate inside the infected primordium cells (Miller and Baker, 1985).

Both infection pathways occur in legumes as well as in actinorhizal symbioses. Similar to the nodule structure, the type of infection is determined by the host plant, but not by the microsymbiont. For example, *Medicago* and *Casuarina* are infected intracellularly, while *Datisca* is assumed to be infected intercellularly (Pawlowski, 2002).

1.4.3. Nodule structure

Mature legume nodules have a stem-like organization in that they have a peripheral vascular system (Figure 1.2), with infected cells in the inner tissue. Actinorhizal nodules, as well as nodules induced by rhizobia on *Parasponia*, are composed of modified lateral roots without root caps, a central vascular system (Figure 1.2) and infected cells in the expanded cortex. It has been suggested that the structural differences between legume and other root nodules may be due to the availability of a unique developmental program in legumes (Joshi et al., 1993; Hirsch and LaRue, 1997). Some legume cultivars can spontaneously form bacteria-free nodules (Truchet et al., 1989; Blauenfeldt et al., 1994) which are rich in amyloplasts, indicating that nodules may originally have developed as carbon storage organs (Joshi et al., 1993).

There are two types of legume nodules: determinate and indeterminate. Which type of nodule is formed depends on the host plant (Mylona et al., 1995; Doyle et al., 1997). Indeterminate nodules contain an apical meristem. As a consequence, a developmental gradient of infected cells is established along the nodule axis (Figure 1.2; Vasse et al., 1990) that can be divided into five zones. Directly below the meristem (I), cells become infected in the prefixation zone (II). At the distal end of the infection zone, rhizobia are released from infection threads, enclosed by plasma membrane-derived

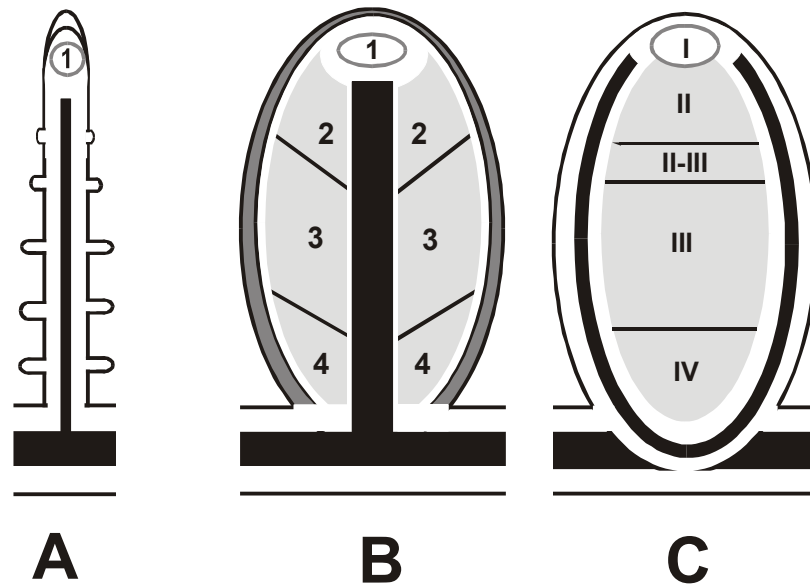


Figure 1.2. Schemes of longitudinal sections of roots and root nodules. **(A)** Scheme of a lateral root. The vascular system is labelled in black. Calyptra and root hairs are shown. 1 - meristem. **(B)** Scheme of an actinorhizal nodule lobe. The nodule periderm is labelled in dark grey. **(C)** Indeterminate legume root nodule. The zone containing the infected cells is labeled in light grey. Due to the activity of the apical meristem, a developmental gradient of infected cells is established along the nodule axis: 1(I) – meristem; 2(II) – pre-fixation zone/infection zone; II-III – intermediate zone of indeterminate legume nodule (C); 3(III) – nitrogen-fixation zone; 4(IV) – senescence zone. ■ - vascular system.

peribacteroid membranes, and start to differentiate into their symbiotic form, the bacteroids. In the interzone (II-III), bacterial nitrogen fixation starts and takes place throughout the nitrogen fixation zone (III). In the senescence zone (IV), bacteria are degraded. In determinate nodules, the nodule meristem stops its activity early in nodule development, and new infected cells are formed by division of already infected cells. Accordingly, all cells of the inner tissue are more or less at the same developmental stage, and the spatial developmental gradient of the indeterminate nodules is substituted by a temporal one (Newcomb, 1981).

Actinorhizal nodules are coralloid organs composed of multiple modified lateral roots, the nodule lobes. Like lateral roots, actinorhizal nodule lobes have an indeterminate growth pattern, i.e. they also show a developmental gradient in the nodule cortex (Figure 1.2; Ribeiro et al., 1995). The meristem (1) is followed by the infection zone (2) where cells are invaded by *Frankia* hyphae and gradually filled with *Frankia* material, surrounded by the invaginating plasma membrane. When *Frankia* has differentiated for nitrogen fixation, either by vesicle formation or by differentiation of hyphae, the nitrogen fixation (3) zone starts. In the senescence zone (4), *Frankia* hyphae and vesicles are degraded by the plant. While in most actinorhizal nodules infected and uninfected cells are interspersed

in the cortex, in nodules formed on roots of *Datisca*, the infected cells form a continuous patch on one side of the acentric stele (Figure 1.3; Hafeez et al., 1984).

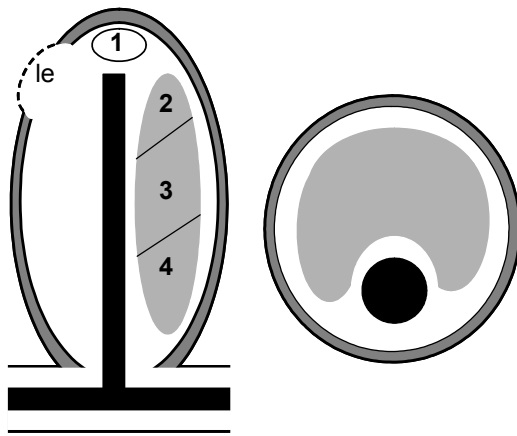


Figure 1.3. Scheme of a root nodule from *Datisca* sp. in longitudinal and cross section. The vascular system is labelled in black. Nodule lobes are surrounded by periderm which is shown in dark grey. For aeration, the periderm may be interrupted by lenticels (le). The infected cells are labelled in light grey. A developmental gradient of infected cells is established along the nodule axis: 1 – meristem; 2 – infection zone; 3 – nitrogen fixation zone; 4 – senescence zone.

1.4.4. Phylogenetic relationship of root nodule symbioses

According to recent molecular phylogenetic analysis (Soltis et al., 1995), legume and actinorhizal symbioses belong to a single clade, the so-called rosid I clade, i.e. they go back to a common ancestor (Figure 1.4). These data suggest a single evolutionary origin of the susceptibility to gain the ability to enter nitrogen-fixing root nodule symbioses.

Independent studies concerning the molecular phylogeny of legumes and of actinorhizal plants have led to the hypothesis that on the basis of a common predisposition, symbiosis has developed independently three or four times in both systems, which is supported by the differences in nodule morphology and infection mechanisms within both systems (Doyle et al., 1997; Swensen, 1996). The question arises which feature was acquired by the ancestor of the rosid I clade that represented the predisposition that allowed the development of a root nodule symbiosis. This feature must be common to all root nodule-forming plants, and is likely to be basal in nodule development.

1.4.5. Carbon sources supplied by the host plant to nitrogen-fixing microsymbionts

Within the symbiosis, the bacteria provide the plant with fixed nitrogen, while the plant provides the bacteria with carbon sources. In legume nodules, bacteria are supplied with dicarboxylic acids by the host plant (reviewed by Streeter, 1995). It has been assumed that dicarboxylic acids might also be the carbon source for symbiotic *Frankia*. While the analysis of enzyme activities in *Frankia* vesicle clusters isolated from nodules of *Alnus*

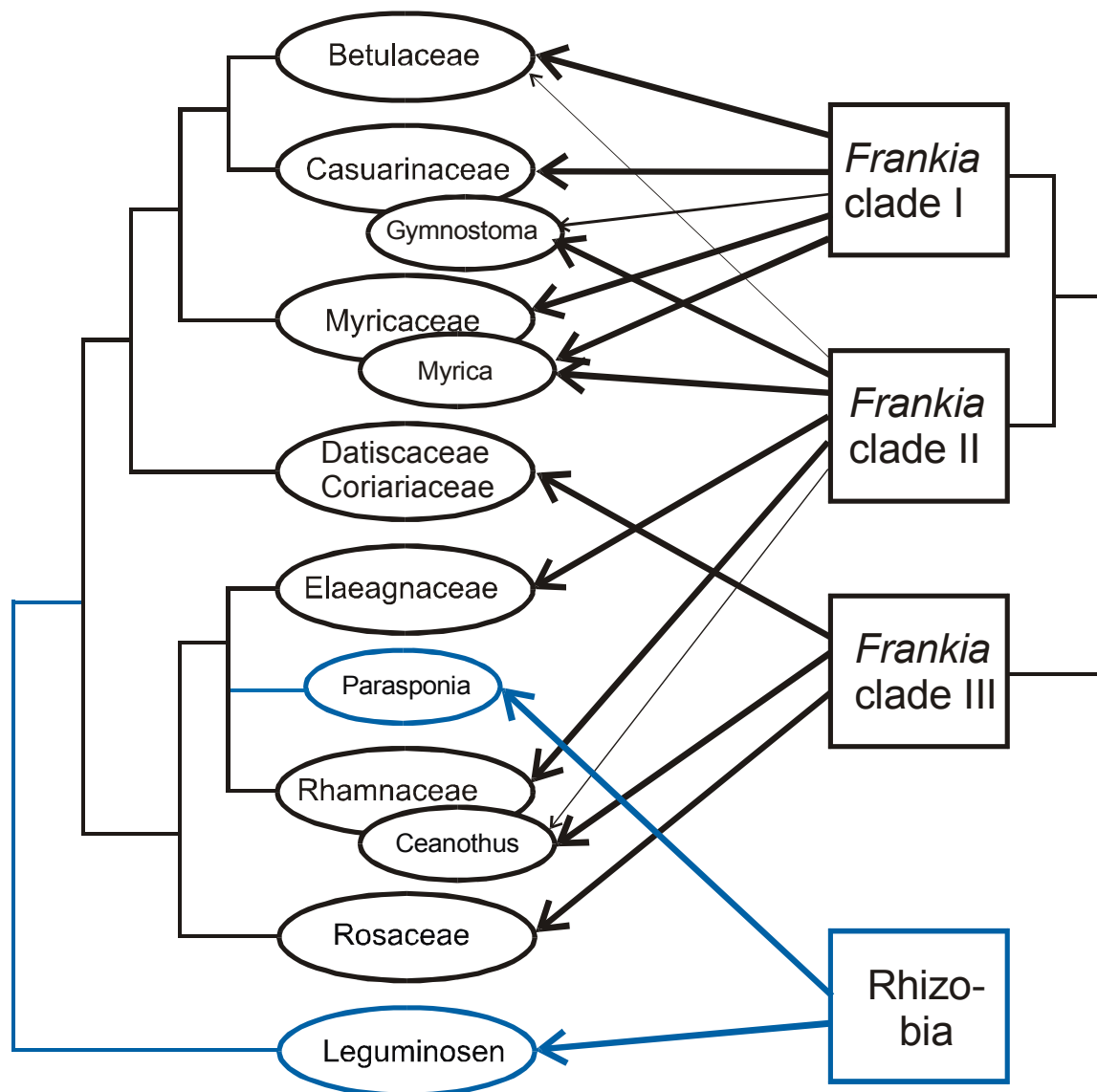


Figure 1.4. The relationships between groups of symbiotic plants and rhizobia and *Frankia* are shown in a simplified scheme (Wall, 2000; Benson and Clawson, 2000). Thick arrows connecting *Frankia* clades with the plant families/genera indicate that members of those clades are commonly associated with the plants. Thin arrows indicate that members of those clades have been isolated from or detected in an effective or ineffective nodule of a member of the plant genus/family at least once. Some actinorhizal genera (*Gymnostoma*, *Myrica*, *Ceanothus*) differ in microsymbiont specificity from the rest of the plant family they belong to. No members of *Frankia* Clade III have been isolated yet. Host specificity exists within the *Frankia* clades, *i.e.*, not all members of a clade can nodulate all plants associated with that clade. (Figure modified after Pawlowski, 2002).

and *Hippophae* yielded results consistent with this hypothesis (Akkermans et al., 1983), experiments on $^{14}\text{CO}_2$ uptake of detached *Alnus* nodules were inconclusive (Huss-Danell, 1990; see review by Huss-Danell, 1997). The carbon preferences of *Frankia* in the free-living state might provide a clue. *Frankia* strains have been divided into two genomic groups A and B based on DNA homology (Lechevallier and Lechevallier, 1990), and into four different clades based on 16S rRNA sequences (Normand et al., 1996). Clade IV comprises *Frankia*-like strains that cannot fix nitrogen; hence, there are three different clades of symbiotic *Frankia* strains. This grouping does not map with the differentiation into genomic groups. Furthermore, the 16S rRNA taxonomy includes non-culturable *Frankia* strains that could not be assigned to a genomic group. In the free-living state, *Frankia* strains of genomic group A tend to grow fairly on both sugars and organic acids, while strains of genomic group B grow variably on organic acids and poorly, if at all, on sugars. The carbon source mostly used in culturing *Frankia* strains is propionic acid. However, the endosymbionts of several actinorhizal plants, including *Datisca*, have not been isolated yet. Based on their 16S rRNA and *nifH* gene sequences, it has been concluded that many non-isolated *Frankia* strains including the endosymbiont of *Datisca* do not belong to any group of *Frankia* strains isolated so far (Mirza et al., 1994; Normand et al., 1996; Figure 1.4). Hence it is unclear whether this group of strains in particular, or *Frankia* strains in general, are fed other carbon sources than dicarboxylates during symbiosis.

1.4.6. Carbon transport and metabolism in nitrogen-fixing root nodules

Root nodules represent strong carbon sinks. They need assimilates as energy source for the microsymbionts, to provide carbon skeletons for the assimilation of the ammonium produced by the microsymbionts, for growth and, with the exception of *Casuarina* (E. Duhoux, personal communication) for starch biosynthesis.

In legume root nodules, several lines of evidence indicate that SuSy is essential for the cleavage of sucrose translocated from the shoots to the roots in support of nodule metabolism. First, the levels of SuSy mRNA and protein in soybean nodules are 10-20 times higher than those in root tissues (Thummler and Verma, 1987). Second, the SuSy gene is known to be predominantly expressed in nodules from *Vicia faba* and *Medicago truncatula* compared to uninfected roots, stems, leaves and other organs (Küster et al., 1993; Hohnjec et al., 1999). Third, several authors have demonstrated that various abiotic stress conditions (e.g. drought, salt, nitrate treatments) that decrease symbiotic nitrogen fixation in soybean nodules also dramatically reduce the mRNA, protein and activity levels

of SuSy (Gordon et al., 1997; González et al., 1995). Finally, a pea mutant with severely reduced activity of nodule-enhanced SuSy was incapable of an effective root nodule symbiosis (Gordon et al., 1999). These results, however, do not preclude that invertases present in nodules (Gordon, 1991) play an important role in nodule carbon metabolism in specific stages of development.

Few studies have been performed on the possibilities of symplastic and apoplastic carbon transport in nodules. Ultrastructural investigation of nodules of 27 genera of legumes demonstrated plasmodesmal connections between sieve element and pericycle cells and also showed that pericycle cells, like infected cells and endodermal cells, were symplastically connected (Pate et al., 1969). For seven genera of legumes, transfer cells were described in the pericycle, but precise investigation showed that they are localized next to xylem elements and cell wall protuberances are especially developed on the walls contiguous with the xylem (Pate et al., 1969). Light and electron microscopy of indeterminate *Vicia faba* nodules also revealed a block between vascular tissue and inner cortex, represented by Casparian bands on the radial cell walls of the vascular endodermis and the so-called nodule endodermis, a cell layer in the nodule cortex surrounding the inner tissue and the nodule vascular system, and by the suberin coat of endodermis cells (Abd-Alla et al., 2000).

But symplastic metabolite passage is possible due to high plasmodesmal frequencies found between the vascular endodermis and the inner cortex (Abd-Alla et al., 2000). It was also demonstrated that there are very few plasmodesmata between infected cells of the central tissue, whereas uninfected cells can represent a symplastic continuity (Abd-Alla et al., 2000).

1.5. Aim of this thesis

One very basal feature in root nodule development is the establishment and maintenance of the carbon sink function of the nodule. The aim of this thesis was to characterize sugar partitioning mechanisms in nitrogen-fixing root nodules. Three diverse model systems were chosen (Table 1.1): one legume symbiosis (*Medicago truncatula* – *Sinorhizobium meliloti*) and two actinorhizal symbioses from different *Frankia* subclades (Figure 1.4; *Datisca glomerata*, *Casuarina glauca*). The possibilities were (a) that carbon partitioning mechanisms in nodules would resemble those established in roots. If all three model plants would be similar here, root carbon partitioning mechanisms might represent the common basic feature that was required for the establishment of nitrogen-fixing symbiosis. If all three would be different, the symbiosis would put no specific requirements

on carbon partitioning mechanisms. On the other hand, if (b) carbon partitioning mechanisms in roots of the three model systems differed, while those in nodules were similar, the symbiosis would put specific requirements on carbon partition. Either way, the results of the comparison would deepen our understanding of the interaction between plants and nitrogen-fixing bacteria.

Table 1.1. Characteristics of the studied model systems for root nodule symbioses.

Characteristics	<i>Medicago truncatula</i>	<i>Datisca glomerata</i>	<i>Casuarina glauca</i>
Microsymbiont	<i>Sinorhizobium meliloti</i>	<i>Frankia</i> subclade III	<i>Frankia</i> subclade I
Infection mechanism	Intracellular	Intercellular	Intracellular
Oxygen-carrying protein	Leghemoglobin	No hemoglobin found	Symbiotic hemoglobin
Oxygen barrier	Nodule parenchyma	Mitochondria at vesicle base	Strong lignification of infected cells
Microsymbiont in free culture	+	Not isolated	+
Phloem loading mechanism	Apoplastic	Not examined	Symplastic

To characterize carbon partitioning mechanisms in these three systems, the following aspects were examined:

- Contents and identity of dominating sugars in nodules compared to roots
- Activities of SuSy and of the different invertases
- Localization of sucrose-cleaving enzymes
- Expression levels of SuSy and sugar transporters
- Isolation of the cDNAs of hexose transporters expressed in nodules, and biochemical characterization of their protein products

The last of these aims was proposed since in nodules of *Datisca*, the expression of a monosaccharide transporter had been localized by *in situ* hybridization specifically to the infected cells (Wabnitz, 1998).

2. Materials and methods

For all methods, except for biochemical methods, only sterile pipette tips, glass and plastic ware were used. All solutions for molecular biological methods were prepared using water of MilliQ grade (dd H₂O), autoclaved or filter sterilised, if not otherwise described.

2.1. Materials

2.1.1. Plant material

Medicago truncatula: cv. Jemalong, genotype A-17 (Barker et al., 1990)
Datisca glomerata: seeds were kindly provided by Alison M. Berry, University of California (Davis, CA, USA)
Casuarina glauca: seeds were supplied by the Desert Development Centre (Cairo, Egypt)

2.1.2. Bacterial and yeast strains

Plant infection:

Host plant	Symbiont	Reference
<i>Medicago truncatula</i>	<i>Sinorhizobium meliloti</i> 1021	Meade et al., 1982
<i>Datisca glomerata</i>	actinomycetes from crushed nodules	
<i>Casuarina glauca</i>	<i>Frankia</i> strain <i>Thr</i>	Girgis et al., 1990

Cloning:

Escherichia coli DH5 α (Woodcock et al., 1989).

Genotype: F⁻ (ϕ 80*dlacZ* Δ M15) *recA1 endA1 gyrA96 thi-1 hsdR17*(r_k⁻m_k⁺) *supE44 relA1 deoR* Δ (*lacZYA-argF*) U169

Analysis of transport activity for plant hexose transporters:

Saccharomyces cerevisiae strain EBY.VW4000 (Wieczorke et al., 1999)

Genotype: *hxt13Δ::loxP hxt15Δ::loxP hxt16Δ::loxP htx14Δ::loxP htx12Δ::loxP htx9Δ::loxP htx11Δ::loxP htx10Δ::loxP htx8Δ::loxP htx514Δ::loxP htx2Δ::loxP htx367Δ::loxP gal2Δ stl1Δ::loxP agt1Δ::loxP ydl247wΔ::loxP yjir 160cΔ::loxP*

2.1.3. Oligonucleotides (Primers)

Name	Sequence
<i>DgHT fs5</i>	5'-CCC TTC TCT CTT TAT CTC C-3'
<i>DgHT fs3</i>	5'-CAG ATA CAT CAA ATT TGA CCC-3'
<i>DgHT 5'race1</i>	5'-GTC GGG AAG GAG TAG CGA-3'
<i>DgHT 5'race2</i>	5'-CTC CTC TGT ACT TGT AGG GA-3'
<i>for</i>	5'-GTA AAA CGA CGG CCA GT-3'
<i>MtHT fs</i>	5'-CCC AAC CAG CAT AGA ATT AAA CTA ACA GTG-3'
<i>MtHT 5'race1</i>	5'-GAA GAA CAC GAC CCA AAA TGA GC-3'
<i>MtHT 5'race2</i>	5'-ATC CTT AGA CAA AAC AGC GTT CGA-3'
<i>MM1</i>	5'- GGC CAC GCG TCG ACT AGT ACG GGI IGG GII GGG IIG - 3'
<i>MM2</i>	5'- GGC CAC GCG TCG ACT AGT AC - 3'
<i>MM3</i>	5'- CTC GAG GAT CCG CGG CCG CT ₁₈ - 3'
<i>MM4</i>	5'- CTC GAG GAT CCG CGG CCG C - 3'
<i>PmDgHT-for</i>	5'-CCG GAA TTC AAG CTT GTA AAA GAA ATG CCG GCC GTC GGA GG-3'
<i>PmDgHT-rev</i>	5'-CTA AAA ATA ACC CTC CCC CCA AAC-3'
<i>PmMtHT-for</i>	5'-CCG CTC GAG AAG CTT GTA AAA GAA ATG GCT GGT GGG GTT TTA CCA GTG-3'
<i>PmMtHT-rev</i>	5'-TTC ACT AGT GAT TCT CGA GGA TCC GC-3'
<i>Rev</i>	5'-AGC GGA TAA CAA TTT CAC ACA GGA-3'
<i>T3</i>	5'- TAA CCC TCA CTA AAG GGA - 3'
<i>T7</i>	5'- TAA TAC GAC TCA CTA TAG GG - 3'
<i>dT₂₀</i>	5'-TTTTTTTTTTTTTTTTTTTTTTT-3'

2.1.4. Plasmids

p-Bluescript [®] II KS (+)	Amp ^R	Stratagene, La Jolla, CA, USA
p-GEM [®] -T Easy	Amp ^R	Promega, Madison, WI, USA
pNEV-E	Amp ^R ; URA3	Sauer and Stolz (1994)

pNEV-X	Amp ^R ; URA3	Sauer and Stolz (1994)
pP001-VS	Amp ^R	B.Reiß, personal communication
pRT 105	Amp ^R	Topfer et al. (1993)
pSPORT	Amp ^R	Gibco BRL, Eggenstein, Germany

2.1.5. Enzymes

2.1.5.1. Restriction enzymes

Restriction enzymes *Xba*I, *Eco*R321 (*Eco*RV), *ACC*65I (*Kpn*I), *Sma*I, *Pst*I, *Sda*I (*Sse*8387I), *Eco*105I (*Sna*BI) were obtained from MBI Fermentas (Vilnius, Lithuania) and *Bam*HI, *Hind*III, *Eco*RI, *Sst*I, *Sst*II, *Sal*I, *Pst*I from Gibco BRL (Eggenstein, Germany).

2.1.5.2. Other enzymes and kits

<i>Taq</i> -Polymerase	Biometra, Göttingen, Germany
DNA-Polymerase I Large Fragment (Klenow Fragment)	MBI Fermentas, Vilnius, Lithuania
MLV Reverse Transcriptase	MBI Fermentas, Vilnius, Lithuania
Thermoscript TM -RT-PCR System	Gibco BRL, Eggenstein, Germany
RNase A	Sigma, Deisenhofen, Germany
T4 DNA-Ligase	Gibco BRL, Eggenstein, Germany
Lysozyme	Sigma, Deisenhofen, Germany
Mung bean nuclease	Epicentre Technologies, Madison, WI, USA
ABI PRISM dRhodamine Terminator Cycle Sequencing Ready Reaction Kit	PE Applied Biosystems, Weiterstadt, Germany
Qiagen Gel Extraction Kit	Qiagen, Hilden, Germany
Qiaprep Spin Miniprep Kit	Qiagen, Hilden, Germany
Qiaprep Spin Maxiprep Kit	Qiagen, Hilden, Germany
Peq Lab E.Z.N.A. Plasmid Miniprep II Kit	Peq Lab Biotechnologie GmbH, Erlangen, Germany
Invisorb Spin-Plant-RNA Mini Kit	Invitek, Berlin, Germany

2.1.6. Chemicals

Agar	Gibco BRL, Eggenstein, Germany
Agarose	Gibco BRL, Eggenstein, Germany
Ampicillin	Sigma, Deisenhofen, Germany
Arbutin	Sigma, Deisenhofen, Germany
Bovine Extract	Difco, Becton Dickinson GmbH, Heidelberg, Germany
Casamino Acids (CAA)	Difco, Becton Dickinson GmbH, Heidelberg, Germany
Coomassie Brilliant Blue G 250	Serva, Heidelberg, Germany
5-Bromo-4-chloro-3-indolyl β -D-galactopyranoside (X-Gal)	Roche Molecular Biochemicals, Mannheim, Germany
Dimethylformamide (DMF)	Sigma, Deisenhofen, Germany
Dimethyl sulfoxide (DMSO)	Sigma, Deisenhofen, Germany
Deoxynucleotide triphosphates (dNTPs)	Roche Molecular Biochemicals, Mannheim, Germany
Dithiothreitol (DTT)	Gibco BRL, Eggenstein, Germany
Ethidium bromide	Sigma, Deisenhofen, Germany
Ethylendiamine tetraacetic acid (EDTA)	Merck, Darmstadt, Germany
D(+)-Glucose	Merck, Darmstadt, Germany
Yeast extract	Gibco BRL, Eggenstein, Germany
Yeast nitrogen base w/o amino acids	Difco, Becton Dickinson GmbH, Heidelberg, Germany
Isopropyl β -D-thiogalactopyranoside (IPTG)	AppliChem, Darmstadt, Germany
Kanamycin	Sigma, Deisenhofen, Germany
β -Mercaptoethanol	Merck, Darmstadt, Germany
Orange G	Sigma, Deisenhofen, Germany
Polyclar AT	Serva, Heidelberg, Germany
D(+)-Sucrose	Carl Roth GmbH & Co, Karlsruhe, Germany
Select Pepton 140	Gibco BRL, Eggenstein, Germany
Trishydroxymethylaminomethane (Tris)	Sigma, Deisenhofen, Germany
Other chemicals	Merck, Darmstadt, Germany Sigma, Deisenhofen, Germany

2.1.7. Other materials and devicesFilters and membranes:

Hybond N	Amersham Pharmacia Biotech, Freiburg, Germany
3MM-filter paper	Whatman, Madistone, Kent, UK
Miracloth	Schütt Labortechnik GmbH, Göttingen, Germany

Devices:

Transilluminator FLX-20M	Vilber Lourmat, Marne La-Vallet, France
ABI Prism 310 Genetic Analyser	PE Applied Biosystems, Foster City, CA, USA
Phospho-Imager Fuji BAS-1000	Raytest, Sprockhövel, Germany
Thermocycler PTC-100	Biozym, Hessisch Oldendorf, Germany
Personal Cycler	Biometra, Göttingen, Germany
Liquid scintillation analyzer 1900TR	Canberra Packard GmbH, Dreieich, Germany

Centrifuges:

Megafuge 1.0	Heraeus Sepatech, Osterode, Germany
Biofuge pico	Heraeus Sepatech, Osterode, Germany
Eppendorf centrifuge 5415 R	Eppendorf AG, Hamburg, Germany
SORVALL®-RC-3B Refrigerated Superspeed Centrifuge	Sorvall GmbH, Bad Homburg, Germany
Ultracentrifuge L-80	Beckman Instruments, München, Germany

2.1.8. Culture media**2.1.8.1. Plant media**Hydroculture medium (Hoagland und Arnon, 1938)

	Strength		<i>Macro element stock solutions:</i>
	$\frac{1}{2}$	$\frac{1}{4}$	
per 1l:	2 ml	1 ml	1 M KH_2SO_4
	4 ml	2 ml	1 M $\text{MgSO}_4 \cdot 7\text{H}_2\text{O}$
	10 ml	5 ml	1 M KNO_3
	10 ml	5 ml	1 M $\text{Ca}(\text{NO}_3)_2 \cdot 4\text{H}_2\text{O}$

2 ml	1 ml	<i>Micro elements stock solution</i>
		2.86 g/l H ₃ BO ₃
		1.81 g/l MnCl ₂ ·4H ₂ O
		0.22 g/l ZnSO ₄ ·7H ₂ O
		0.08 g/l CuSO ₄ ·5H ₂ O
		0.025 g/l Na ₂ MoO ₄ ·2H ₂ O
		0.025 g/l CoCl ₂ ·6H ₂ O
10 ml	5 ml	<i>Fe-EDTA-stock solution:</i>
		5.56 g/l FeSO ₄ ·7H ₂ O
		7.45 g/l Na ₂ -EDTA
		adjust pH to 5.5

Aeroponic culture medium (Lullien et al., 1987)

5,5	mM	K-PO ₄ -buffer pH 7.0
1	mM	CaCl ₂
0.52	mM	K ₂ SO ₄
0.25	mM	MgSO ₄
0.04	µM	CoCl ₂
0.2	µM	CuSO ₄
0.7	µM	ZnSO ₄
10	µM	MnSO ₄
30	µM	H ₃ BO ₃
50	µM	Na ₂ -EDTA
50	µM	FeSO ₄
1	µM	Na ₂ Mo ₄

K-PO₄-buffer was prepared as sterile 100× stock solution, pH 7.0, containing 58.92 g/l K₂HPO₄ and 41.08 g/l KH₂PO₄. For the other components 1000× stocks were prepared separately and autoclaved. FeSO₄ solution should be made fresh.

Fåhraeus Medium (Fåhraeus, 1957)

For 1 l of medium (nodulation nitrogen-free medium):

0.5 ml	1,0 M	MgSO ₄
1.0 ml	0,7 M	KH ₂ PO ₄
2.0 ml	0,4 M	NaH ₂ PO ₄
2.5 ml	20 mM	Fe EDTA
100 µl	1 mg/l	MnSO ₄
100 µl	1 mg/l	CuSO ₄
100 µl	1 mg/l	ZnSO ₄
100 µl	1 mg/l	H ₃ BO ₄
100 µl	1 mg/l	Na ₂ MoO ₄

The pH was adjusted to 6.5 with H₂SO₄ and then 1.25 ml of 1 M CaCl₂ was added.

2.1.8.2. Bacterial media

- Media for *Escherichia coli*:

LB Medium (Luria-Bertani Medium) (Sambrook et al., 1989)

Per liter:

5 g	Yeast Extract
10 g	Select Pepton 140
10 g	NaCl

The pH was adjusted to 7.5 with 5 N NaOH. For solid LB medium, 1.5 % (w/v) agar per liter were added.

SOC-Medium (Sambrook et al., 1989)

All glassware used for the preparation of SOC medium was autoclaved filled with dd H₂O to remove remains of detergents.

Per liter:

5 g	Yeast Extract
20 g	Select Pepton 140
10 ml	1 M NaCl
2.5 ml	1 M KCl

The volume was adjusted to 1 liter with dd H₂O. After autoclaving for 10 minutes filter sterilized solutions were added:

10 ml	1 M MgCl ₂
10 ml	1 M MgSO ₄
10 ml	1 M Glucose

TB Medium [Terrific Broth] (Tartof and Hobbs, 1987)

Per liter:

To 900 ml of dd H₂O were added:

12 g	Select Pepton 140
24 g	Yeast Extract
4 ml	Glycerol

After autoclaving for 20 minutes, the solution was cooled to 60 °C or less, and 100 ml of a sterile solution of K-PO₄-buffer (0.17 M KH₂PO₄, 0.72 M K₂HPO₄) were added. For K-PO₄-buffer 2.31 g KH₂PO₄ and 12,54 g K₂HPO₄·3H₂O were dissolved in 90 ml of dd H₂O, the volume was adjusted to 100 ml with dd H₂O.

- Media for *Sinorhizobium meliloti*:

TY-medium

Per liter:

5 g	Select Pepton 140
3 g	Yeast Extract
0.9 g	CaCl ₂ ·2H ₂ O

YEB-medium (van Larebeke et al., 1977)

Per liter:	5 g	Bovine Extract
	1 g	Yeast Extract
	5 g	Select Pepton 140
	5 g	Sucrose

The pH was adjusted to 7.2-7.3 with NaOH

- Medium for *Frankia*:

BAP Medium (Fontaine et al., 1986)*Stock solutions:*

Per liter:	10 ml	13.5 mM	CaCl ₂ ·2H ₂ O
	5 ml	40.5 mM	MgSO ₄ ·7H ₂ O
	1 ml	195 mM	FeNa ₂ EDTA
	5 ml	1 M	NH ₄ Cl
	5 ml	1 M	Sodium propionate
	1 ml		Oligoelements
	1 ml		Vitamins
	10 ml		K-PO ₄ -buffer

<i>Oligoelements:</i>	2.86 g/l	H ₃ BO ₃
	1.81 g/l	MnCl ₂
	0.22 g/l	ZnSO ₄ ·7H ₂ O
	0.08 g/l	CuSO ₄ ·5H ₂ O

<i>Vitamin stocks:</i>	11.21	mg/10 ml	Thiamin HCl
	50	mg/10 ml	Pyridoxin HCl
	50	mg/10 ml	Nicotinic acid
	10	mg/10 ml	Calcium pantothenate
	10	mg/10 ml	Folic acid
	10	mg/10 ml	Riboflavin
	9	mg/0.5 ml	Biotin, dissolved in 0.5 ml KOH, then diluted to 4 ml with dd H ₂ O

Vitamin stocks were stored at -20 °C. To prepare 100 ml vitamin mix 1 ml of each stock was used.

<i>K-PO₄- buffer:</i>	560 ml	1 M	KH ₂ PO ₄
	320 ml	1 M	K ₂ HPO ₄ ·3H ₂ O
	pH was adjusted to 6.7 with 10 N KOH		

2.1.8.3. Media for *Saccharomyces cerevisiae*

<u>YPM – medium</u>	1 % (w/v)	Yeast extract
	2 % (w/v)	Peptone
	2 % (w/v)	Maltose

<u>CAA – medium</u>	1 % (w/v) Casamino Acids
	2 % (w/v) Maltose
	0.67 % (w/v) YNB w/o amino acids
Supplements:	1:50 (v/v) 1 mg/ml Tryptophan stock solution

For agar plates 2 % agar (w/v) were added before autoclaving. L-Tryptophan was dissolved at 60-70 °C. The solution was filter-sterilized and stored at 4 °C. Tryptophan was added to CAA-medium at 50 °C before making plates.

2.1.8.4. Medium additives

Additives	Solvent	Stock solution concentration	Final concentration
Ampicillin	H ₂ O	100 mg/ml	100 µg/ml
Kanamycin	H ₂ O	50 mg/ml	50 µg/ml
IPTG	H ₂ O	0,1 M	0,2 mM
X-Gal	DMF	2 % (w/v)	0,004 %

Stock solutions dissolved in H₂O were filter sterilized. All medium additives were kept at –20 °C.

2.2. Plant culture methods and growth conditions

Datisca glomerata and *Casuarina glauca* seeds were germinated and grown for three and five to six months, respectively, in soil (T 25 Frühstorfer Erde®) mixed with one third volume of sand. Then they were transferred into aerated hydroculture in ¼ strength Hoagland's medium (Hoagland and Arnon, 1938; see 2.1.8.1.).

Noninfected plants of *Medicago truncatula* genotype A-17 (cv. Jemalong) were grown in a soil-sand mixture (see above) for three weeks and then transferred either to hydroculture in Fåhraeus Medium (Fåhraeus, 1957; see 2.1.8.1.) for root material or in aeroponic culture with Lullien medium for root and nodule material (Lullien et al., 1987; see 2.1.8.1.). After one week in aeroponic culture they could be infected with *Sinorhizobium meliloti* 1021 cells (Meade et al., 1982) grown in TY medium and washed with dd H₂O. Nodules were harvested after 10-14 days (aeroponic culture).

D. glomerata was infected with actinomycetes from crushed nodules of *D. glomerata* plants grown in soil and *C. glauca* was infected with *Frankia* strain *Thr* (Girgis et al., 1990) grown in BAP Medium (Fontaine et al., 1986, see 2.1.8.2.) and washed with dd H₂O 3-4 times. Nodules of *D. glomerata* and *C. glauca* were harvested 4-8 weeks after infection.

The greenhouse conditions were: temperature 22 °C/18 °C (day/night), light intensity 200 μmol photons×m⁻²×s⁻¹ in winter and 400 μmol photons m⁻² s⁻¹ in summer, 60-65 % humidity.

2.3. RNA isolation from plant tissue

2.3.1. RNA isolation from *Medicago truncatula* and *Datisca glomerata* (modified after Burgos et al., 1995)

Homogenization Buffer (HB):	100 mM	Tris/HCl , pH 9.0
	100 mM	NaCl
	15 mM	EDTA
	0.5 %	N-Lauroylsarcosin (Sigma)
	Store at room temperature in 50 ml aliquots	

Plant tissue was ground in liquid nitrogen into a fine powder and transferred into 50 ml Falcon tubes, containing 5 ml homogenization buffer, 5 ml phenol/chloroform mixture (1:1) and 35 μl β-mercaptoethanol per 1 g of plant material. After homogenizing for 2 minutes using a IKA Ultra-Turrax® T-25 Basic Homogenizer (Ika-Werke GmbH & Co. KG, Staufen, Germany), 350 μl 3 M sodium acetate (pH 5.4) were added per g tissue, and the mixture was homogenized again for 30 sec. Then the homogenate was poured into phenol/chloroform resistant 13 ml tubes and centrifuged in a SORVALL®-RC-3B Refrigerated Superspeed Centrifuge (SORVALL GmbH, Bad Homburg, Germany) in a SS 34 rotor at 10 krpm for 10 min at 4 °C.

After centrifugation, the proteins of the cell homogenate formed a solid interphase between the water phase and the organic phase. The water phase was transferred into a new 13 ml tube, an equal volume of phenol/chloroform was added, and the tube was vortexed and centrifuged again at 10 krpm for 10 min at 4 °C. Then the supernatant was transferred again into a new 13 ml tube and an equal volume of isopropanol was added. After vortexing, the mixture was incubated at – 20 °C for 20-60 minutes. At this step

nucleic acids precipitated and could be pelleted by a 10 min centrifugation step in the SS 34 rotor at 10 krpm and 4 °C.

The pellet was washed with 2 ml 70 % (v/v) ethanol to remove salts and centrifuged for 5 min in a SS 34 rotor at 10 krpm and 4 °C. The pellet was resuspended in 900 µl dd H₂O and transferred into an 1.5 ml Eppendorf tube for extraction with 500 µl phenol/chloroform mixture (1:1) followed by an extraction of supernatant with 500 µl chloroform. The supernatant was then transferred to a new Eppendorf tube and the volume was adjusted to 900 µl. 300 µl (1/3 Vol.) 8 M LiCl were added and RNA was precipitated on ice for 3 hours, followed by 10 min of centrifugation at 4 °C and 13 krpm. The pellet was washed with 70 % (v/v) ethanol, resuspended in 50–100 µl H₂O at 65 °C for 5 min and then cooled on ice. The insoluble material was removed by a 5 min centrifugation step. The supernatant was transferred to a new Eppendorf tube, and the intactness and concentration of the isolated RNA was tested on a 1 % (w/v) agarose gel (see 2.6.1.) in a detergent-treated gel chamber.

2.3.2. RNA isolation from *Casuarina glauca*

The RNA isolation from *Casuarina* is difficult because of the high polyphenol content of the plant that interferes with nucleic acid isolation procedures. Therefore different methods and kits were applied for *Casuarina* RNA isolation. The best results were obtained with the „Invisorb Spin Plant RNA Mini Kit“ (Invitex, Berlin, Germany). The purification procedure was conducted according to recommendations of the manufacturer with a few adaptations.

About 100 mg plant material were ground in liquid nitrogen with ca. 50 mg of Polyclar® AT (Serva, Heidelberg, Germany) to a fine powder and transferred into a 2 ml Eppendorf tube. After the liquid nitrogen had evaporated, 500-800 µl of Lysis Solution RP were added to the plant powder followed by vortexing for 1 min and 2 min of incubation at room temperature. To remove cell debris, the sample was centrifuged for 5 min at 13 krpm. The supernatant was pipetted onto a DNA-Binding Spin Filter which was placed in a 1.5 ml Eppendorf tube and incubated for 1 min at room temperature. After a centrifugation for 1 min at 10 krpm at room temperature, ½ vol. of absolute ethanol was added to the RNA-containing flow-through and the mix was transferred onto an RNA-Binding Spin Filter in a 1.5 ml Eppendorf tube. After 1 min incubation at room temperature, the sample was centrifuged for 30 sec at 10 krpm in order to bind the RNA to the filter. The flow-through was discarded, and the filter was washed with 600 µl wash buffer R1 by a centrifugation for 30 sec at 10 krpm. This step was repeated twice with 500 µl of wash buffer R2. Then the filter was centrifuged again for the removal of remains of wash buffer at 12 krpm for 2

min and placed in a new Eppendorf tube. The RNA was eluted by direct pipetting of 40-60 µl elution buffer onto the membrane, followed by 2 min of incubation at room temperature and a centrifugation for 1 min at 10 krpm. After this step, the RNA was kept on ice before testing the RNA concentration on an 1 % agarose gel (see 2.6.1.), or stored at $-80\text{ }^{\circ}\text{C}$.

2.4. Isolation of plasmid DNA from bacteria and yeast

2.4.1. Plasmid mini-preparation protocol „ Triton Boiling“

This method comprised an effective and fast method for the isolation of plasmid DNA from bacteria for a quick characterization with restriction enzymes.

4 ml of LB medium (see 2.1.8.2.), containing an appropriate antibiotic, were inoculated with a single bacterial colony and incubated overnight at $37\text{ }^{\circ}\text{C}$ with vigorous shaking. 1.5 ml of overnight culture were poured into an Eppendorf tube and spun down at 13 krpm for 1 min. The remainder of the overnight culture could be stored at $4\text{ }^{\circ}\text{C}$ for 1-2 days. The supernatant was removed to leave the bacterial pellet as dry as possible. Bacterial pellets were resuspended by vortexing in 150 µl cold STEL buffer (8 % sucrose; 5 % Triton X 100; 50 mM Tris-HCl, pH 8.0; 50 mM EDTA; 0.5 mg/ml lysozyme) and boiled for 30 sec at $100\text{ }^{\circ}\text{C}$. Cell debris with genomic DNA was sedimented by 20 min of centrifugation at 13 krpm at room temperature. The pellet was removed with a sterile toothpick, and the supernatant was mixed with 180 µl isopropanol and centrifuged again at 13 krpm for 5 min to pellet the plasmid DNA. The pellet was then washed with 500 µl 70 % ethanol, spun down for 5 min at 13 krpm, dried at $37\text{ }^{\circ}\text{C}$ and finally resuspended in 50 µl RNase- H_2O (0.2 mg/ml RNase A) for 10 min at $37\text{ }^{\circ}\text{C}$. DNA was stored at $-20\text{ }^{\circ}\text{C}$.

2.4.2. Mini preparation of bacterial plasmid DNA for the sequence analysis

For sequence analysis, the plasmid DNA was isolated using a QIAprep® Spin Miniprep Kit (Qiagen, Hilden, Germany), which allows a fast preparation of pure DNA. The QIAprep miniprep procedure is based on the alkaline lysis of bacterial cells followed by the adsorption of DNA on a silica gel membrane in the presence of a high salt concentration. The DNA was eluted from the column with 50 µl dd H_2O .

2.4.3. Maxi preparation of bacterial plasmid DNA

This method was used for the preparation of large amounts of plasmid DNA from bacteria. For this procedure, 50 ml of TB medium (see 2.1.8.2.), containing an appropriate antibiotic, were inoculated with a single bacterial colony and incubated overnight at 37 °C with vigorous shaking. The overnight culture was distributed over four 13 ml centrifugation tubes and centrifuged for 10 min at 4.3 krpm in a Megafuge 1.0 (Heraeus Sepatech, Osterode, Germany). The supernatant was discarded, and the pellet could be stored at -20 °C.

For DNA preparation the Peq Lab E.Z.N.A. Plasmid Miniprep Kit II (Peq Lab Biotechnologie GmbH, Erlangen, Germany) was used, which allows to isolate large amounts of very pure plasmid DNA. This procedure, conducted as described in the standard Peq Lab protocol, is based also on the alkaline lysis of bacterial cells followed by the adsorption of DNA to a silicagel membrane. 13 ml of overnight culture was used per preparation. The plasmid DNA was eluted from the column with 120 µl dd H₂O with a 5 min incubation step at 37 °C before the last centrifugation.

2.4.4. Preparation of plasmid DNA from yeast

For the quick preparation of plasmid DNA from yeast, a medium size yeast colony (Ø ca. 3 mm) was picked and transferred to 200 µl of lysis buffer (100 mM NaCl, 10 mM Tris (pH 8.0), 1 mM EDTA, 0.1% (w/v) SDS). Then an equal volume of glass beads (Ø 0.45 mm) was added, and the sample was vortexed at top speed for 1 min. After an extraction with 200 µl of a phenol/chloroform mixture (2:1), the plasmid DNA was precipitated with ethanol (see 2.5.1.) and finally resuspended in 50 µl of dd H₂O. To obtain enough DNA for the characterization of the plasmid by digestion with restriction enzymes, *E.coli* was transformed with 5-10 µl of plasmid DNA prepared from yeast (2.13.2.) and a plasmid DNA minipreparation (2.4.1.) was performed.

2.5. Concentration and purification of DNA or RNA solutions

2.5.1. Precipitation of nucleic acids

DNA or RNA precipitation was used to concentrate very dilute samples of nucleic acids or to change salt/buffer composition. For this purpose, the DNA (or RNA) sample was mixed

with 0.1 volume of 3 M sodium acetate (pH 5.2) and 2.5 volumes of absolute ethanol, and precipitated at $-20\text{ }^{\circ}\text{C}$ for at least one hour. After centrifugation for 15 min at 13 krpm, the supernatant was taken off and the pellet was washed with 70 % ethanol to remove excess salt. After centrifugation for 10 min at 13 krpm, the pellet was dried at $37\text{ }^{\circ}\text{C}$ to remove the remains of ethanol. Finally, the pellet was resuspended in an appropriate volume of dd H_2O or buffer.

2.5.2. Phenol-chloroform extraction and precipitation of DNA

To remove proteins from DNA solution the same volume (at least 200 μl) of a phenol/chloroform mixture (1:1, v/v) was added. The mixture was vortexed and centrifuged for 5 min at 13 krpm. Then the supernatant was extracted the same way with one volume of chloroform. After this step, 0.1 volume of 3 M sodium acetate (pH 5.4) and 2.5 volume absolute ethanol were added to the supernatant to precipitate DNA as described above (2.5.1.).

This method was used to purify for instance the linearised form of a cloning vector from restriction enzymes and buffer salts before ligation.

2.6. Electrophoretic separation of DNA and RNA

2.6.1. TEA-Agarose gel electrophoresis

DNA and RNA concentrations or fragment size were tested on 1 % (w/v) agarose gels in $1\times$ TEA buffer (40 mM Tris-acetate pH 8.3; 2 mM EDTA) as gel- and running buffer. The gel was supplied with 0.25 $\mu\text{g}/\text{ml}$ ethidium bromide (Sigma, Deisenhofen, Germany) to make nucleic acids visible under UV-light (366 nm wave length; Transilluminator FLX-20M, Vilber Lourmat, Marne La-Vallet, France).

1 μl of DNA or RNA solution was mixed with 2 μl of orange loading dye (50 % glycerol; 10 mM NaH_2PO_4 , pH 7.0; 0.4 % Orange G (Sigma, Deisenhofen, Germany)). The electrophoresis was conducted at 70 V. 1 μg of λ -Phage DNA, restricted with *Pst*I was used as length and quantity standard. Gel documentation was performed using the program PhotoFinish® 3.0 (WordStar Atlante Technology Center Inc., Marietta, GA, USA).

For quantification and quality estimation of RNA, gel box, combs and gel carrier were pre-treated with 1 % SDS solution (w/v) for 1 h to denature RNases. Afterwards they were thoroughly rinsed with tap water to remove remains of SDS, which bind ethidium bromide.

2.6.2. Separation of RNA on agarose gel for Northern blots

For Northern blots, RNA samples were separated on denaturing formaldehyde agarose gels (1.2 % (w/v) agarose). For a gel of 13.5×16 cm, 3 g agarose were dissolved in 150 ml dd H₂O by heating in a microwave oven. After cooling to 70 °C, 20 ml 10× MEN buffer (200 mM MOPS, 10 mM EDTA, 80 mM sodium acetate, pH adjusted to 7.0 with NaOH) and 33 ml 37 % formaldehyde solution were added and the gel was poured.

Per slot, ca. 10 µg of RNA in 9 µl H₂O were denatured at 65 °C for 10 min together with 21 µl of Northern mix (3 µl 10× MEN; 12 µl deionised formamide; 3 µl 37 % formaldehyde solution; 3 µl blue marker-mix, prepared from 15 µl 10 mg/ml ethidium bromide stock and 85 µl blue loading dye (0,1 % (w/v) xylene cyanol; 0,2 g/ml sucrose; 250 mM EDTA; 0,5 mg/ml bromphenol blue)). After loading of the RNA samples, all slots were filled with 1× MEN running buffer. Electrophoresis was performed for ca. 2.5 hours at 100-130 V. Ca.1 h after start of the electrophoresis, the gel was photographed to document the quantities of RNA loaded.

2.7. Northern blot hybridization

2.7.1. RNA transfer to nylon membranes (Northern blotting)

The gel with electrophoretically separated RNA samples (see 2.6.2.) was put on blotting paper (3 MM, Watman, Maidstone, UK) that had been soaked in 20× SSC (3M NaCl, 300 mM sodium citrate, pH 7.0) and the ends of which were placed in 20× SSC solution. Then a nylon membrane (HybondTM-N, Amersham Pharmacia Biotech, Buckinghamshire, UK), wetted in dd H₂O was incubated for 15-20 min in 20× SSC, placed on the gel and covered with 3 layers of whatman 3 MM paper soaked in 20× SSC and finally with a dry, about 5 cm thick stack of paper towels of about 5 cm height. A weight of about 1 kg was placed on the paper towel stack and the capillary transfer of RNA onto the membrane proceeded

overnight. The Hybond-N membrane was washed in 2× SSC, followed by baking for 2-3 hours at 80 °C. The membrane was stored in a plastic bag at 4 °C before use.

2.7.2. DNA probe labelling with α -[³²P]-dATP

About 25 ng of DNA fragment isolated from a gel were denatured for 5 min at 100 °C in a total volume of 27 μ l and then put on ice. 6.5 μ l OLB-buffer, 1 μ l 20 μ g/ μ l of BSA, 1 μ l (2U/ μ l) Klenow Fragment (DNA-Polymerase I Large Fragment; MBI Fermentas, Vilnius, Lithuania) and 2 μ l α - [³²P]-dATP (ca. 20 μ Ci, specific activity 111 Tbq/mmol; Hartmann Analytic, Braunschweig, Germany) were added. After incubation for 45-60 min at 37 °C, nonincorporated nucleotides were removed using the Concert™ Rapid PCR Purification System (Gibco BRL, Eggenstein, Germany). The labelled probe was boiled for 5 min at 95 °C for denaturation and then shortly cooled down on ice before being added to the hybridization buffer (see 2.7.3.).

OLB-buffer: mix solutions A : B : C as 10 : 25 : 30

Solution O: 1.25 M Tris/HCl, pH 8.0
0.125 M MgCl₂

Solution A: 1 ml solution O
18 μ l β -Mercaptoethanol
5 μ l 100 mM dCTP
5 μ l 100 mM dGTP
5 μ l 100 mM dTTP

Solution B: 2 M HEPES, pH 6.6 adjusted with NaOH

Solution C: 21.6 OD₂₆₀ units/ml Hexadeoxynucleotides (Amersham Pharmacia Biotech, Freiburg, Germany), dissolved in TE (10 mM Tris/HCl, pH 7.5; 1 mM EDTA)

2.7.3. Hybridization

A Northern blot of ca. 4×7 cm² was sealed into a plastic bag containing 13 ml of hybridization buffer and incubated in a shaking water bath at 65 °C for at least 45 min before the denatured radio-labelled probe (see 2.7.2.) was added. Hybridization was performed for at least 16 hours at 65 °C in a shaking water bath. After hybridization, the membrane was washed twice at 65 °C for 20 min in 2× SSC, 0.1 % SDS (low stringency wash) or once for 20 min in 2× SSC, 0.1 % SDS and once for 20 min in 0.5× SSC, 0.1 %

SDS (high stringency wash) at 65 °C to remove non-specifically bound DNA. Then the membrane was dried on 3MM paper, wrapped up in plastic foil and exposed in a phosphorimager cassette (Fuji BAS-1000; Raytest, Sprockhoevel, Germany) for a maximum of 72 hours. The image was analyzed with the computer program Tina 2.0 (Raytest, Sprockhoevel, Germany).

Hybridization buffer: 5× SSC, 5× Denhardt's, 0.5 % SDS

Stock solutions: 20× SSC: 3 M NaCl, 0.3 M sodium citrate, pH 7.0
50× Denhardt's: 1% (w/v) Ficoll 400
1% (w/v) PVP 40
1% (w/v) BSA

The hybridization buffer and stock solutions were stored at -20 °C

2.8. First strand cDNA synthesis (Reverse transcription)

For cDNA synthesis ca. 2-3 µg RNA and 500 pmol of 5'-specific primer or oligo(dT₂₀) primer (see 2.1.3.) were incubated for 5 min at 65 °C in a volume of 11 µl to denature the secondary structure of RNAs and to allow the primer to bind to the mRNA, and then placed on ice. For 5'-RACE, a gene specific primer was used on 20 µg total RNA.

Afterwards, the cDNA synthesis mix from ThermoScript™ RT-PCR System (Gibco BRL, Karlsruhe, Germany) was added:

4 µl 5× cDNA synthesis buffer
1 µl 100 mM DTT
2 µl dNTP-mix (10 mM each)
1 µl RNase OUT™ (RNase inhibitor)
1 µl ThermoScript RT

The reaction mixture was incubated for 1 hour at 55 °C and then the reaction was stopped by 5 min heating at 85 °C. cDNA was kept at -20 °C until use.

2.9. Amplification of DNA fragments

DNA sequences localized between two known sequences can be amplified using the polymerase chain reaction (PCR; Mullis and Faloona, 1987)

2.9.1. Polymerase chain reaction (PCR)

A typical program for PCR includes denaturing, annealing and elongation steps. Denaturation occurs at 94 °C, which separates both strands of the DNA. The following cooling to the annealing temperature, for example 55 °C, allows the hybridization of primers to single stranded DNA molecules. Then at 72 °C, the optimal temperature for *Taq* polymerase (from the thermophilic bacterium *Thermus aquaticus*), the primer is elongated, forming a double-stranded DNA molecule, identical to the original DNA. The multiple repetition of this cycle leads to the exponential amplification of the sequence between the primer binding sites.

For a standard PCR the following components were pipetted together:

5	μl	10× Buffer (500 mM KCl, 100 mM Tris-HCl pH 9.0)
1.5	μl	25 mM MgCl ₂
1	μl	dNTP-Mix (10 mM each)
1	μl	forward primer (100 pmol/μl)
1	μl	reverse primer (100 pmol/μl)
2-5	μl	DNA template
1	μl	<i>Taq</i> -polymerase (1 U) (Promega, Mannheim, Germany)
dd H ₂ O was adjusted to 50 μl		

The programmed DNA thermal cyclers MJ Research PTC™ 100 (Biozym, Hessisch Oldendorf, Germany) or TGradient (Biometra, Göttingen, Germany) were used with the standard program:

1.	94 °C	5 min	
2.	94 °C	1 min	} 25-35 cycles
3.	T _{Ann}	1 min	
4.	72 °C	n min (ca. 1 min per 1 kb product)	
5.	72 °C	10 min	
6.	4 °C	∞	

T_{Ann} is the annealing temperature of the primer pair used and it should be 2-3 °C lower than the melting temperature (T_m) of this primer pair (see 2.9.2.). After the reaction, 5 μl of the reaction mixture were analyzed on a TEA-agarose gel (see 2.6.1.).

2.9.2. Design of synthetic oligonucleotide primers

PCR primers should be composed of 18-30 nucleotides, with a GC content of 40-60 % and end on a G or C nucleotide. The primers used together in one PCR should have approximately the same melting temperature. This temperature can be calculated as follows:

$$T_m[^\circ\text{C}] = 69.3 + 0.41 \cdot [\% \text{ G/C}] - 650/n,$$

where n is the number of nucleotides in the primer. The primers should not be able to form any strong secondary structures in order to allow successful hybridisation with the complementary DNA sequence.

2.10. Rapid amplification of cDNA ends (RACE): 5'-RACE

The RACE (Frohman et al., 1988) is used to obtain full size cDNA sequences, when only a partial cDNA is available. To amplify the sequence between the known fragment and the 5'-end, a 5'-RACE is performed.

At first, a reverse transcription reaction is performed with a gene-specific primer derived from the known part of the sequence. This is followed by cDNA tailing with dATP or dCTP using terminal deoxynucleotidyl transferase. The homopolymeric tails of the cDNAs are used to bind an anchor primer (5'- CTC GAG GAT CCG CGG CCG CT₁₈ - 3' or 5'-GGC CAC GCG TCG ACT AGT ACG GGI IGG GII GGG IIG-3', respectively) in the following PCR, together with a second gene-specific primer that binds within the known sequence upstream of the primer used for reverse transcription. Here, ca. 20 µg total RNA were used for cDNA synthesis according to 2.8.

To remove unincorporated nucleotides after the RT reaction, the ConcertTM Rapid PCR Purification System (Gibco BRL, Eggenstein, Germany) was used. The cDNA was eluted from the column with 50 µl of 1× TdT buffer. The purified cDNA was used in the terminal deoxynucleotidyl transferase (TdT) reaction (Roychoudhury et al., 1976). The reaction mixture contained:

50 µl cDNA in 1× TdT buffer (Promega, Madison, WI, USA)
1 µl 5× TdT buffer
1,5 µl 1 mM dCTP
1 µl TdT (15 U/µl; Promega, Madison, WI, USA)
1,5 µl H₂O

The reaction was carried out at 37 °C for 30 min and then stopped by 5 min incubation at 70 °C.

The PCR reaction for amplification of the 5'-part of the cDNA could be conducted in two different ways. For one step PCR, the anchor primer (see above) was used together with the second gene specific primer. For two-step PCR, first the template was amplified in a reaction involving the anchor primer and the first gene-specific primer, and then a second reaction was performed with a primer hybridizing to the non-homopolymeric part of the anchor primer (MM4 or MM4 new, see 2.1.3.) and the second gene specific primer.

In each case, 5 µl of the TdT-reaction was used for the first PCR. The second PCR was based on 2 µl of the first PCR-mixture product.

2.11. DNA sequencing

DNA sequencing was based on the principle of Sanger et al. (1977), using a kit containing dideoxynucleotides labelled with dRhodamin („ABI PRISM dRhodamine Terminator Cycle Sequencing Ready Reaction Kit“; Perkin Elmer Applied Biosystems, Weiterstadt, Germany). The differently labelled ddNTPs have different absorption and emission spectra from 450 to 650 nm, so that each of the four nucleotide types could be detected individually on a sequencer. The following reaction mixture for the polymerase reaction was used:

2 µl	Terminator Ready Reaction Mix
200-300 ng	Plasmid DNA
5 pmol	Sequencing primer
ad 10 µl	dd H ₂ O

Mostly, vector specific primers were used as sequencing primers (T3, T7, *for* (M13 forward primer), *rev* (M13 reverse primer); see 2.1.3.). The polymerase reaction was conducted in the programmed Thermocycler PTC™ (Biozym, Hessisch Oldendorf, Germany) with the following program:

96°C 10 sec	} 25 cycles
50°C 5 sec	
60°C 4 min	

After the reaction, un-incorporated nucleotides were removed via an ethanol precipitation. 1 µl Na-acetate/EDTA buffer (1.5 M Na acetate; 250 mM EDTA, pH ≥ 8.0) and 36 µl of 99.6 % ethanol were added to the reaction mixture, mixed with a pipette and incubated for at least 45 min on ice. The precipitate was collected by centrifugation for 15 min at 13 000 rpm, washed in 100 µl of 70 % ethanol and centrifuged again for 10 min at 13 000 rpm. Afterwards the supernatant was discarded. The pellet was dried at 90 °C for 1 min, resuspended in 20 µl of Template Suppression Reagent (Perkin Elmer Applied Biosystems, Weiterstadt, Germany) and finally denatured at 95 °C for 2 min. The sample was sequenced automatically in an ABI Prism 310 Genetic Analyser (Perkin Elmer Life Sciences Ltd, UK).

Amino acid and nucleotide sequences of known cDNAs, proteins and vectors were obtained from GenBank at the National Center for Biotechnology Information (Altschul et al., 1990; <http://www.ncbi.nlm.nih.gov>). For the alignment of sequences, the Wisconsin Package program from Genetics Computer Group (GCG; Madison, WI, USA) was applied which was available through the Gesellschaft für wissenschaftliche Datenverarbeitung Göttingen (GWDG). The programs *seqed*, *map*, *bestfit*, *lineup*, *assemble*, *peptidesort* and *translate* were used.

The full length sequences of the *M. truncatula* and *D. glomerata* hexose transporter cDNAs were obtained from SEQLAB Sequence Laboratories Göttingen GmbH (Göttingen, Germany).

2.12. Cloning methods

2.12.1. Digestion with restriction enzymes

Restriction enzymes recognize sequences in double-stranded DNA and cut them corresponding to enzyme specificity, producing „blunt ends“, or cohesive („sticky“) ends of DNA with overhanging 5´- or 3´-ends. Reaction conditions were as recommended by the manufacturers. For characterization of plasmid DNA mini-preparation (see 2.4.1.) 5 U restriction enzyme were used per 1 µg DNA. For fragment isolation from clone vector or vector linearization 20 U enzyme per 10 µg DNA were used. Digestion was carried out for at least 1 hour at 37 °C.

2.12.2. Phosphatase treatment

To increase the probability of the insertion of a fragment into a plasmid during ligation, the digested plasmids were in some cases treated with alkaline phosphatase. This enzyme removes the phosphate residue on the 5´-end of a DNA double strand, and thus prevents vector religation. Afterwards only ligation with an insert carrying an intact 5´-phosphate group is possible. Phosphatase treatment can be very helpful when ligating (see 2.12.5.) vector and insert with “blunt” ends, which otherwise results in very low insertion efficiency.

After digestion (2.12.1) with a restriction enzyme, the reaction mixture was supplied with 0.1 volume of 10× dephosphorylation buffer and 1 µl of alkaline phosphatase (20 U/µl, stored at 4 °C; Roche Molecular Biochemicals, Mannheim, Germany). Then incubation followed at 37 °C for 30 min. Before ligation, the linearized plasmid was purified

from restriction enzyme and phosphatase by phenol-chloroform extraction (2.5.2.) and ethanol precipitation (2.5.1.).

10× dephosphorylation buffer:	Tris/HCl pH 8.5	0.5 M
	EDTA	1 mM

2.12.3. Filling-in of 5' overhanging ends with Klenow fragment

When a fragment had to be cloned, but no compatible restriction site was available in the vector, blunt-end cloning was performed. In this case, restriction enzymes producing either blunt or 5' overhanging ends were used, and for the latter, single-stranded DNA ends were filled-in using Klenow fragment (MBI Fermentas, Vilnius, Lithuania) to obtain blunt ends. A fill-in reaction contained:

10× Klenow buffer	4 µl (MBI Fermentas)
Klenow fragment 2 U/µl	1 µl (ca. 1 U per µg DNA)
10 mM dNTPs	4 µl
DNA	2 µg
dd H ₂ O	ad 40 µl

The reaction took place at 37 °C for no longer than 20 min to prevent that Klenow polymerase, after using up the free dNTPs, acted as 3'→5' exonuclease. The DNA fragment was purified from enzyme and nucleotides via an agarose gel using the QIAquick™ Gel Extraction Kit (see 2.12.4.).

2.12.4. Isolation of DNA fragments from agarose gels

After the digestion of DNA with restriction enzymes or after PCR, the fragments produced could be separated on an agarose gel (see 2.6.1.) with large slots holding up to 50 µl of reaction mixture. The DNA band of interest was excised with a scalpel under UV-light and then extracted from the gel using the QIAquick™ Gel Extraction Kit (Qiagen, Hilden, Germany). This kit is based on the selective binding of nucleic acids to kiesel gel particles at high salt concentrations. DNA was eluted with 25 µl dd H₂O, and the DNA concentration in the eluate was determined by running 1/10 volume on an agarose gel.

2.12.5. Ligation

Ligation is the formation of a phosphodiester bond between the 5'-end and 3'-end of one or two DNA molecules, catalyzed by DNA ligase. DNA ligase requires a free -OH group at the 3'-end of one DNA chain and a phosphate group at the 5'-end of the other. If either both fragments or open plasmid have "blunt" ends or if they have compatible cohesive ends, ligation is possible.

Ligations were conducted at 15 °C overnight in a volume of 10 µl, containing about 10 ng vector, 100 ng insert, 2 µl 5× ligation buffer (660 mM Tris/HCl, pH 7.6; 50 mM MgCl₂; 10 mM DTT; 10 mM ATP) and 1-5 units of T4-Ligase (Gibco BRL, Eggenstein, Germany).

PCR products were ligated into the cloning vector pGEM®-T Easy (Promega, Madison, WI, USA). This vector has 3' overhanging T-residues on both sides of the insertion site which makes it suitable for the cloning of PCR products because *Taq* and *Tth* polymerases leave overhanging A residues on the 3'-ends of amplified DNA fragments. In this case a ligation reaction contained:

0.5 µl pGEM®-T Easy Vector (50 ng/µl)
5.0 µl 2× Ligase buffer (Promega)
1.0 µl T4 DNA ligase (Promega)
3.5 µl PCR product

2× T4 DNA ligase buffer: 60 mM Tris/HCl pH 7.8
20 mM MgCl₂
20 mM DTT
2 mM ATP

Five µl of a ligation reaction were used for transformation of *E.coli* DH5α (see 2.13.2.), the rest of the reaction was kept for a few days at 4 °C in case that the transformation had to be repeated.

2.13. Transformation of *Escherichia coli*

2.13.1. Preparation of competent *E.coli* cells

To obtain optimal competent cells, the glassware used in the protocol had to be free of any detergents. For this purpose, glassware was first autoclaved filled with dd H₂O to remove traces of detergents, and then autoclaved again empty.

The preparation of competent *E.coli* cells (strain DH5α, see 2.1.2. for genotype) was conducted according to the method of Inoue et al. (1990) with some modifications. This

method produces competent cells with high transformation efficiency, which could be stored for a long time at $-80\text{ }^{\circ}\text{C}$.

Five ml SOC medium in a 50 ml Falcon tube were inoculated with DH5 α and incubated (shaking) overnight at $37\text{ }^{\circ}\text{C}$. Then the overnight culture was transferred into a 2 l Erlenmeyer flask containing 200 ml SOC medium and incubated further at $37\text{ }^{\circ}\text{C}$ up to an OD₆₀₀ of 0.2. Then the incubation proceeded at $18\text{ }^{\circ}\text{C}$ until an OD₆₀₀ of 0.3-0.4 was reached and the cells could be harvested. For this purpose the culture was divided into four Falcon tubes and centrifuged at 4 000 rpm in a Megafuge 1.0 (Heraeus Sepatech, Osterode, Germany) at $4\text{ }^{\circ}\text{C}$ for 10 min. Each of the bacterial pellets was resuspended on ice in 15 ml of cold transformation buffer, followed by incubation on ice for 15 min. Afterwards, the cell suspensions were collected into two Falcon tubes and centrifuged for 10 min at 4 000 rpm and $4\text{ }^{\circ}\text{C}$. Each pellet was resuspended in 10 ml of cold transformation buffer and supplied with 350 μl of DMSO under light shaking. After 5 min incubation on ice, 350 μl of DMSO were added again to the cell suspension under light shaking, followed again by 5 min incubation on ice. Then the competent cells were aliquoted into sterile Eppendorf tubes (200 μl per tube) and shock-frozen in liquid nitrogen. Competent cells were stored at $-80\text{ }^{\circ}\text{C}$.

Transformation buffer:	10 mM PIPES
	15 mM CaCl ₂
	250 mM KCl
	pH adjusted to 6.7 with KOH
	ad 55 mM MnCl ₂
	sterile filtration

2.13.2. Transformation of competent *E.coli* cells

To transform *E.coli* DH5 α , a 200 μl aliquot of competent cells was thawed on ice. Then 5 μl of ligation mixture (see 2.12.5.) or 0.5 - 1 μl of plasmid DNA was added to the competent cells, mixed by pipetting and incubated on ice for 20 min. After a 30 sec heat shock at $42\text{ }^{\circ}\text{C}$, the sample was transferred back on ice and 1 ml SOC medium (see 2.1.8.2.) was added. In SOC medium, the bacteria were incubated for 1 hour at $37\text{ }^{\circ}\text{C}$. Then, they were plated on two plates (200 and 1000 μl of culture, respectively) for selection on LB-agar with the appropriate antibiotics and incubated overnight at $37\text{ }^{\circ}\text{C}$.

2.13.3. Characterization of transformants

The appearance of antibiotic resistant colonies shows the success of the transformation. The presence of the insert in the vector has to be shown by plasmid isolation and restriction.

Some vectors (for example, pGEM[®]-T Easy (Promega, Madison, WI, USA) or pBluescript[®] II KS (+/-) (Stratagene, La Jolla, CA, USA)) allow a blue-white colony selection on LB-Amp-IPTG-X-Gal indicator plates (see 2.1.8.2. and 2.1.8.4.). These vectors contain a poly-linker in the coding region of *E.coli* gene *lacZ'*, encoding the α peptide of β -galactosidase, and part of the *lac* operon promoter. Bacteria containing a vector without insert are characterized by an intact *lacZ* gene. IPTG induces the expression of the *lac* promoter, i.e. of β -galactosidase, which metabolises the colourless X-Gal into a blue product, so colonies containing the empty vector can be recognised by their blue colour. Successful cloning of an insert in pGEM[®]-T Easy or pBluescript[®] II KS (+/-) interrupts the coding sequence of the β -galactosidase, and therefore, recombinant clones can usually be identified by their white colour on IPTG/X-Gal containing plates. In some cases, however, blue colonies can result from inserts that are cloned in-frame with the *lacZ* gene.

For plasmid characterization, plasmid DNA has to be isolated (see 2.4.1.) from selected clones followed by digestion with (an) appropriate restriction enzyme(s) (see 2.12.1.). This reveals the presence and the size of insert after electrophoretic separation of the digested DNA on an agarose gel.

If white-blue selection of clones is not possible, a PCR (see 2.9.1.) can be applied for the identification of positive (insert-containing) colonies: the so-called "colony PCR". At the same time, colony PCR can be used to determine the orientation of the insert in the vector (sense or antisense), using an insert-specific and vector-specific primer. For this purpose, single growing bacterial colonies were picked with a toothpick and each was first used to inoculate 10 μ l dd H₂O in 0.5 ml Eppendorf tubes, and then 4 ml LB medium with the appropriate antibiotic. For a screening 20-40 colonies were picked. LB cultures were incubated overnight at 37 °C with shaking. The Eppendorf tubes containing dd H₂O with bacteria were used for colony PCR. Insert- or vector-specific primers were used.

After the PCR program was finished the products could be electrophoretically separated on an agarose gel (see 2.6.1.) to choose a clone with an insert of the expected size/orientation for mini-preparation of plasmid DNA (see 2.4.1.).

Colony PCR reaction mixture:

2.5 μ l 10 \times *Taq*-buffer
 1.5 μ l 25 mM MgCl₂
 0.5 μ l 10 mM dNTP
 0.5 μ l 3'-primer
 0.5 μ l 5'-primer
 0.5 μ l *Taq* polymerase
 10 μ l template (dd H₂O
 inoculated with bacteria)
 ad 25 μ l H₂O

PCR program:

94 °C 5 min (lysis of bacteria)
 94 °C 30 sec
 T_{Ann} 30 sec
 72 °C 1 min/1kb product } 30 cycles
 72 °C 10 min

2.14. Yeast transformation

The yeast strain *Saccharomyces cerevisiae* EBY.VW.4000 (Wieczorke et al., 1999; see 2.1.2. for genotype) was used to investigate *in vivo* transport activity of plant hexose transporters. Yeast transformation was carried out corresponding to the protocol of Sauer and Stolz (2000).

Cells were grown overnight in 25 ml of complete medium YPM (see 2.1.8.3.) on a rotary shaker at 29 °C. Then the OD₆₀₀ of the cells was determined and they were diluted into 50 ml of pre-warmed (29 °C) YPM to a final OD₆₀₀ of 0.5. Afterwards, cells were grown to an OD₆₀₀ of 2.0 and harvested by centrifugation at 3 000 \times g for 3 min. The medium was discarded, and cells were resuspended in 25 ml ddH₂O and centrifuged again. After the supernatant had been discarded, cells were resuspended in 1 ml of 100 mM lithium acetate and transferred to a 1.5 ml microcentrifuge tube. The cells were pelleted at top speed for 15 sec. The supernatant was removed with a pipette. Finally, cells were resuspended in 0.5 ml of 100 mM lithium acetate and divided into 10 portions of 50 μ l each, yielding 10 samples for 10 transformations. The cells were pelleted for 15 sec and, after the supernatant had been removed with a pipette, to each tube was added in the given order:

240 μ l 50 % (w/v) PEG
 36 μ l 1 M lithium acetate
 25 μ l carrier DNA (see below)
 50 μ l dd H₂O with 1-5 μ g of plasmid DNA

Each tube was vortexed vigorously to resuspend the cells and then incubated first at 30 °C for 30 min, and then at 42 °C for 20 min. After centrifugation for 60 sec at 5 000 \times g, the supernatant was removed with a pipette and the pellet was resuspended in 1 ml of dd H₂O by pipetting up and down. Aliquots of 2-200 μ l were plated on selection medium (CAA for NEV-constructs; see 2.1.8.3.), and plates were incubated at 29 °C for 2-4 days.

Carrier DNA: High molecular weight DNA from salmon testes was added to TE buffer (10 mM Tris/HCl pH 8.0, 1 mM EDTA) to a final concentration of 2 mg/ml and dispersed by repeated pipetting and vigorous stirring on a magnetic stirrer. Stirring was stopped when the viscosity of the solution had decreased. Aliquots were stored at – 20 °C and heat-denatured by boiling at 100 °C for 5 min prior to use, followed by quick chilling on ice.

2.15. Bacterial and yeast glycerol cultures

Original strains of *E. coli*, *S. meliloti* or *S. cerevisiae*, or strains containing characterized plasmids were grown overnight in 5–20 ml of full medium supplemented with the appropriate antibiotic(s) (for bacterial strains) at the appropriate temperature (37°C for *E. coli*, 28-30 °C for yeast). 200 µl of 87% glycerol were pipetted into plastic tubes with screw tops and autoclaved. 800 µl of bacterial or yeast culture were added, vortexed, shock-frozen in liquid nitrogen and stored at –80 °C.

2.16. Extraction of sugars

2.16.1. Chloroform-methanol extraction

To isolate water-soluble sugars from roots and nodules, chloroform-methanol extraction was used. Nodules or roots were frozen in liquid nitrogen, stored at –80 °C and ground to a fine powder in liquid nitrogen using mortar and pestle. About 300 mg of powder were put in a pre-cooled 10 ml plastic tube on ice containing 5 ml of a chloroform/methanol mixture (1.5 : 3.5 v/v), mixed shortly and incubated on ice for 30 min. Then 3 ml of dd H₂O were added to the homogenate, and the sample was mixed vigorously for 2 min. The separation of two phases (the upper water/methanol phase and the lower chloroform phase) was achieved by centrifugation of the samples at 5000 rpm for 5 min in a Hettich EBA 3 S centrifuge (Hettich, Tuttlingen, Germany). The upper (aqueous) phase was saved in a round-bottom evaporation glass and the rest was extracted once again with 3 ml of water. The aqueous phases were combined and dried completely in a rotary evaporator at 37 °C. The dried residues were dissolved in 1.5 ml ultra pure H₂O (Millipore), filtered through a syringe with a cellulose-nitrate membrane filter (0.45 µm; Schleicher and Schuell, Dassel, Germany) and stored at –80 °C.

2.16.2. Preparative isolation of unknown sugars / sugar derivates from *Datisca*

Analysis of the sugars from *Datisca glomerata* roots and nodules showed these organs contained high concentrations of an unknown sugar derivate (up to 6 and 13.5 $\mu\text{mol/g}$ FW in roots and nodules, respectively, when calculated on the basis of molecular weight of ribitol, a sugar with the nearest retention time to the unknown HPLC peak). This unknown metabolite ("D") was isolated for the analysis of its chemical structure by NMR, conducted at the Institute for Organic Chemistry, University of Göttingen.

The method of Pharr *et al.* (1987) was used with some modifications. 150 g of *D. glomerata* were ground to a powder in liquid nitrogen and extracted in 1.5 l of a chloroform/methanol mixture on ice for 30 min (see 2.16.1.). Then, 900 ml dd H₂O were added and phases were separated by centrifugation for at least 20 min at 11 600 \times g (Sorvall DuPont, Dreieich, Germany; rotor GS3). The upper (aqueous) phase containing the water-soluble metabolites was saved. The rest was extracted once again with 900 ml dd H₂O. The upper phases from both centrifugation steps were combined and the volume was reduced to 100 ml in a rotary evaporator at 37 °C. Then, cations were removed from the extract by adding 20 g of a cation exchanger Dowex® 50W \times 8 (200-400 mesh, in H⁺-form) (Serva Electrophoresis, Heidelberg, Germany) and stirring for 30 min. The extract was filtered through a paper to remove Dowex particles, and the procedure was repeated with 1/10 volume of Polyclar® AT (Serva) to remove polyphenols and polysaccharides. Polyclar® AT was pelleted by 10 min centrifugation in a Megafuge 1.0 (Heraeus Sepatech, Osterode, Germany). The volume of the supernatant was reduced to 10 ml in a rotary evaporator at 37 °C and the concentrate was applied to an anion exchange column of 50 cm length and 2.8 cm diameter filled with Dowex® 1 \times 8 (100-200 mesh, OH⁻-form). Passing the extract through the column allowed to remove anions and at the same time provided a separation of the extract into fractions with different sugar composition. The elution was done with 0.2 M NaOH at a rate of 2.5 ml/min. 200 fractions of 5 ml per fraction were collected. Sugar composition of the fractions was determined by HPLC (see 2.17.). "D" eluted after about 2 hours and was found in the fractions No. 59 to 70. No other sugars were detectable in these fractions. The "D"-containing fractions were combined and neutralized using 5 M HCl. This step was necessary because the presence of 0.2 M NaOH in the eluate might lead to the condensation (caramelisation) of sugars under alkaline conditions during the following concentration of the combined fractions. Then, the volume of the combined fractions was reduced to 10 ml in the rotary evaporator at 37°C. In this step a very high concentration of NaCl (up to 2M) was achieved which could disturb the following sugar analysis. Therefore, NaCl and "D" were separated by descendent paper chromatography. Two pieces of 18 cm x 45 cm chromatography paper

Whatman Chr 17 were used. The running solution was n-propanol : ethyl acetate : H₂O = 7 : 1 : 2 (v/v). For the detection of the isolated sugars, thin strips were cut off and developed in detection solution (2.5 ml of a saturated AgNO₃ solution in 500 ml acetone) for 2.5 min. The strips were then transferred to the stop solution (10 g NaOH in 15 ml H₂O added to 500 ml of 96% ethanol). NaCl moved along the chromatogram faster than "D". The part of the chromatogram containing "D" was cut into pieces and "D" was eluted with 200 ml dd H₂O in an ultrasonication bath for 20 min (Branson Sonifier B 15, Branson Ultrasonics Corp., Geneva, Switzerland). The elution was repeated three times. The eluates (600 ml in total) were combined and the volume was reduced in a rotary evaporator at 37 °C to concentrate "D". Then, the end concentration of "D" was determined by HPLC (see 2.17.). A 1 ml aliquot of this solution was dried in a Speed Vac concentrator and used for analysis of the chemical structure by NMR at the Institute for Organic Chemistry at the University of Göttingen.

Analysis of the sugar contents of *Datisca glomerata* roots and nodules revealed also a high concentration of another sugar related compound with a HPLC retention time close to that of myo-inositol, called "M". Its preparative isolation was carried out simultaneously with the isolation of "D" (described above) from the same extract. "M" was detected in fractions No. 30 to 50. No other sugars were detectable in these fractions. Isolation proceeded as described above. Aliquots of M were also dried in a Speed Vac Concentrator (Bachofer, Reutlingen, Germany) and used for the analysis of its chemical structure by nuclear magnetic resonance spectroscopy (NMR) and mass spectroscopy, and the NMR correlation spectroscopy methods H,H-COSY and C,H-COSY by Dr. R. Fortte at the Institute for Organic Chemistry at the University of Göttingen (in laboratory of Prof. Tietze).

2.16.3. Ethanol extraction

About 300 mg root material was frozen in liquid nitrogen and then transferred into 8 ml scintillation tubes with 2 ml 10 mM HEPES buffer in 80 % ethanol (pH 7.0) prewarmed to 80 °C, and incubated in a shaking water bath at 80 °C for 30 min. Then the supernatant was transferred to a round-bottom evaporation glass and the rest was extracted again with 1 ml 10 mM HEPES buffer in 70 % ethanol (pH 7.0). The supernatant was combined with the extract in a round-bottom evaporation glass, and the pellet was extracted again with 1 ml 10 mM HEPES buffer in 50 % ethanol (pH 7.0) for 30 min in a shaking water bath at 80 °C. All supernatants were combined in the evaporation glass and dried completely in a rotary evaporator at 37 °C. The dried residues were dissolved in 2 ml ultra

pure H₂O (Millipore), filtered through a syringe with a cellulose-nitrate membrane filter (0.45 µm; Schleicher and Schuell) and stored at –80 °C.

2.16.4. Perchlorate extraction

About 300 mg root material was frozen in liquid nitrogen, stored at –80 °C and ground to a fine powder in liquid nitrogen using mortar and pestle. After the liquid nitrogen was evaporated, 1 ml perchloric acid solution (10 % HClO₄, 5 mM EGTA) was added to the powder and ground further without cooling. After the sample had melted, it was transferred into an Eppendorf tube using a pipette with a cut-off tip and centrifuged for 3 min at 13 krpm. The supernatant was transferred into new 2 ml Eppendorf tubes, neutralized to pH 7.0-7.5 using potassium hydroxide-triethanolamine solution (5M KOH, 1M TEA) and incubated for 15 min on ice. Then precipitated KClO₄ was spun down by 10 min centrifugation at 13 krpm, and the supernatant was saved in a new Eppendorf tube and stored at -80 °C.

2.16.5. Acetone extraction

Roots were frozen in liquid nitrogen, stored at –80 °C and ground to a fine powder in liquid nitrogen using mortar and pestle. About 650 mg of powder were put in a pre-cooled 10 ml plastic tube on ice containing 5 ml of 90 % acetone. Sugars were extracted overnight by shaking at 4 °C. Afterwards, the sample was centrifuged at 4300 rpm in a Megafuge 1.0 (Heraeus Sepatech, Osterode, Germany) at 4 °C for 10 min. The supernatant was transferred to a round-bottom evaporation glass and dried completely in a rotary evaporator at 37 °C. The dried residues were dissolved in 1.5 ml ultra pure H₂O (Millipore), filtered through a syringe with a cellulose-nitrate membrane filter (0.45 µm; Schleicher and Schuell) and stored at –80 °C.

2.17. Sugar analysis by high-performance liquid chromatography (HPLC)

Sugars in root and nodule extracts were assayed by HPLC using pulse amperometrical detection. The sugars were separated over an anion exchange column MA1 (CarboPAC10; Dionex Corp, Sunnyvale, CA, USA) with a pre-column (CarboPAC10 Guard; Dionex Corp), which allowed a better resolution of polyols and cyclitols, and eluted with 600 mM NaOH using a LC-9A pump from Shimadzu (Kyoto, Japan) with a flow rate of

0.4 ml min⁻¹. Sodium hydroxide solution was prepared using Millipore water purified with helium for 15 min to prevent the formation of NaHCO₃. NaOH (50 %) of the purest commercially available quality was used (Malinckrodt Baker B.V., Deventer, The Netherlands) in order to obtain a stable baseline.

The autosampler (# 2157, LKB Pharmacia, Gräfelfing, Germany) was thermostated at 12 °C. Sugars were detected by a thin layer amperometric cell (ESA, Model 5200, Chelmsford, MA, USA) with a gold electrode. A Pulse Amperometric Detector (Coulchem II, ESA, Chelmsford, MA, USA) was set according to the following scheme:

pulse mode	voltage	duration	Measure
Measurement	50 mV	500 ms	400 ms
Clearance	700 mV	540 ms	
Regeneration	-800 mV	540 ms	

The calibration was done with sugar concentrations of 50 µM, 100 µM, 250 µM and 500 µM. Myo-inositol, sorbitol, ribitol, mannitol, glucose, fructose, ribose, sucrose, raffinose, verbascose and stachyose were used as standards and showed a linear range of the detector response between 50 and 500 µM ($r^2 = 0.99$). Sugar hydrolysis products were compared with another calibrated standard, containing *myo*-inositol, arabitol, xylitol, fucose, ribose, galactose, glucose, fructose and rhamnose. Plant samples were diluted before measurements to provide concentrations within the linear range. The evaluation of chromatograms was performed with the integrated program Peaknet 5.1 (Dionex, Idstein, Germany).

2.18. Sugar analysis

To identify the unknown saccharides isolated from *Datisca glomerata* and termed "M" and "D" (see 2.16.2), the identity of the sugar residues and the conformation of the bonds had to be determined. For this purpose, M and D were hydrolyzed using both hydrochloric acid and with different glycosidases.

2.18.1. Acid hydrolysis

For hydrolysis of D and M by hydrochloric acid, each saccharide was boiled for 1 hour in 1 M HCl in the total volume of 50 µl with a substrate concentration of about 0.5-1 mM. In preparation for HPLC analysis, the sample was twice vacuum evaporated and then dissolved in 50 µl dd H₂O. For HPLC analysis the sample was diluted 1:2.

2.18.2. Enzymatic hydrolysis

To determine whether the isolated saccharides represented α -galactosylated compounds, an α -galactosidase reaction was performed in 30 mM sodium citrate buffer (pH 4.6) with a substrate concentration in a range of 0.5-1 mM. The reaction volume was 50 μ l, and the reaction was started by adding 1 μ l α -galactosidase from green coffee bean (0.05 U/ μ l; Sigma). The reaction was stopped after 5, 10 and 20 min, respectively, by boiling for 3 min. The samples were centrifuged for 5 min at 13 000 rpm, and the supernatants were diluted 1:2 for HPLC analysis (see 2.17.).

To determine whether the isolated saccharides contained glucose at the non-reducing end, they were treated with α - and β -glucosidases, which hydrolyze terminal non-reducing α - and β -D-glucose residues, respectively. The reactions were performed in acetate buffer (71 mmol/l; EDTA 0.96 mmol/l) with pH 6.0 for the α -glucosidase reaction and 5.0 for the β -glucosidase reaction. The acetate buffer stock solution (0.1 M; EDTA 1.35 mM) was prepared the following way: 0.57 ml acetic acid (96 %) were added to 80 ml of dd H₂O, then 50 mg EDTA disodium salt monohydrate was dissolved in this solution, the pH was adjusted to 6.0 with 1 N sodium hydroxide and the final volume was adjusted to 100 ml with dd H₂O. The reaction was performed in a volume of 50 μ l with a substrate concentration in the range of 0.5-1 mM and was started by adding either 1 μ l α -glucosidase from *Saccharomyces* sp. (0.05 U/ μ l; ICN, Irvine, CA, USA) or β -glucosidase from almonds (0.05 U/ μ l; Sigma). In each case, the reaction was stopped after 5, 10 and 20 min, respectively, by boiling for 3 min. The samples were centrifuged for 5 min at 13 krpm, and the supernatants were diluted 1:2 for HPLC analysis (see 2.17.).

To prove the bond configuration between rhamnose and glucose in the isolated sugars, as well as the position of rhamnose at the non-reducing end, they were hydrolyzed with naringinase (α -rhamnosidase) from *Penicillium decumbens* (0.05 U/ μ l; Sigma). The reaction was conducted in 50 μ l of 0.1 M sodium acetate buffer (pH 4) with a substrate concentration in the range of 0.5-1 mM at 40 °C, and started by adding 1 μ l enzyme. The reaction was stopped after 5, 10 and 20 min, respectively, by boiling for 3 min. The samples were centrifuged for 5 min at 13 000 rpm, and the supernatants were diluted 1:2 for HPLC analysis (see 2.17.).

2.19. Sucrose synthase extraction and assay

2.19.1. Extraction of sucrose synthase (SuSy)

The procedure was based on the method described by Winter *et al.* (1998). Plant tissue was ground to a fine powder in a mortar under liquid nitrogen and homogenized with 4 ml/g plant material extraction buffer A (100 mM MOPS, pH 7.5; 10 mM MgCl₂; 0.5 mM CaCl₂; 1 mM EDTA; 2 mM DTT; 20 mM NaF; 1 mM PMSF; 100 mM sucrose). The homogenate was filtered through four layers of Miracloth (Schütt Labortechnik GmbH, Göttingen, Germany) and centrifuged at 100 000 × g for 1 h at 4 °C. The supernatant was desalted by centrifugal filtration on Sephadex-G25 (PD 10 desalting columns; Amersham Pharmacia Biotech, Freiburg, Germany), equilibrated with desalting buffer B (50 mM MOPS, pH 7.5), and concentrated in Fugisep Maxi®-30 concentrators (Intersep, Witten, Germany) for 1 h at 4 °C. Afterwards SuSy activity was assayed immediately. The protein concentration was determined according to Bradford (1976; see 2.23.).

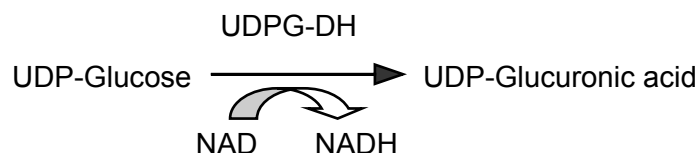
2.19.2. Sucrose synthase activity assay

For the sucrose synthase assay, the following reaction mixture was prepared in a microcentrifuge tube and kept for a few minutes at the room temperature:

60 µl	Buffer B (50 mM MOPS, pH 7.5)
30 µl	8 mM UDP in buffer B
30 µl	14 mM MgCl ₂ , 0.3 mM CaCl ₂
30 µl	0.8 M sucrose in buffer B

The reaction was started by adding 100 µl extract, incubated for 10 min at 30 °C and stopped by boiling for 10 min. Then, denatured protein was spun down by centrifuging for 10 min at 4 °C, and the supernatant was transferred into a new microcentrifuge tube.

Sucrose synthase is a glycosyltransferase, converting sucrose into UDP-glucose and fructose in the presence of UDP. The sucrose synthase activity was analysed via determination of the UDP-glucose concentration in the following assay:



For the spectrophotometric assay of UDP-glucose, 900 μl of assay buffer (200 mM glycine, pH 8.9; 5 mM MgCl_2), 20 μl 0.1 M NAD^+ and 100 μl of sample were mixed in a cuvette. The reaction was started by adding 10 mU UDP-Glucose-Dehydrogenase (Sigma). The measurements were conducted on a two wavelength spectrophotometer (Sigma ZFP 22; Sigma instrumente GmbH, Berlin, Germany). The activity was calculated as the increase in absorbance due to the formation of NADPH using a molar extinction coefficient for NADPH of $6.18 \text{ mmol}^{-1}\text{cm}^{-1}$ at 334 nm.

2.20. Invertase extraction and assay

2.20.1. Extraction of invertase

Plant tissue was ground to a fine powder in liquid nitrogen and homogenized with homogenization buffer (2 ml/g fresh weight (FW) tissue). PVPP (200 mg/g FW) was added to *D. glomerata* and *C. glauca* powder to bind polyphenols and polysaccharides. The homogenate was centrifuged at $6000 \times g$ for 10 min at 4 °C. The supernatant (cytosolic and vacuolar fraction) represented the soluble enzyme preparation. The pellet (cell-wall fraction) was washed three times with dd H_2O at 4 °C and finally resuspended again in dd H_2O . Both enzyme preparations were dialyzed against 12.5 mM K-Phosphate buffer (pH 7.4 adjusted with KH_2PO_4) for 45 min twice and then overnight at 4 °C. Afterwards the probes were collected into Eppendorf tubes and assayed for invertase activity (see 2.20.2.) or stored at -80 °C before analysis.

Homogenisation buffer:

	for 40 ml:
200 mM HEPES/NaOH, pH 7.5	16 ml 0.5 M stock
3 mM DTT	240 μl 0.5 M stock
3 mM MgCl_2	120 μl 1 M stock
1 mM EDTA	80 μl 0.5 M stock
2 % glycerol	920 μl 87 % stock

10 ml aliquots of the homogenization buffer were kept at -20 °C. PMSF (Merck, Darmstadt, Germany), dissolved in ethanol, and benzamidine (Sigma-Aldrich, Taufkirchen, Germany), dissolved in dd H_2O , were added to the homogenisation buffer to the final concentrations of 0.1 mM and 1 mM, respectively, directly before use.

2.20.2. Invertase activity assay

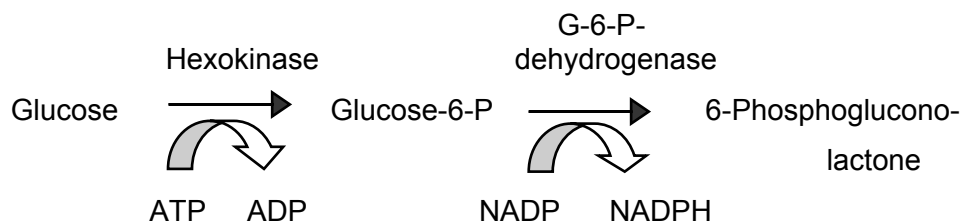
Invertase activity was tested according to the method described by Sung et al. (1989) with some modifications. Invertase is a hydrolase, cleaving sucrose irreversibly into glucose and fructose. For the assay, 30 μ l of 1 M sucrose stock solution were mixed with 470 μ l of reaction buffer in an Eppendorf tube. K_2HPO_4 /citric acid buffers were used for the different enzymes (pH 4.35 for apoplasmic invertase, pH 5.0 for vacuolar invertase, pH 6.8 for cytosolic invertase). 100 μ l extract (cytosolic or vacuolar invertase) or cell wall suspension (apoplasmic invertase) was added to start the reaction. The reaction mixture was incubated for 30 min at 26 °C, then put on ice and immediately analysed for glucose concentration (see below).

Reaction buffer type 40/70 for apoplasmic invertase	40 mM citric acid 70 mM K_2HPO_4 adjusted to pH 4.35
--	--

Reaction buffer type 40/70 for vacuolar invertase	40 mM citric acid 70 mM K_2HPO_4 adjusted to pH 5.0
--	---

Reaction buffer type 20/160 for cytosolic invertase	20 mM citric acid 160 mM K_2HPO_4 adjusted to pH 6.8
--	--

To determine the glucose concentration in the invertase reaction mixture the following combined assay was used:



For each glucose determination, the following solutions were mixed in a cuvette: 475 μ l of reaction buffer for glucose determination (100 mM HEPES, pH 7.2; 5 mM $MgCl_2$), 25 μ l of mastermix (400 μ l 100 mM ATP; 400 μ l 30 mM $NADP^+$; 35 U of G-6-PDH in 200 μ l reaction buffer) and 100 μ l invertase assay mixture. The reaction was started by adding 2 U of hexokinase.

The concentration of NADPH formed was detected photometrically on a double-beam photometer Uvikon 932 (Kontron, Milan, Italy). The glucose concentration was calculated as the increase in absorbance due to the equivalent formation of NADPH using a molar extinction coefficient for NADPH of $6.22 \text{ mmol}^{-1}\text{cm}^{-1}$ at 340 nm. The reaction was considered complete when there was no more increase of the OD_{340} .

The amount of glucose formed in the invertase reaction is equivalent to the amount of sucrose cleaved in this reaction. Therefore, results of invertase activity assay are presented as nmol sucrose cleaved per milligram protein per minute. Protein content in extracts was determined according to the method of Bradford (1976, see 2.23.). BSA was used for the calibration curve.

2.21. *In situ* glucose and acid (apoplastic) invertase activity staining

Glucose can be detected via the formation of a coloured reaction product by glucose oxidase and peroxidase in the presence of diaminobenzidine (DAB). About 200 μm thick tissue slices were hand cut. For glucose staining the slices were denatured at 65 °C in dd H_2O for 3 -10 min and transferred to reaction medium. To stain the sites of invertase activity the slices were washed extensively in dd H_2O to remove endogenous glucose and then transferred into reaction medium, supplied with 100 mM sucrose. The reaction was carried out for 3 - 4 hours at 37 °C (or overnight at room temperature).

After the incubation, the slices were washed with dd H_2O and then photographed under a microscope. Brown precipitate indicates the presence of glucose or acid (apoplastic) invertase activity, respectively.

<u>Reaction medium:</u>	200 mM	Tris/citrate pH adjusted to 6.0 with a citric acid
	20 $\mu\text{g}/\text{ml}$	glucose oxidase (Sigma Chemical, St. Louis, MO, USA)
	250 $\mu\text{g}/\text{ml}$	horseradish peroxidase (Sigma)
	300 $\mu\text{g}/\text{ml}$	diaminobenzidine (DAB) (Sigma)

2.22. Total protein isolation from plant material

Plant tissue (50 -100 mg) was ground to a fine powder in a mortar under liquid nitrogen, transferred into a 1.5 ml Eppendorf tube and immediately supplied with 200 μl extraction buffer (see below). An identical volume of TE-saturated phenol was added to the sample, vortexed and incubated on ice for at least 5 minutes. For phase separation, the

homogenate was centrifuged for 10 min at $10\,000 \times g$ at $4\text{ }^{\circ}\text{C}$. The phenol phase (upper phase) was transferred into a new Eppendorf tube. Protein precipitation was achieved by adding five volumes of 100 mM ammonium acetate (w/v) in methanol and incubating for 16 h at $-20\text{ }^{\circ}\text{C}$. After a centrifugation step at $10\,000 \times g$ for 10 min at $4\text{ }^{\circ}\text{C}$ the supernatant was discarded and the pellet was washed with 80 % acetone (v/v) and dried under vacuum in a Speed Vac Concentrator (Bachofar, Reutlingen, Germany). The pellet was dissolved in a small volume (20-50 μl , depending on protein quantity) of denaturing buffer and incubated for 1 min at $100\text{ }^{\circ}\text{C}$. Then protein concentration of the sample was determined according to Bradford (see 2.23.). Protein samples were stored at $-20\text{ }^{\circ}\text{C}$.

Extraction buffer	700 mM	sucrose
	500 mM	Tris-HCl
	100 mM	KCl
	50 mM	EDTA
	pH 9.5	
	2 % (v/v)	β -mercaptoethanol, freshly added
Denaturing buffer	10 mM	Tris-HCl
	2 % (w/v)	SDS
	pH 9.5	
	2 % (v/v)	β -mercaptoethanol, freshly added

2.23. Bradford protein concentration determination

The Bradford test (Bradford, 1976) is a colorimetric method to quantify the protein content of solutions. The amount of Coomassie Brilliant Blue G 250 (Serva, Heidelberg, Germany) binding to protein is determined. The staining develops within 5 -10 min. Then the protein complex is stable for about 30 min. By comparison with a calibration curve obtained with a standard protein (fatless BSA), the protein concentration in a sample can be estimated. Every experiment requires a new calibration curve.

5 μl of the sample was filled up with dd H_2O to a total volume of 500 μl . Then 500 μl staining solution was added to the sample, mixed and incubated for 10 min at room temperature. The OD_{595} was measured in a spectrophotometer (Uvikon 932; Kontron, Milan, Italy). As a reference, 5 μl of sample buffer was taken and prepared as described for the protein sample.

Staining solution: 70 mg/50 ml abs. EtOH Coomassie Brilliant Blue G-250

600 ml H₂O

100 ml 85% H₃PO₄

volume was adjusted to 1000 ml with dd H₂O

and the solution was filtered through 3MM paper

2.24. Sodiumdodecyl sulfate polyacrylamide gel electrophoresis (SDS-PAGE)

The SDS-PAGE method is based on the method of Laemmli (1970). SDS is an anionic detergent that has two effects on proteins: first, it leads to disbanding of oligomeric structures, resulting in a relaxed conformation and, second, it binds in excess in a constant relation (1.4 g SDS/1 g protein) to the protein, which leads to an equal negative charge per mass unit. Therefore, in the presence of SDS, proteins can be separated based on their molecular weight.

The negatively charged SDS-protein complexes run towards the anode in an electrical field. To separate these complexes, the molecular-sieve properties of polyacrylamide gel (PAA-Gel) are used, where the mobility of most proteins is reversely proportional to the decimal logarithm of their molecular weight. The discontinuous buffer system of Laemmli (1970) leads to the concentration of probes on the transition state between a stacking gel and a separation gel, resulting in a higher resolution of the following separation of proteins. To determine the molecular weight of unknown proteins, a marker containing some proteins with molecular weights of 14-97 kDa („Low Molecular Weight Calibration Kit“; Amersham Pharmacia, Freiburg, Germany) or 9 to 185 kDa (“Bench Mark™ Prestained Protein Ladder”, Invitrogen, Groningen, Netherlands) was loaded on the same gel. The pore size of a PAA-gel depends on relation between the concentrations of acrylamide to cross-linking N-N'-methylenbisacrylamide. The acrylamide quota and the cross-linking degree are the values that characterize a polyacrylamide gel. To separate total protein extracts and detect sucrose synthase (SuSy), consisting of 92- to 93-kDa subunits (Hohnjec et al., 1999), a PAA-gel containing 6 or 7.5 % polyacrylamide in the separating gel and 4 % acrylamide in the stacking gel were prepared. The separating range was 60 to 200 kDa in 6 % and 40 to 200 kDa in 7.5 % PAA-gel. Gel plates, spacer and combs as well as gel camera were ordered from Biometra (Göttingen, Germany).

2.24.1. Buffers and solutions for analytic SDS-PAGE

Acrylamide / Bisacrylamide (30 % T/2.7 % C) stock solution (30%)	29.2 % (w/v) acrylamide 0.8 % (w/v) N,N'-methylene bisacrylamide
	Dissolve in 100 ml dd H ₂ O and filter through 3 MM paper Store at 4-10 °C
4 × Stacking gel buffer	500 mM Tris-HCl pH 6.8 0.4 % (w/v) SDS
4 × Separating gel buffer	1.5 M Tris-HCl pH 8.8 0.4 % (w/v) SDS
10 % Ammonium persulfate	10 % (w/v) Ammonium persulfate (in dd H ₂ O) (APS) solution stored at 10 °C
10 × SDS Electrophoresis buffer	250 mM Tris 1.92 M Glycine 1 % (w/v) SDS pH 8.2-8.4 (not adjusted)
5 × Sample buffer	60 mM Tris-HCl (pH 6.8) 2 % (v/v) β-Mercaptoethanol 25 % (v/v) Glycerol 2 % (w/v) SDS 0.1 % (v/v) Bromphenol blue

2.24.2. Pouring the SDS-Polyacrylamide gel

Glass gel plates were cleaned with acetone or ethanol, silicon spacer tubes and combs were cleaned with water. The glass plates were joined together to form the cassette and clamped in vertical position. Solutions for stacking and separating gel were mixed as described in the table below. To start the polymerisation, TEMED (N,N,N',N'-Tetramethylene diamine) solution was added to the separating gel solution. The gel solution was mixed and poured into the gel chamber up to 1 cm under the ends of the

comb slots. To ensure that the gel polymerized with a smooth surface, a 2 mm layer of dd H₂O was carefully poured on the gel using a Pasteur pipette. Because of the great difference in density between dd H₂O and the gel solution, the water is spread across the surface of the gel without much mixing. When the gel was set, a clear refractive index change could be seen between the polymerised gel and the overlaying water. Then the overlaying water was poured off and TEMED was added to the stacking gel solution to start polymerisation. The stacking gel was poured into the gel cassette until the solution reached the upper edge and the slot-forming comb was put into the solution before leaving the gel to set. 30 min to 1 hour later, the comb was removed from the gel, and the gel slots were rinsed with electrophoresis buffer to remove any rests of non-polymerised acrylamide solution.

The data of the following table are based on the stock solutions and buffers given in 2.24.1. The volume is sufficient for two mini gels (8.5 cm × 7.5 cm).

Separating gel, 7.5 % (15 ml):	Acrylamide stock solution (30 %)	3.750 ml
	4 × Separating gel buffer	3.750 ml
	dd H ₂ O	7.410 ml
	10 % APS solution	75 µl
	TEMED (add before pouring the gel)	15 µl
Stacking gel, 4 % (5 ml):	Acrylamide stock solution (30 %)	0.670 ml
	4 × Stacking gel buffer	1.250 ml
	dd H ₂ O	3.050 ml
	10 % APS solution	30 µl
	TEMED (add before pouring the gel)	5 µl

The resulting end concentrations were:

	Stacking gel	Separating gel
Tris/HCl pH 6.8	0.13 M	-
Tris/HCl pH 8.8	-	0.38 M
SDS	0.1 % (w/v)	0.1 % (w/v)
Acrylamide	4.6 % (w/v)	7.5 % (w/v)
N,N-Methylene bisacrylamide	0.12 % (w/v)	0.33 % (w/v)
APS	0.06 % (w/v)	0.05 % (w/v)

2.24.3. Probe preparation and SDS polyacrylamide gel electrophoresis (SDS-PAGE)

Ca. 15 µg protein per slot were used for immunoblotting and 10-30 µg protein for Coomassie stained gels.

The samples were supplemented with sample buffer to a final concentration of $\geq 1\times$ sample buffer to ensure proper solubilisation of the proteins and solubilised for 15 min at RT by sucking the solution up and down with a pipette. Then the samples were boiled at 95 °C for 3 min and centrifuged afterwards at top speed (13 000 rpm) for 5 min in a table top microcentrifuge to sediment insoluble material. After removing the spacers, the gel cassette was assembled with the electrophoresis unit, and first the top and then the bottom reservoir were filled with 1× SDS electrophoresis buffer (see 2.24.1.). Then the appropriate volume of sample was filled up to 10 µl with sample buffer (see 2.24.1.) and loaded into the SDS gel slot using a microsyringe. Every empty slot on the gel was filled in with 10 µl sample buffer. The electrophoresis was run under a constant current of 25 mA (500 V, 100 W) and was continued until the Bromphenol blue reached the bottom of the gel (about 1.5 hours). Then the gel cassette was removed from the electrophoresis unit and opened, and the gel was taken out to stain in Coomassie or to mount a Western blot.

2.24.4. Coomassie staining of SDS polyacrylamide gels

Coomassie staining serves to detect proteins in an SDS polyacrylamide gel. For this purpose, the gel was fixed after electrophoresis and stained in staining solution (see below) for at least 30 min and then destained in wash solution for about 1-2 hours until the gel background was colourless. After washing, the gel could be stored for a long time in dd H₂O. Alternatively, it could first be soaked in 10 % glycerol for 30 min and then dried under vacuum.

Coomassie staining solution	0.25 % (w/v)	Coomassie® Brilliant Blue R 250
	40 % (v/v)	Methanol
	10 % (v/v)	Acetic acid
Washing solution	50 % (v/v)	Methanol
	10 % (v/v)	Acetic acid

2.25. Western blot

With Western blotting it is possible to identify and quantify proteins in a total protein extract by use of specific antibodies.

2.25.1. Protein transfer to a nitrocellulose membrane

After the separation of protein probes by SDS-PAGE (see 2.24.3.) the gel was fixed in a Western blot camera. The mounting order of the blot was the following (from anode to kathode):

- three layers of blotting paper (3MM), wetted in blotting buffer
- SDS gel, equilibrated in blotting buffer for 15 min
- nitrocellulose membrane (Hybond ECL Nitrocellulose Membrane; Amersham Pharmacia Biotech, Freiburg, Germany), wetted in blotting buffer, cut corresponding to gel size.
- three layers of wet 3MM blotting paper

Protein transfer was performed overnight at 4 °C in the Western blot chamber filled with blotting buffer at a constant current of 90 mA.

Blotting buffer:	Tris	25 mM
	Glycine	192 mM
	Methanol	20 % (v/v)

2.25.2. Staining of the blot

The nitrocellulose membrane was taken out of the blotting system and stained for two minutes in Ponceau red solution to check the protein transfer. The staining is reversible, so after washing with dd H₂O the bands of marker proteins and the sample order were marked with a pencil on the protein side of the membrane. Then, the blot was cut off to the required size.

Ponceau red solution:	Ponceau S	2 % (w/v)
	Trichloroacetic acid	3 % (w/v)

2.25.3. Immunological detection of transferred proteins

Specific proteins were identified on the nitrocellulose membrane by the indirect immunological method. First a non-labelled primary antibody binds to the antigen. In the second step, this antigen-antibody complex is bound by the secondary antibody which represents the bacterial protein A that binds immunoglobulins of many species. The secondary antibody is conjugated with an enzyme, horseradish peroxidase. This allows visualising the labelled proteins after incubation with a horseradish peroxidase substrate, which is converted into a coloured or luminescent product.

Reaction with antibodies

To reduce the unspecific binding capacity of nitrocellulose, the membrane was incubated with the primary antibodies in an appropriate dilution (1:1000 to 1:5000) in the presence of Block buffer for 2 hours at room temperature on a swinging shaker. Then the blot was washed once shortly and three times for 15 min with TBS-T to remove unspecifically bound IgG molecules. Then followed an incubation with secondary antibodies conjugated with peroxidase (1:3000 to 1:10000 in TBS-T) "Anti Rabbit-Protein A Horseradish Peroxidase Conjugate"; Bio-Rad, München, Germany) for 1 h at room temperature. Afterwards the wash steps with TBS-T were repeated: shortly once and three times for 15 min and finally one 15 min wash step with TBS.

TBS:	Tris/HCl pH 7.5	50 mM
	NaCl	150 mM
TBS-T:	Triton-X-100	0.1 % (v/v)
	in TBS	
Block buffer:	Dry milk powder	1 % (w/v)
	in TBS-T	

Peroxidase detection by "Enhanced Chemiluminiscence"

The method of "Enhanced Chemiluminiscence" (ECL) serves as a sensitive detection of a protein A-coupled peroxidase. Under alkaline conditions, peroxidase catalyses the oxidation of luminol by H₂O₂, which results in the emission of light. This reaction is enhanced by phenol. The half time of this reaction is about 1 h.

The nitrocellulose membrane was put flat, without air bubbles, on a thin plastic foil with the protein side up. 2 ml ECL-Solution 1 and 2 ml ECL-solution 2 (Amersham

Pharmacia Biotech, Freiburg, Germany) were mixed, poured on the membrane and incubated for 1 min under swinging. After the reaction, the liquid was removed and the membrane was covered by plastic foil without air bubbles and immediately exposed to Hyperfilm ECL (Amersham Pharmacia Biotech) for 1 min in the dark. Another exposition for 10 min was performed and based on the results a third exposition was performed for the optimal time period (10 sec, 30 sec or 1 hour). After taking off, the film was developed in Kodak Develop and Fix Solutions (Kodak, Rochester, NY, USA).

2.26. Measurement of sugar uptake in yeast

Yeast cells transformed with a pNEV-based expression construct with the putative hexose transporter (2.14.) were grown overnight in the appropriate selection medium (2.1.8.3.) up to an OD₆₀₀ of 1. Then the cells were harvested by centrifugation for 5 min at room temperature in a Megafuge 1.0 at 4500 rpm, and the pellet was washed twice with 50 mM Na-P_i-buffer pH 5.5 (for determination of the pH optimum, buffers with pH in the range of 3.0 – 7.3 had been tested) with centrifugation steps as described above. Finally, the cells were resuspended in the same buffer to an OD₆₀₀ of 10. Before sugar uptake measurements, the cell suspension was stored on ice for a maximum of 10 hours.

For a series of measurements, 1 ml of cell suspension was pre-incubated in a 25 ml Erlenmeyer flask for 1-2 min at 30 °C under vigorous shaking. Then 11 µl of 10 mM [¹⁴C]-labelled substrate was added to a final substrate concentration of 100 µmol in the mixture to start the sugar uptake. The labelled substrate solution was prepared by mixing 10 µl 10 mM of non-radioactive (“cold”) substrate and 1 µl of [¹⁴C]-labelled substrate (for example, ca. 0.2 µCi [¹⁴C]-glucose from Amersham Pharmacia Biotech, Little Chalfont, UK).

Samples of 100 µl were taken at given intervals after adding the substrate (10 sec, 30 sec, 1, 2, 3, 5, 10 min), filtered on nitrocellulose filters (0.8 µm pore size; Hölzer, Dorfen, Germany) and washed with an excess of dd H₂O. Incorporation of radioactivity was determined by scintillation counting. For every measurement series, 100 µl of the total sample was counted to obtain the value for overall radioactivity. To calculate the concentration of substrate accumulated in yeast cells, the cell volume (in µl of packed cells, p.c.) was determined using Hematocrite tubes for the centrifugation of 1 ml cell sample for 5 min at 3000 × g. 30 % of the total volume was taken up by the intracellular volume.

For analyzing energization, 10 μl of absolute ethanol were added after 1 min of pre-incubation, and incubated for one min before the uptake test was started. To analyze the influence of inhibitors on the uptake of glucose, the plasma membrane uncouplers CCCP (carbonyl cyanide m-chlorophenylhydrazone) and DNP (2,4-Dinitrophenol) were added to the sample to a final concentration of 50 μM before the uptake reaction was started.

2.27. Statistic evaluation of experimental data

The results shown represent either the typical results of the all experimental series conducted or the summary results. In the last case the arithmetic average value \pm the standard deviation (SD) are performed. The number of the conducted experiments was at least 3, when it is not otherwise noted in the text.

$$\text{Average value} = \frac{\Sigma \text{ Arguments of single measurements}}{\text{Number of measurements (n)}}$$

$$\text{SD} = \sqrt{\frac{\sum_{i=1}^n (x_i - \bar{x})^2}{n - 1}}$$

3. Results

3.1. Sugar contents in roots and nodules

In most plants, sucrose is the main form of carbon transported in the phloem from source to sink organs. After phloem unloading, it can reach the sink cells in the form of sucrose or as its component hexoses, glucose and fructose (Sonnewald and Willmitzer, 1992). In addition to supporting sink cell metabolism in roots, carbon allocated to the roots also supports nodule formation and the growth of symbiotic microorganisms in root nodules. To get an overview of the sugar metabolism in roots and root nodules, it was important first to analyse the soluble sugars in roots and nodules of the three model systems: one legume symbiosis (*Medicago truncatula* – *Sinorhizobium meliloti*) and two actinorhizal symbioses from different *Frankia* subclades (see 1.5). Extracts of soluble sugars from roots and nodules were obtained using the chloroform-methanol extraction (2.16.1). Sugar contents were determined via HPLC (2.17).

3.1.1. Sugar contents in roots and nodules of *Medicago truncatula*

The main sugars detected in *Medicago* extracts were glucose and sucrose. The relative amounts of these two sugars were similar in roots and nodules, with the sucrose concentrations being about 2 times higher than the glucose concentrations (Figure 3.1). The contents of fructose were below the detection limit. The only compound with increased amounts in nodules compared to roots was a substance that had similar retention time to sugar-alcohols in analysis by HPLC, but which could not be identified with available standards (“unknown M1” in Figure 3.1). This compound might represent pinitol (1-D-3-O-methyl-*chiro*-inositol), the major cyclitol of legumes, which is present in all organs of the plant (Smith and Phillips, 1980) or D-ononitol (4-O-methyl-*myo*-inositol), which has been described as a nodule-specific sugar alcohol for *Pisum sativum* (Skøt and Egsgaard, 1984; Romanov et al., 1995). Another unknown sugar (“unknown M2” in Figure 3.1) was detected only in *Medicago* root extracts, not in nodule extracts.

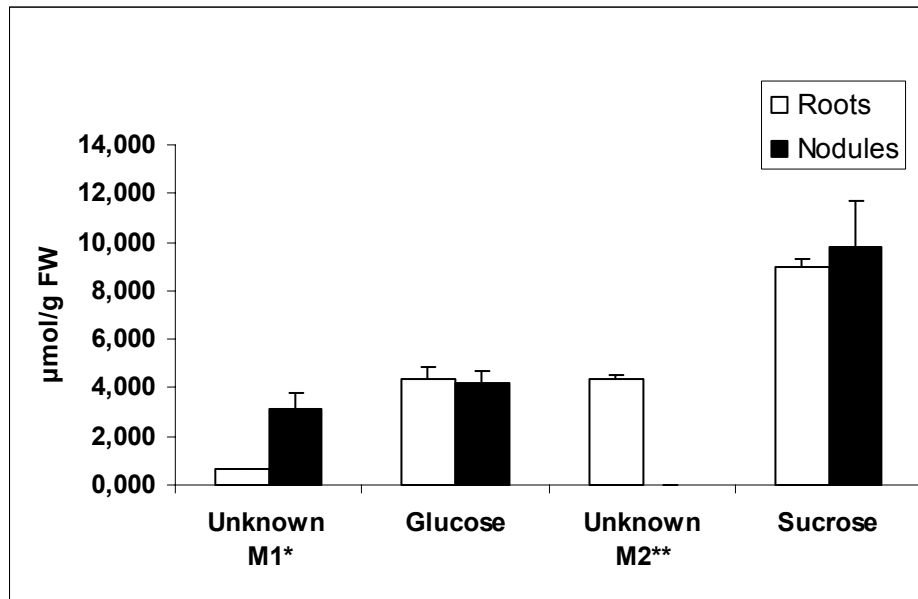


Figure 3.1. Concentrations of soluble sugars in roots and nodules of *Medicago truncatula* ($\mu\text{mol/g FW}$). The concentrations of the unknown sugars were estimated on the basis of the molecular weight of the standard components with the most similar retention time: * - *myo*-inositol; ** - fructose. A representative result of three independent experiments with three parallel samples each is shown.

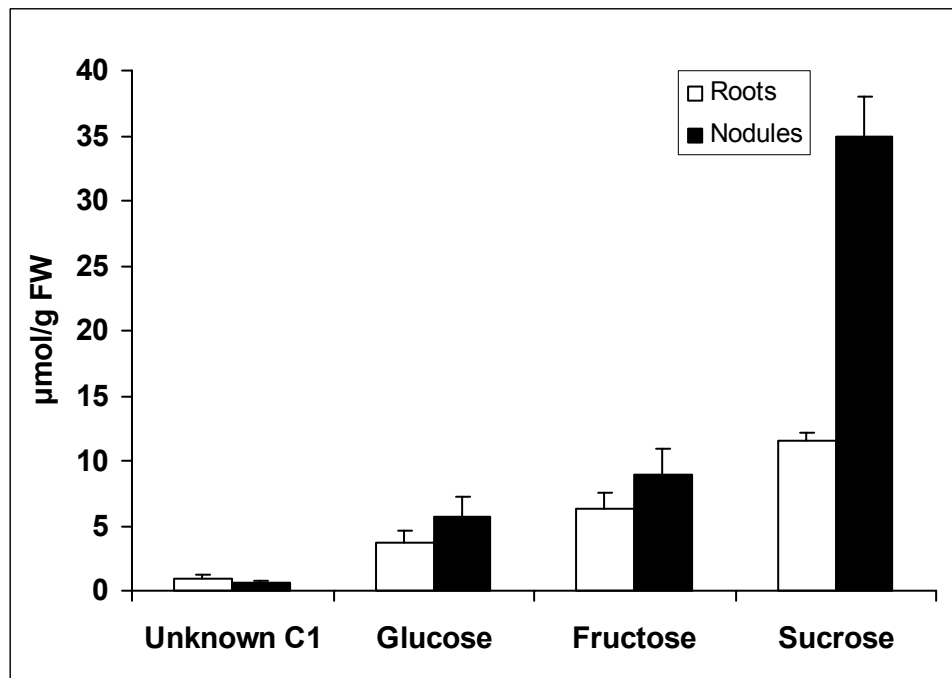


Figure 3.2. Concentrations of soluble sugars in roots and nodules of *Casuarina glauca*. The concentration of the unknown compound C1 was estimated based on the molecular weight of *myo*-inositol, the sugar-alcohol with the most similar retention time. A representative result of three independent experiments with three parallel samples each is shown.

3.1.2. Sugar contents in *Casuarina glauca*

In extracts of roots and nodules of *Casuarina glauca*, glucose, fructose, sucrose and small amounts of sugar-alcohols were detected (Figure 3.2).

Concentrations of glucose and fructose were not significantly different in roots and nodules. The main sugar compound in roots as well as in nodules of *Casuarina* was sucrose. Moreover, sucrose contents were strongly increased in nodules compared to roots, with a nodule sucrose concentration of about 35 $\mu\text{mol/g}$ FW, compared to about 12 $\mu\text{mol/g}$ FW in roots.

3.1.3. Sugar contents in *Datisca glomerata*

The sugar profile of *Datisca glomerata* (Figure 3.3) was very different from those of *Medicago* and *Casuarina*. Altogether, the total sugar content was higher in *Datisca* nodules compared to roots. In nodules, glucose and sucrose concentrations were similar (about 4.5-4.8 $\mu\text{mol/g}$ FW), whereas fructose concentrations were as high as 8 $\mu\text{mol/g}$ FW. As with *Medicago* nodules, two unknown compounds were found, the concentrations of which were strongly increased in *Datisca* nodules compared to roots. One of these substances was termed "M", because its retention time in HPLC was most similar to that of *myo*-inositol (Figure 3.3; Figure 3.4).

The other major unidentifiable component of *Datisca* soluble sugar extracts had a retention time close to that of ribitol (Figure 3.3; Figure 3.4). Based on the molecular weight of ribitol, the concentrations of the unknown sugar in roots and in nodules were about 5 and 13.5 $\mu\text{mol/g}$ FW, respectively. This compound was termed "D", from *D**atisca*.

3.1.3.1. Isolation and characterization of two unknown carbohydrates from *Datisca glomerata*

For identification of the two unknown compounds in soluble sugar extracts from *Datisca*, large-scale sugar isolation was performed for D and M as described in 2.16.2, using chloroform-methanol extraction, separation of sugar extract into fractions using anion exchange column and sodium hydroxide as eluate and paper chromatography purification from sodium chloride formed after neutralisation.

The detailed analysis of the chemical structure of D and M was conducted by nuclear magnetic resonance spectroscopy (NMR) and mass spectroscopy, and the NMR

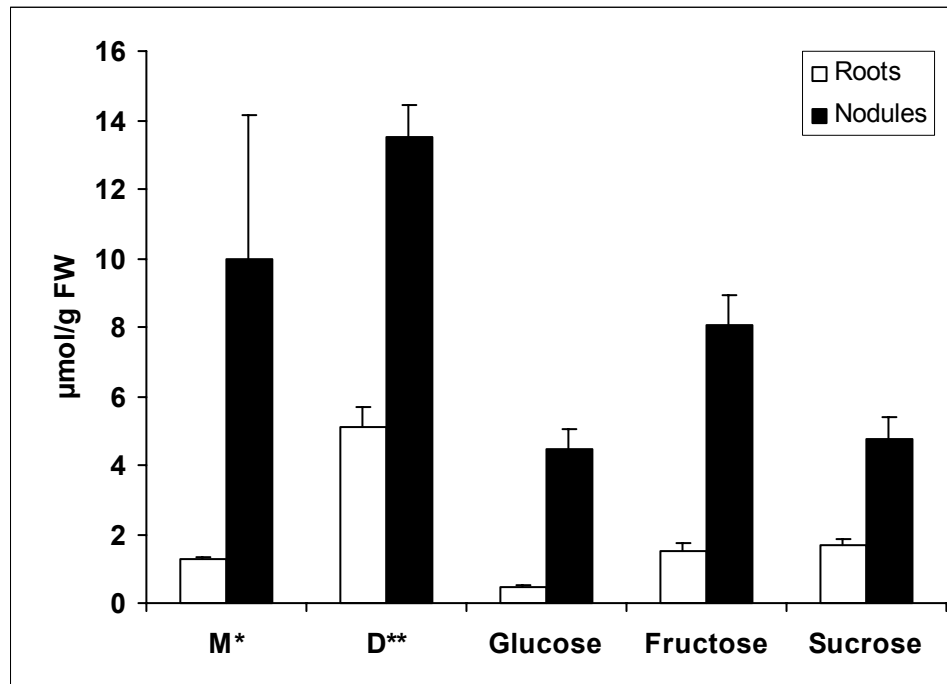


Figure 3.3. Concentrations of soluble sugars in roots and nodules of *Datisca glomerata*. The concentrations of the unknown sugar components were estimated based on the molecular weight of *myo*-inositol (*) and ribitol (**), the sugar compounds with the HPLC retention times most similar to that of M and D, respectively (see text).

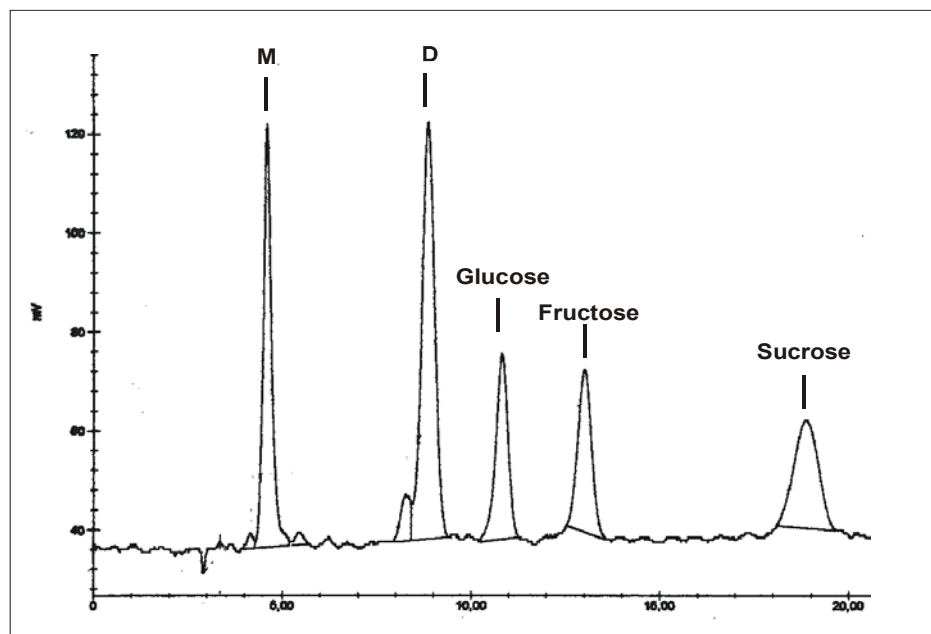


Figure 3.4. HPLC diagram of an extract of soluble sugars from nodules of *Datisca glomerata*. Two components, M and D, could not be identified with the standards available. X-axis: time [min], Y-axis: HPLC detection signal [mV].

correlation spectroscopy methods H,H-COSY and C,H-COSY by Dr. R. Fortte at the Institute for Organic Chemistry at the University of Göttingen in the laboratory of Prof. Tietze.

The ^{13}C -NMR spectrum of D showed twelve signals, whereas in the NMR spectrum of M 13 signals were observed, indicating that M contains an additional C1-unit. According to the ^{13}C -NMR spectrum, D does not contain any carbonyl groups or aromatic or olefinic carbons, but an acetal and one anomeric hemiacetal carbons. These signals were found at $\delta = 98$ and $\delta = 88.93$, respectively. The methyl group resonates at $\delta = 17.59$. The ^{13}C -NMR spectrum of compound M was similar to D, except for the presence of an additional O-methyl group at $\delta = 58$.

Based on the first NMR results, it was proposed that the isolated compounds represent disaccharides one of which was methylated. To determine the monosaccharide components of these disaccharides, acid catalysed hydrolysis of D and M was performed using 1 M HCl at 100 °C for 1 hour. The products were D-glucose and L-rhamnose (Figure 3.5) in a 1:1 ratio as determined by HPLC on a MA1 column with 0.5 M NaOH as eluant. Therefore, it was assumed that D and M were glycosides of L-rhamnose and D-glucose. Since enzymatic digestion of D and M by α -glucosidase and β -glucosidase (2.18.2), respectively, did not lead to hydrolysis, glucose could not be the sugar at the non-reducing end of either D or M. Since no methylated sugar was detected in the HPLC analysis, it was assumed that the O-methyl group of M was located at the anomeric C atom.

Based on the results of NMR and mass spectrometry as well as on results of enzymatic digestions, the structures of M and D represented in Figure 3.6 were proposed. However, the configurations of the glycosidic bonds and the O-methyl bond were still unclear.

To find out the connected positions of the monosaccharide units, acyl protection of all hydroxy groups was performed with an 1:2 mixture of acetic acid anhydride (Ac_2O) and pyridine and catalytic amounts of 4-dimethylaminopyridine (DMAP) (see Figure 3.7). The connected positions were identified via the NMR correlation spectroscopy methods H,H-COSY and C,H-COSY. The acylation of a secondary hydroxyl group leads to the chemical shift of protons at the corresponding carbon atom and shows a δ value of about 5.0. This shift was detected for the secondary hydroxyl groups at 2a/b, 3a/b and 4a/b. The corresponding 6a-protons showed a shift about $\delta = 3.7$, indicating that this carbon atom carried no free hydroxyl group. Hence, these results showed that the connection between the monosaccharides is 1b to 6a.

For the determination of the configuration of the bond between the monosaccharide units the H,H-COSY and C,H-COSY NMR-spectroscopy was used. Here, for the proton at

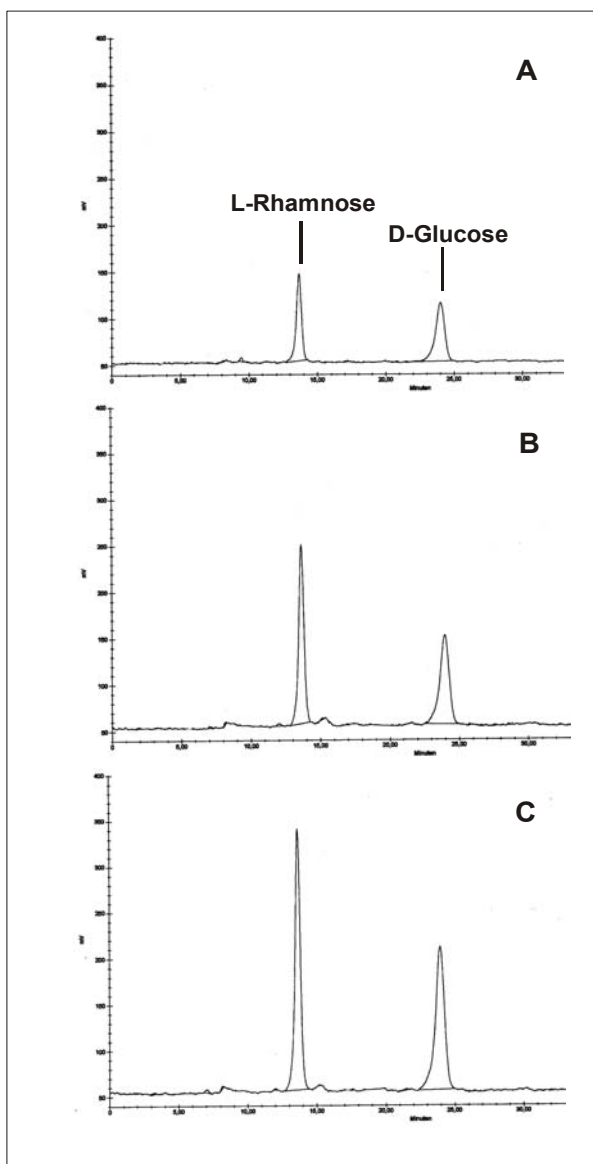


Figure 3.5. HPLC identification of the hexose components of the disaccharide D from *Datisca glomerata*. **A:** Standard representing a solution of L-rhamnose and D-glucose (200 μmol each); **B:** Products of the HCl-hydrolysis of D; **C:** standard **A** was added to the hydrolysis product **B**, and since no additional signals appear, the two peaks of **B** represent L-rhamnose and D-glucose, respectively. X-axis: time [min], Y-axis: HPLC detection signal [mV].

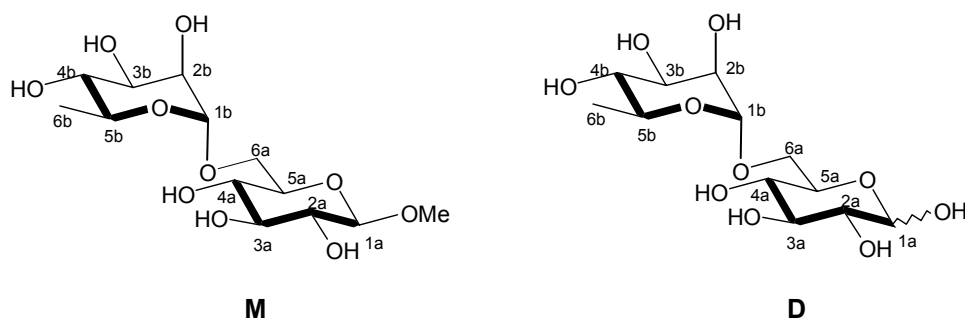


Figure 3.6. Structures of the compounds M and D. Both sugars are comprised of L-rhamnose and D-glucose moieties, with the difference that M represents O-methyl-ester of D at the C1 atom of glucose. Thus, D represents α -L-rhamnopyranosid-(1 \rightarrow 6)-glucose (rutinose), and M represents α -L-rhamnopyranosid-(1 \rightarrow 6)-(1-O- β -D-methylglucose) (methylrutinose).

the position 1b of M' and D' , a singlet was found at $\delta = 4.76$ and 4.62, respectively, that is typical for a α -glycosidic linkage.

For the proton at carbon atom 1a of compound M' a doublet was found with a coupling constant of 8.0 Hz that represents the expected value for a β -glycosidic linkage. Therefore, it was concluded that the bond between glucose and the O-methyl group in M has the β configuration.

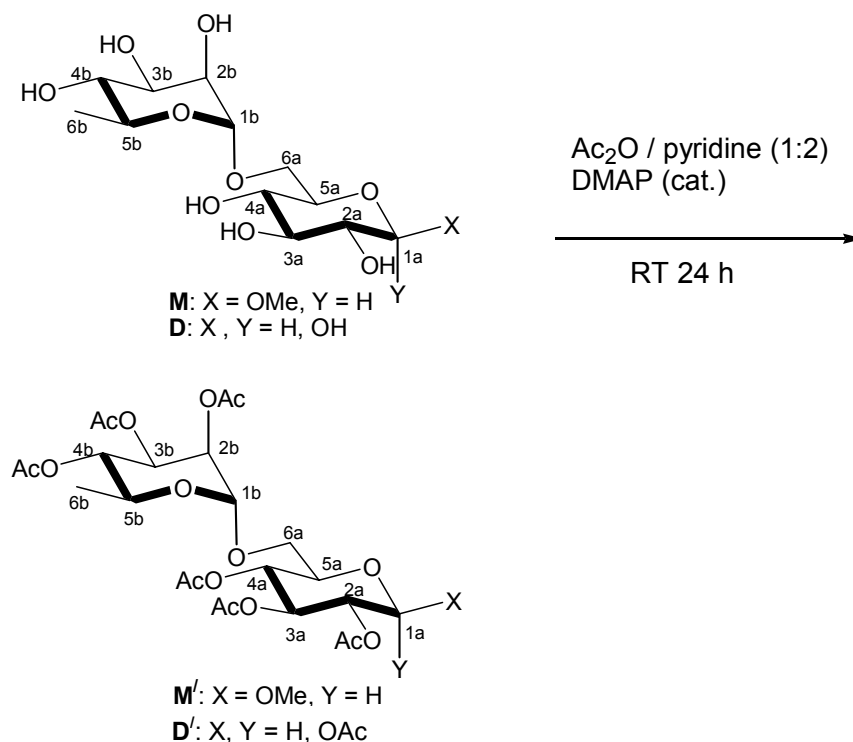


Figure 3.7. Scheme of the acylation of the free hydroxyl groups for the identification of the glycosidic bond in M and D .

The molecular mass of compounds M (340 g/mol) and D (326 g/mol) was confirmed by the electron spray ionisation method (ESI) and the chemical ionisation method (CI): for D it was equal to 349.5 g/mol, which represents the molecular mass of D plus Na^+ (ESI), and for M it represented 358 g/mol which equals the molecular mass of M plus NH_4^+ (CI).

Summarising the data on the chemical structure of the novel compounds D and M isolated from *Datisca glomerata*, they represent α -L-rhamnopyranosyl-(1 \rightarrow 6)-1-O-methyl- β -D-glucose and α -L-rhamnopyranosyl-(1 \rightarrow 6)-D-glucose, respectively (Figure 3.6).

This was confirmed by enzymatic analysis. Treatment of both D and M with naringinase, a α -rhamnopyranosidase from *Penicillium decumbens* (Sigma), yielded L-rhamnose and D-glucose (Figure 3.8), although in case of M the substrate was not cleaved completely; the cleavage stopped after an incubation time of about 5 min.

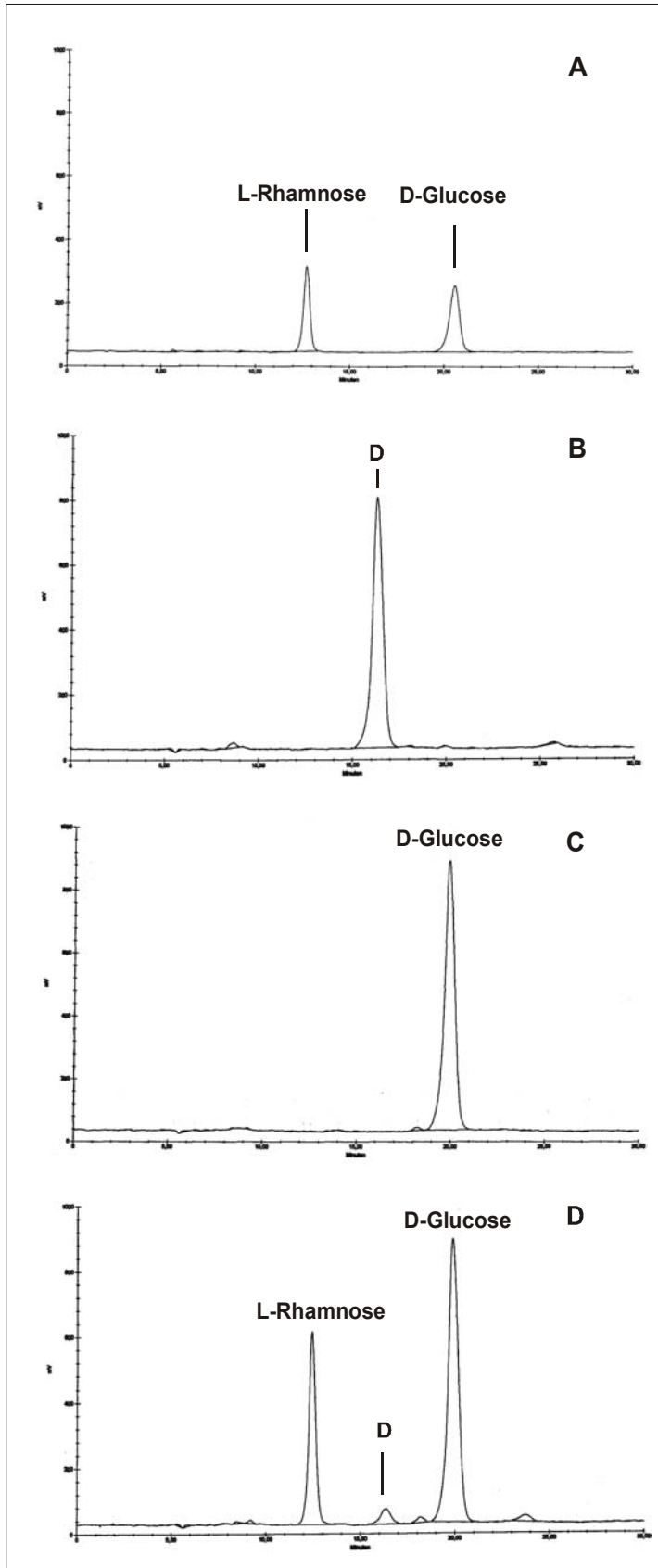


Figure 3.8. HPLC chromatograms demonstrating the enzymatic determination of the configuration of the bond between L-rhamnose and D-glucose of the disaccharide D from *Datisca glomerata* using α -L-rhamnosidase treatment. **A:** Standard representing a solution of L-rhamnose and D-glucose (200 μ mol each); **B:** Standard representing a 2 mmol solution of sugar D; **C:** Control reaction with water without substrate shows a contamination of the commercial enzyme naringinase (α -L-rhamnosidase) with polysaccharides and β -glucosidase, leading to the formation of glucose in the absence of added substrate; **D:** products of the naringinase-mediated digestion of D after 10 min reaction time represent L-rhamnose and D-glucose. X-axis: time [min], Y-axis: HPLC detection signal [mV].

Nevertheless, it was confirmed that both D and M represent disaccharides with L-rhamnose at the non-reducing end and that the bond between their monosaccharide moieties is in the α -configuration. Thus, roots and nodules of *Datisca* contain high amounts of α -L-rhamnosyl-D-glucosides.

A study of the literature on plant glycosides showed that D (α -L-rhamnopyranosyl-(1 \rightarrow 6)-D-glucose) is known as rutinose and has been described as the glycoside part of many flavonglycosides, i.e. rutin, galanginoside, cannabin, datiscin and datinoside. These flavonglycosides have been isolated and characterized from another species of the *Datisceae*, *Datisca cannabina* (Zapesochneya and Pangarova, 1976). Rutinose has not yet been described as a free sugar in plants.

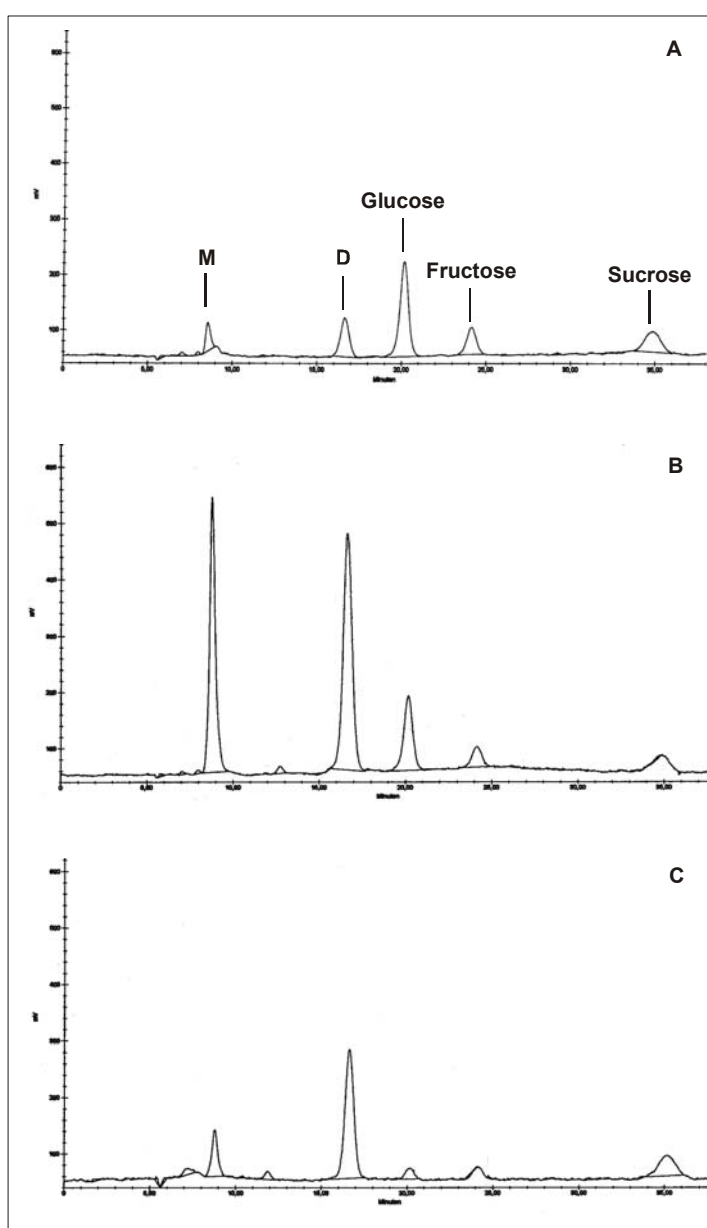


Figure 3.9. HPLC diagrams of the root sugar extracts from *Datisca glomerata*. **A:** Ethanol extract; **B:** Standards of 200 μ mol isolated M (1-O-methylrutinose) and 1 mM D (rutinose) were added to ethanol extracts to confirm the sugar identity; **C:** Chloroform/methanol extract. X-axis: time [min], Y-axis: HPLC detection signal [mV].

Accordingly, M (α -L-rhamnopyranosyl-(1 \rightarrow 6)-1-O-methyl- β -D-glucose) could be named 1-O-methylrutinose. Like rutinose, this sugar is not known among free plant metabolites. To ensure that the methylation of the anomeric C-atom was no artefact of the isolation method, namely the chloroform/methanol extraction (2.16.2), alternative methods for total sugar extractions were applied to confirm the natural occurrence of 1-O-methylrutinose. HPLC analysis of *Datisca* root extracts obtained with ethanol, perchlorate or acetone (2.16.3-2.16.5) confirmed the occurrence of 1-O-methylrutinose in total sugar extracts independently of the presence of a potential methyl donor. The HPLC diagram of the ethanol extract is shown in Figure 3.9, whereas the results for perchlorate and acetone extractions are not shown.

Moreover, methylrutinose and ethylrutinose were chemically synthesised from rutinose by Dr. R. Fortte at the Institute for Organic Chemistry at the University of Göttingen in laboratory of Prof. Tietze. The comparison of the synthesised alkylated products with rutinose and 1-O-methylrutinose isolated from *Datisca* via NMR and thin layer chromatography (TCL) on silicagel plates showed that during chemical synthesis, only α -methyl- and α -ethylglycosides of rutinose were formed, whereas the natural component represents a β -methylglycoside (see above). Hence, it was confirmed that O-methylrutinose does not represent a chemical artefact in *Datisca* sugar extracts.

3.1.3.2. Sugar contents in roots, nodules and leaves of *Datisca* after determination of the molecular mass of the novel sugars

Sugars were extracted with chloroform/methanol for HPLC analysis. The concentrations of the two unknown components termed M and D in the total sugar extracts had previously been estimated based on the molecular weight of *myo*-inositol and ribitol, respectively, as components with the closest retention time (see 3.1.3). After the isolation and determination of chemical structure and molecular mass of the unknown sugar components M (1-O-methylrutinose) and D (rutinose) (see 3.1.3.1), new concentration standards were prepared to estimate the real concentrations of M and D and to compare them with concentrations of glucose, fructose and sucrose in the same extracts. Additionally, leaf extracts were analysed for the presence of methylrutinose and rutinose to find out whether these two sugars are only present in sink- or also in source organs. The results are presented in Figure 3.10.

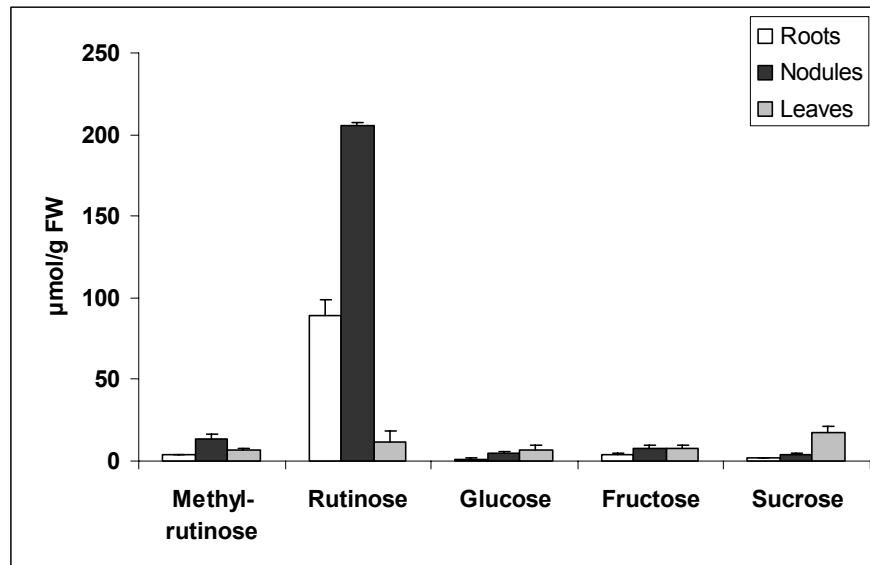


Figure 3.10. Concentrations of soluble sugars in roots, nodules and leaves of *Datisca glomerata*. The concentrations of the novel sugars methylrutinose (M) and rutinose (D) were estimated using concentration standards prepared from the isolates (see 3.1.3.1).

3.2. Activities of sucrose cleaving enzymes in roots and root nodules

Sink organs of most plant species are supplied with carbon and energy in the form of sucrose. The channelling of sucrose into sink metabolism requires its cleavage by one of several isoforms of invertase (cytosolic, apoplastic or vacuolar) or SuSy, which are localized in different subcellular compartments. These activities regulate the entry of sucrose into distinct biochemical pathways, such as respiration or biosynthesis of cell wall polysaccharides and storage reserves. Other vital roles for the sucrose-cleaving enzymes include invertase activity at the site of phloem unloading and vacuolar invertase and sucrose synthase in sink organs, which drives the long-distance transport of sucrose. In order to understand the differences of sugar metabolism in roots and root nodules, the activities of these enzymes were compared.

3.2.1. Invertase activities

Invertase is a hydrolase that cleaves sucrose irreversibly into glucose and fructose. Invertase activities were measured in soluble protein extracts and cell wall suspensions of *Medicago*, *Datisca* and *Casuarina*. The activities of the three different invertase isoforms were analysed based on their pH optima: 4.35 for apoplastic invertase; 5.0 for the

vacuolar invertase and 6.8 for the cytosolic isoform, which is also called alkaline invertase (see 2.20.2). The pH optima of apoplastic and vacuolar invertase were rather similar, but these enzymes could be distinguished based on their solubility, because apoplastic invertase is insoluble.

In *Medicago*, cytosolic invertase activities were somewhat increased in nodules compared to roots, but both apoplastic and vacuolar invertase activities were strongly reduced in nodules compared to roots (Figure 3.11A). In *Datisca*, the activities of all three types of invertases were dramatically reduced in nodules compared to roots (Figure 3.11B). In *Casuarina*, vacuolar invertase activities were similar in nodules and roots, while apoplastic and cytosolic invertase activities were strongly reduced in nodules compared to roots (Figure 3.11C). Thus, in all systems examined, apoplastic invertase activities were strongly reduced in nodules compared to roots. The highest specific activity of apoplastic invertase among the plants examined in this work was observed for roots of *Casuarina* (about 5 nmol sucrose cleaved per min per mg protein). Extremely high vacuolar invertase activities were found in roots of *Datisca*.

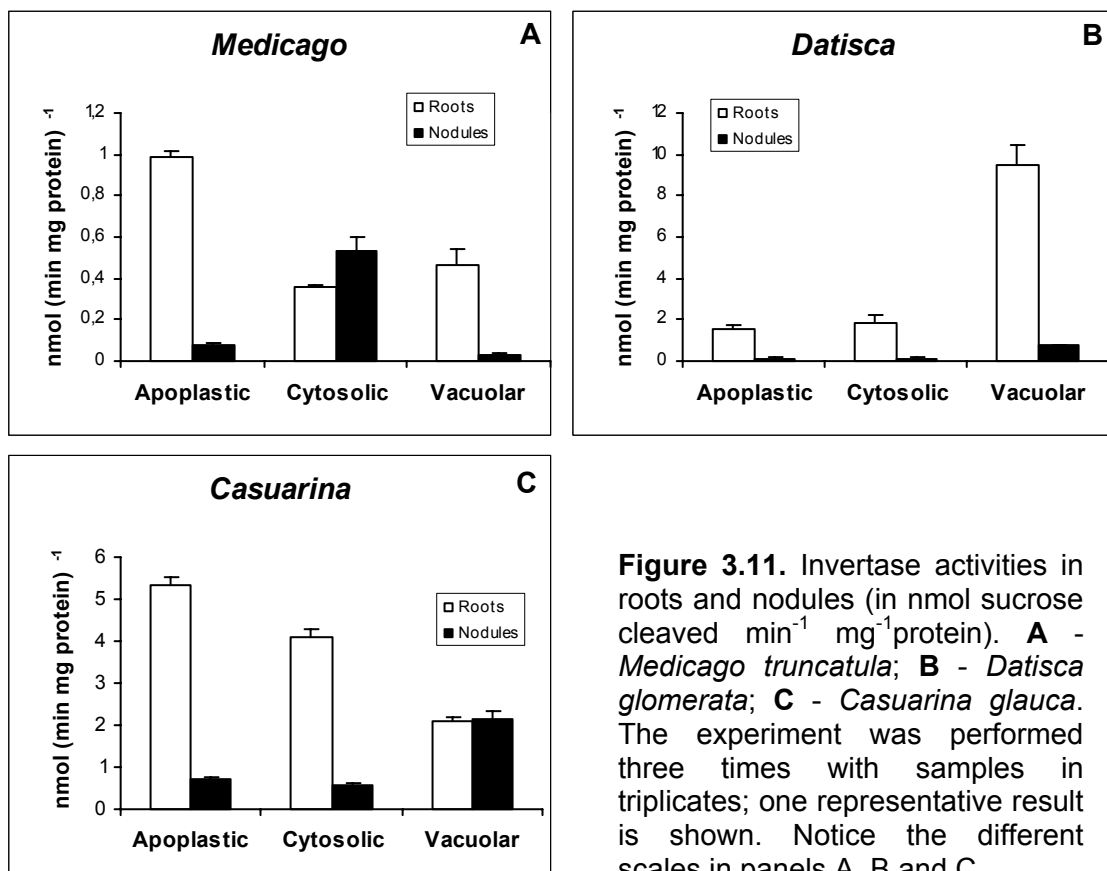


Figure 3.11. Invertase activities in roots and nodules (in nmol sucrose cleaved min⁻¹ mg⁻¹protein). **A** - *Medicago truncatula*; **B** - *Datisca glomerata*; **C** - *Casuarina glauca*. The experiment was performed three times with samples in triplicates; one representative result is shown. Notice the different scales in panels A, B and C.

3.2.2. Sucrose synthase activities

Sucrose degradation by SuSy seems to be the primary pathway in mature legume nodules (Kouchi et al., 1988; Anthon and Emmerich, 1990). Sucrose synthase is a glycosyltransferase that converts sucrose into UDP-glucose and fructose in the presence of UDP. Although SuSy is able to synthesise sucrose under appropriate conditions, there is good evidence that sucrose synthase is primarily involved in its breakdown *in vivo* (Xu et al., 1989; Geigenberger et al., 1993).

SuSy activity was determined via UDP-glucose formation (see 2.19.2). No differences could be found in the SuSy activities of roots and nodules of *Medicago truncatula*, while in *Datisca glomerata* SuSy activity in nodules was slightly reduced compared to roots (Figure 3.12A; Table 3.1). However, when activities were expressed per g fresh weight as compared to the specific activity, SuSy was much more active in nodules than in roots in both plant species (Figure 3.12B; Table 3.1). All attempts to extract SuSy activity from *Casuarina glauca* tissues failed. This may have been due to the fact that 80% of the protein from the extract was lost during desalting. When the desalted extracts were tested for SuSy activity, some apparent UDP-glucose formation as denoted by NAD reduction by UDP-glucose dehydrogenase could be observed in *Casuarina* nodule extracts. However, this activity could not be due to SuSy because it was not inhibited by arbutin, a phenylglycoside inhibitor of SuSy.

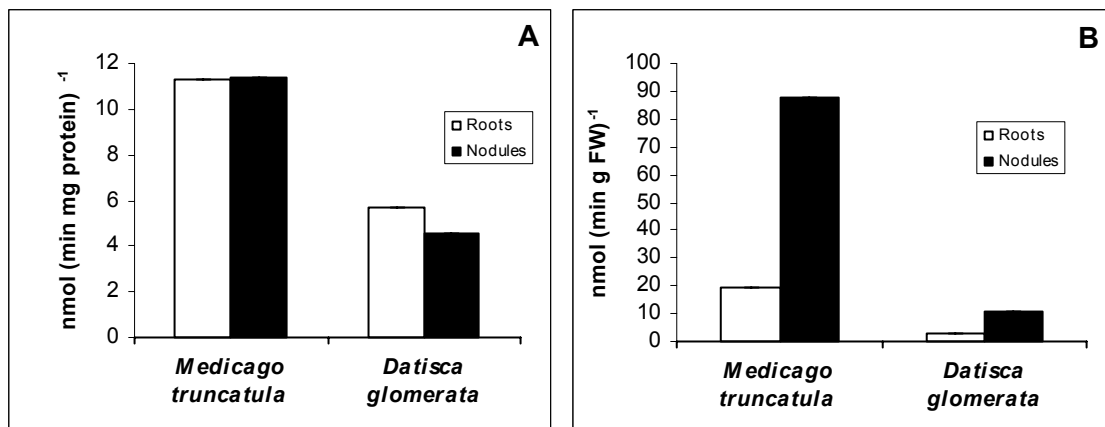


Figure 3.12. Sucrose synthase activity (in nmol sucrose cleaved) in roots and nodules of *M. truncatula* and *D. glomerata*. **A** – activity calculated per mg protein; **B** – activity calculated per g FW. The experiment was performed three times; one representative result is shown. Error bars are not visible since errors were 0.003% maximally (see Table 3.1).

Table 3.1. Sucrose synthase activities in roots and nodules of *M. truncatula* and *D. glomerata*.

Host plant	Roots		Nodules	
	nmol sucrose cleaved/min/mg protein	nmol sucrose cleaved/min/g FW	nmol sucrose cleaved/min/mg protein	nmol sucrose cleaved/min/g FW
<i>Medicago truncatula</i>	11.3 ± 0.0004	19.4 ± 0.0002	11.4 ± 0.0014	88.1 ± 0.0027
<i>Datisca glomerata</i>	5.7 ± 0.0006	2.6 ± 0.0001	4.5 ± 0.0002	10.6 ± 0.0002

In root extracts, NADH formation could already be observed before the UDP-glucose determination was started by the addition of UDP-glucose dehydrogenase. This artefactual activity might be the result of UDP-glucose formation by UDP-glucose pyrophosphorylase in the crude extract.

The data show that generally, in both roots and nodules of *Medicago*, SuSy activities are more than 20-fold higher than cytosolic invertase activities (Figure 3.11A). SuSy activities were also significantly higher than cytosolic invertase activities in nodules and roots of *Datisca* (3 times higher in roots, 34 times higher in nodules; Figure 3.12B).

3.2.3. *In situ* localization of acid invertase activity

A glucose oxidase reaction in the presence of horseradish peroxidase and diaminobenzidine (DAB) causes the production of H₂O₂, which is then used by peroxidase to oxidize diaminobenzidine (DAB), leading to the formation of a brown precipitate. On hand sections of plant material, after removal of apoplastic glucose by washing and the addition of sucrose, this staining method can be used to visualize the places of acid, i.e. apoplastic or vacuolar invertase activity (Kim et al., 2000). Alternatively, when invertases are inactivated by heat treatment before the reaction medium is added, this method allows to visualize sites of glucose accumulation.

The method did not work for both *Casuarina* roots and nodules, because it was impossible to identify brown precipitates in the strongly lignified and polyphenol-containing tissues of this plant. Therefore, only results obtained with *Medicago* and *Datisca* are presented below.

3.2.3.1. *In situ* localization of glucose in roots and nodules

There was no significant staining for glucose in roots of *Medicago* and *Datisca* (Figures 3.13A and 3.13B). It was very surprising to find strong glucose staining in the nitrogen-fixing infected cells of *Datisca* nodules (Figure 3.14A; for *Datisca* nodule morphology, see Figure 1.3). However, this staining turned out to be an artefact, because a similar reaction was also observed when nodules were incubated in reaction mixture without glucose oxidase (Figure 3.14B). It is likely that in *Datisca* nodule sections stained for glucose, the brown precipitate was due to the presence of H_2O_2 (see above) produced by the symbiotic bacteria.

As in roots, no significant staining for glucose was found for *Medicago* nodules, where only infected cells showed weak glucose staining (Figure 3.15A).

3.2.3.2. *In situ* localization of acid invertase in roots and nodules

A different pattern of acid invertase activity was observed in roots of *Medicago* and *Datisca*. *Medicago* roots showed invertase activity in the cortex, whereas *Datisca* roots only showed activity in the stele (Figure 3.13). Thus, in *Medicago* apoplastic hydrolysis of sucrose in the course of apoplastic sugar transport takes place in the entire root cortex, while in *Datisca*, it only takes place in the vascular system, indicating that sugar transport in the root cortex occurs symplastically.

Invertase activity staining could not be performed with *Medicago* nodules, since DAB was reduced in the infected cells independently of the presence of glucose oxidase (Figure 3.15). Like the glucose staining in *Datisca* nodules, this could be explained by the production of H_2O_2 by the bacteria in infected cells. In *Datisca* nodules, no acid invertase activity could be detected (Figure 3.14). In nitrogen-fixing infected cells, a light brown staining was observed sometimes, but it was much weaker than the colouring found in the same cells during glucose staining (Figure 3.14). This is in accordance with the lack of invertase activity in *Datisca* nodules (see 3.2.1.). Thus, either incomplete removal of glucose in the washing steps, and/or also the production H_2O_2 by the bacteria could be an explanation for this weak staining.

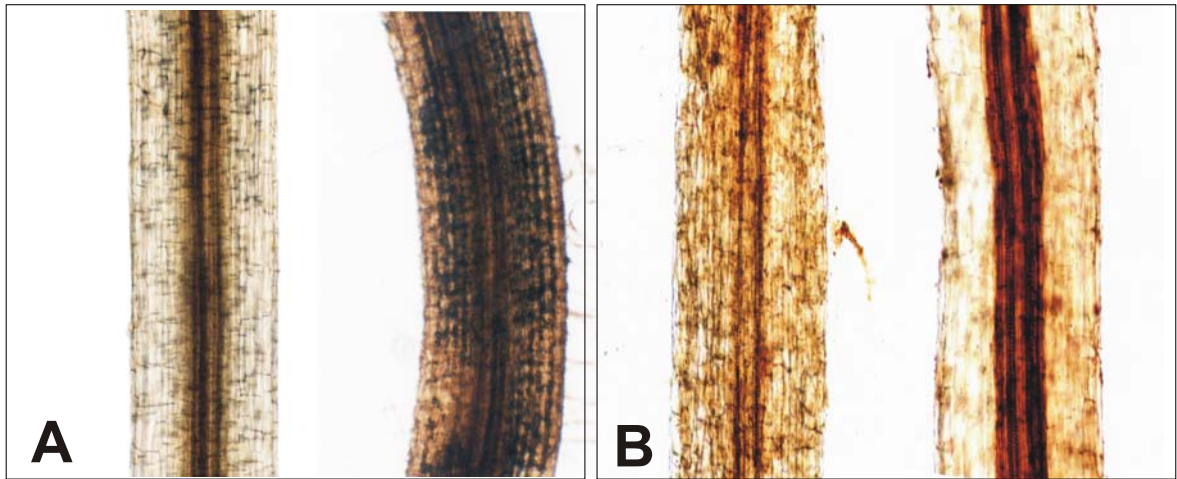


Figure 3.13. *In situ* staining of glucose and apoplastic invertase activity in *Medicago* and *Datisca* roots. **(A)** *Medicago* roots: left - staining of glucose leads to some brown precipitate in the vascular system; right – staining of acid invertase activity yields a brown precipitate all over the root cortex. **(B)** *Datisca* roots: left - staining of glucose yields a weak brown colour in the vascular system; right - staining of acid invertase activity leads to strong accumulation of brown precipitate in the vascular system.

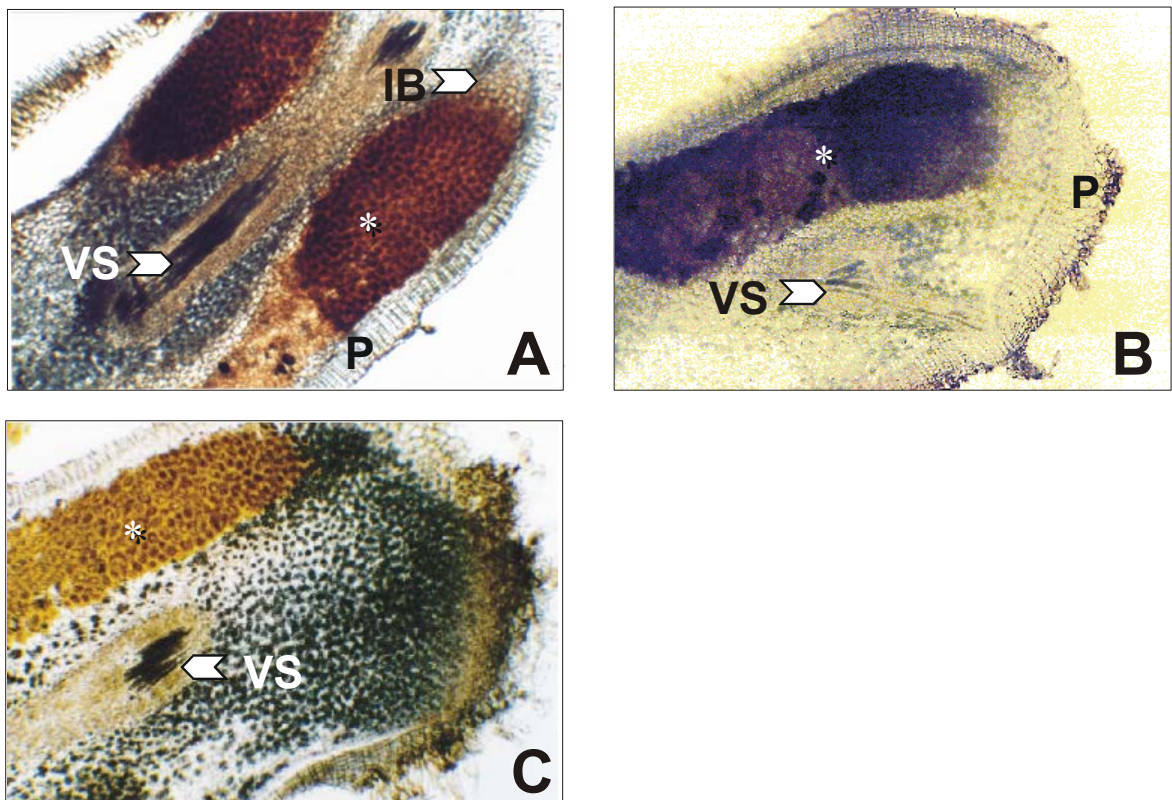


Figure 3.14. *In situ* staining of glucose and acid invertase activity in *Datisca* nodules. VS - vascular system; IB - beginning of infection; P - periderm; * - nitrogen-fixing infected cells. **(A)** Glucose staining: nitrogen-fixing infected cells stained brown due to the presence of glucose. **(B)** Negative control for (A) in the absence of glucose oxidase. The nitrogen-fixing infected cells also accumulated a brown precipitate. **(C)** Staining for invertase activity: no acid invertase activity staining could be found in *Datisca* nodules.

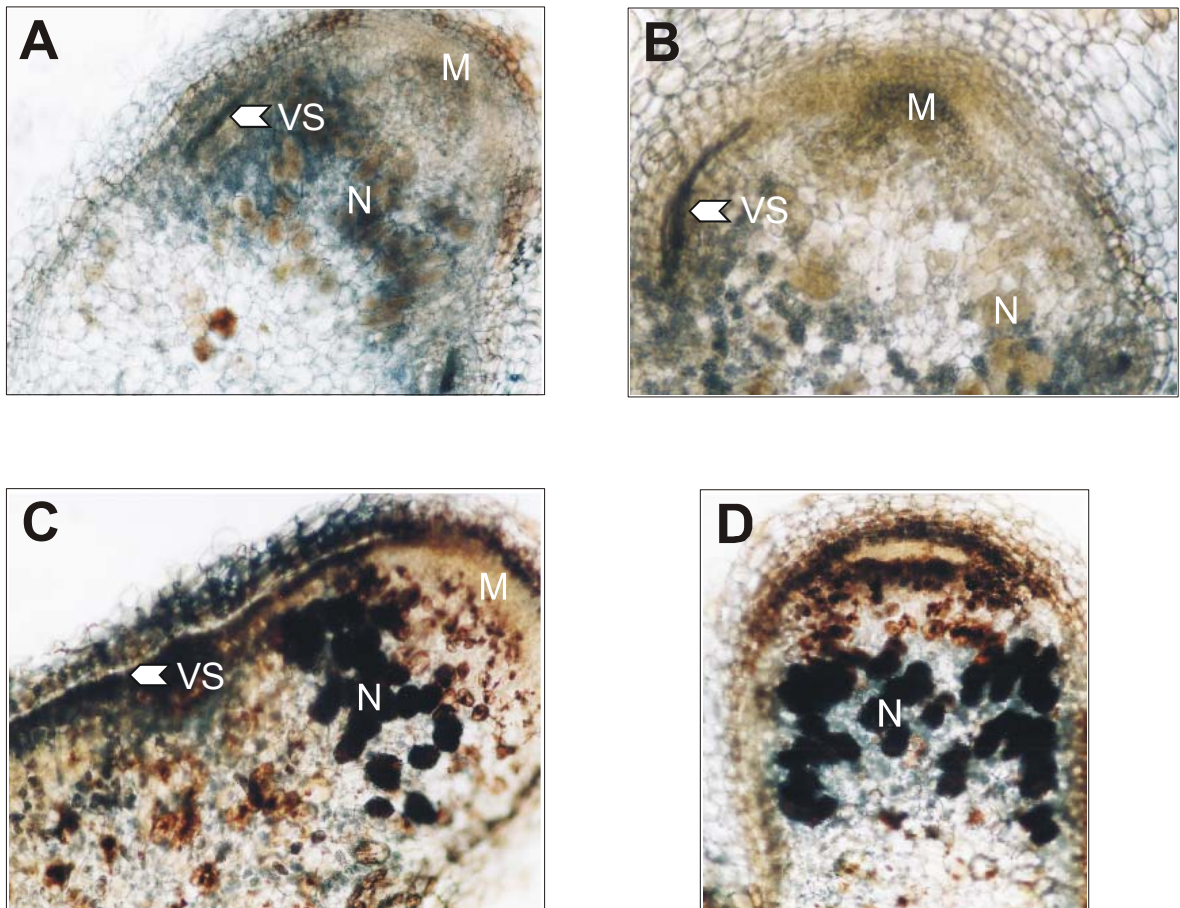


Figure 3.15. *In situ* staining of glucose and acid invertase activity in *Medicago* nodules show background in infected cells. Staining of root nodules for glucose (**A**) and invertase activity (**C**) in complete reaction mixtures led to the accumulation of brown precipitate in the infected cells in (**C**). Control staining without glucose oxidase for glucose (**B**) and invertase activity (**D**) led to similar amounts of brown precipitate in (**D**), but not in (**B**). For nodule structure see Figure 1.2. M – meristem; N – nitrogen-fixation zone; VS – vascular system.

3.3. Expression levels of sucrose synthase and sugar transporters in roots and nodules

Sucrose cleaving enzymes are regulated on the transcriptional and post-translational level, while for sugar transporters, so far only transcriptional regulation has been shown (Winter and Huber, 2000; Krausgrill et al., 1998; Ehneß and Roitsch, 1997; Truernit et al., 1996; Büttner et al., 2000). To understand which control mechanisms are employed to regulate sugar partitioning in nodules and roots, expression levels of SuSy and sugar transporters were examined by RNA gel blot hybridization analysis. Invertase expression could not be analysed this way, since invertases are encoded by large gene families with rather divergent sequences (see e.g. Godt and Roitsch, 1997; Tymowska-Lalanne and

Kreis, 1998), the characterization of which was not possible within the scope of this project.

3.3.1. Expression levels of sucrose synthase (RNA gel blot hybridization analysis)

Expression levels of sucrose synthase were compared in roots, nodules and leaves of the three model plants by RNA gel blot hybridization. The results are shown in Figure 3.16. In order to maximize the chance to detect all members of the sucrose synthase gene family, *Medicago* RNA was hybridized with a heterologous probe, namely a SuSy cDNA fragment from another legume, *Vicia faba* (Küster et al., 1993). *Datisca* and *Casuarina* RNA gel blots were hybridized with homologous cDNA probes (Wabnitz, 1998), since no cDNAs from close relatives were available.

In *Medicago*, SuSy expression was strongly increased in nodules compared to roots, while in *Datisca*, the expression of SuSy was only slightly induced in nodules compared to roots. The RNA gel blot hybridization results of *Casuarina* showed the opposite results: less SuSy transcripts were detected in nodules than in roots (Figure 3.16).

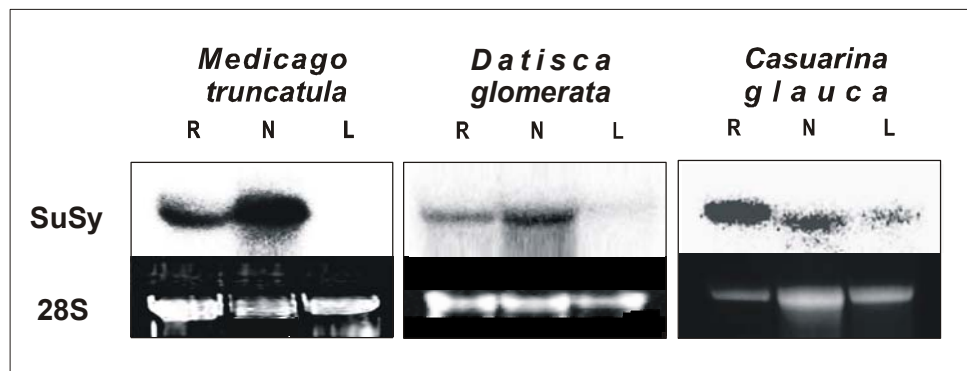


Figure 3.16. SuSy gene expression levels in *Medicago*, *Datisca* and *Casuarina* roots (R), nodules (N) and leaves (L). 28S rRNA served as a control for the amount of RNA per slot. These experiments were performed at least three times. One representative result is shown.

No expression of SuSy was detected in *Medicago* leaves, and very low amounts of SuSy transcripts were detected in *Datisca* leaves. The lack of detectable SuSy transcripts in leaves is normal for source organs, where sucrose is synthesized, and not degraded (Sturm and Tang, 1999). However, the enzyme has also been localized in the sieve tube-companion cell complex of source leaves (Nolte and Koch, 1993), where it appears to be involved in the hydrolysis of a small proportion of the incoming sucrose to maintain a

proton gradient across the plasma membrane of companion cells for phloem loading (Lerchl et al., 1995). The relatively high expression levels of SuSy in *Casuarina* leaves are due to the fact that morphologically, these "leaves" represent branchlets with the true leaves reduced to tiny scales, i.e. mixed leaf and stem material. The role of SuSy in stems is not completely clear, because only hypocotyls of radish, sunflower and cotton were analysed with respect to SuSy (Rouhier and Usuda, 2001; Kutschera and Heiderich, 2002; Ruan et al., 1997). In sunflower hypocotyls the SuSy activity was implicated in cellulose synthesis (Kutschera and Heiderich, 2002) as it had already been shown for developing cotton seeds (Ruan et al., 1997). In hypocotyls of radish, high levels of SuSy were found in companion cells of the phloem (Rouhier and Usuda, 2001), where besides its potential function in the production of precursors for respiration, SuSy could also play a role in callose accumulation, and therefore in the regulation of both cell-to-cell and long-distance transport in plants. However SuSy protein was also found in the xylem parenchyma and some cortical cells, where its role remains unclear (Rouhier and Usuda, 2001).

3.3.2. Levels of sucrose synthase protein (Protein blot analysis)

Enzyme activity can be regulated both on the transcription level and posttranscriptionally. SuSy is extensively regulated on all levels, including reversible protein phosphorylation and interaction with the actin cytoskeleton (Winter and Huber, 2000). The finding that similar levels of SuSy enzyme activity were found in roots and nodules of *Medicago* and *Datisca*, while the levels of SuSy mRNA were different in roots and nodules of all three model plants, raised the question of how SuSy activity is regulated at the posttranscriptional level.

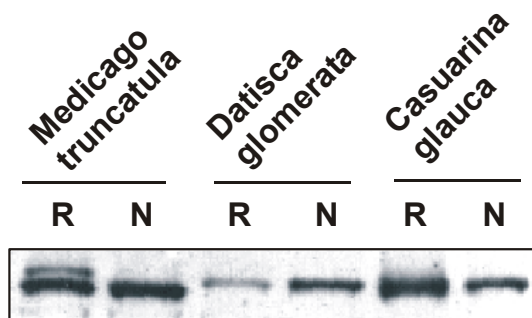


Figure 3.17. Immunodetection of sucrose synthase in total protein extracts from roots (R) and nodules (N) of *Medicago*, *Datisca* and *Casuarina*, separated by PAGE (2.24-2.25). 15 μ g of total protein were applied per slot. This experiment was performed three times. One representative result is shown.

The amounts of SuSy were analysed by the protein blot analysis of total protein extracts from roots and nodules (2.25) from the three plant systems with an antibody raised against SuSy from cotyledons of *Vicia faba* (Ross and Davies, 1992; kindly provided by N. Hohnjec, University of Bielefeld). The results are shown in Figure 3.17. Increase of SuSy protein levels in nodules compared to roots could be found only in nodules of *Datisca*, which contain a single immunoreactive protein of approximately 92-kDa. For *Casuarina glauca*, also a single immunoreactive protein of the same mass was detected, but the amounts of SuSy were reduced in nodules compared to roots. So, for *Datisca* and *Casuarina* the amounts of protein are in accordance with mRNA expression levels. However, in *Medicago* nodules, only a slight increase in the amount of the immunoreactive 92 kDa protein was detected compared to roots. This does not reflect the mRNA levels, but is in accordance with SuSy enzyme activities in both organs (Figure 3.12A). A second immunoreactive protein of slightly higher molecular weight was detected in extracts of uninfected roots of *Medicago*, which is consistent with the results obtained by Hohnjec et al. (1999).

3.3.3. Expression levels of sugar transporters in roots, nodules and leaves

The organ-specific expression of sucrose and hexose transporters was analysed by RNA gel blot hybridisation in roots, nodules and leaves of the three model plants. For the sucrose transporter of *Medicago*, a heterologous probe from *Vicia faba* was used (Weber et al., 1997), while a homologous probe was used for the hexose transporter of *Medicago* (Wabnitz, 1998). The expression levels of the sucrose transporter (*MtST*) were strongly reduced in nodules compared to roots, and the expression levels of the hexose transporter (*MtHT*) in nodules were below the detection limit (Figure 3.18). For *Datisca* only homologous probes were used (Wabnitz, 1998). Here, the expression of the hexose transporter was strongly induced in nodules compared to roots, while sucrose transporter expression was below the detection limit in both nodules and roots as well as in leaves (Figure 3.18; data not shown for the sucrose transporter). For *Casuarina*, only hexose transporter expression was examined since no sucrose transporter cDNA fragment could be amplified by PCR with the degenerate primers that had been used successfully for *Datisca* (Wabnitz, 1998). *Casuarina* hexose transporter expression was strongly induced in nodules compared to roots, as in *Datisca* (Figure 3.18). Interestingly, in both *Casuarina* and *Datisca*, hexose transporter expression levels were very low in roots, while in *Medicago* roots high expression levels of both hexose and sucrose transporters were found, indicating that root sugar partitioning mechanisms differ significantly between the legume *Medicago* and the two actinorhizal plants.

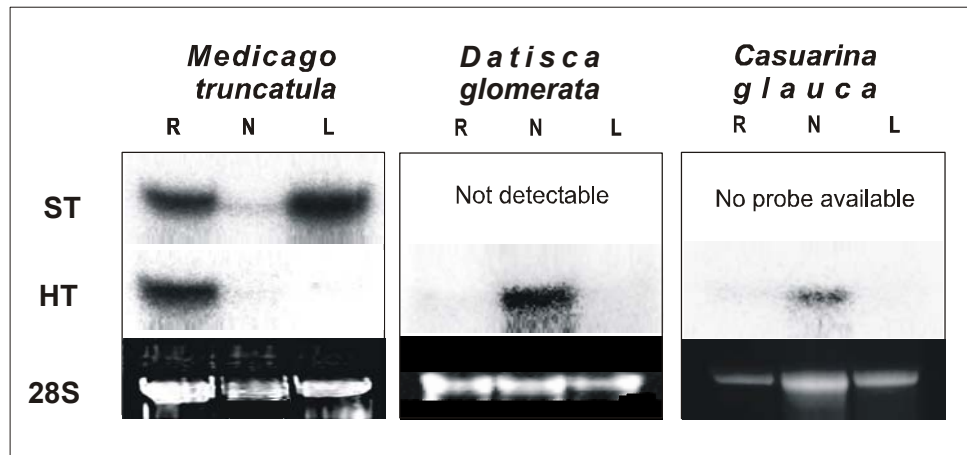


Figure 3.18. Sucrose transporter (ST) and hexose transporter (HT) gene expression in *Medicago*, *Datisca* and *Casuarina* roots (R), nodules (N) and leaves (L). 28S rRNA serves as a control for the amounts of RNA per slot. These experiments were performed at least three times. One representative result is shown.

3.4. Isolation and characterization of hexose transporter cDNAs

In previous studies, evidence had been obtained that the hexose transporters from *Medicago* (Figure 3.19) and *Datisca* (Figure 3.20) had special properties with respect to their primary structure and expression patterns. The hexose transporter cDNA fragment that had been amplified from *Medicago* nodule cDNA differed in the C-terminal region from all other hexose transporters known thus far (Wabnitz, 1998; amino acids 404 to C-terminus in Figure 3.21). *In situ* hybridization analysis of the expression pattern of the hexose transporter from *Datisca* (Figure 3.20) had revealed that its expression was confined to the infected cells of the nodules (Wabnitz, 1998). In combination with the data on the extremely low apoplastic invertase activity in *Datisca* nodules obtained in this thesis (3.2.1.), this expression pattern suggested a function of the transporter in feeding hexose to the microsymbionts (see 4.4.). Therefore, one of the aims of this study was to obtain full size cDNAs from both genes in order to analyse the transport activity of the encoded proteins in yeast.

3.4.1. Full size cDNA of the *Medicago truncatula* hexose transporter (*MtHT*)

At the beginning of this study, only ca. 500 bp of the 3' end of cDNA had been isolated, namely the sequence of the original PCR product and the 3' RACE products (Wabnitz, 1998; Figure 3.19). For *MtHT*, the 3' end of the cDNA had been used to isolate

```

1 GAATTCGATTCCCAACCAGCATAGAATTAACACTAACAGTGATTACCCATAAAGTTAAGTTTGGTGCAT
-----+-----+-----+-----+-----+-----+-----+
71 ATTTTAGAACCTTAAAGGTAGATATATCCTTAGACAAAACAGCGTTTCGAAAATGGCTGGTGGGGTTTTAC
-----+-----+-----+-----+-----+-----+-----+
                                     M A G G V L P 7
141 CAGTGGATAGTACACCAGTGGCAGTAACTGCCATCAATATTTGGTGGCAAGTTAACTCTCAATCATCAT
-----+-----+-----+-----+-----+-----+-----+
      V D S T P V A V T A I N I G G K L T L S I I I 30
211 TACCTGCATAGTTGCTGCATCCGGTGGCCTTCTTTATGGATATGATCTCGGAGTTTCAGGAGGTGTTACA
-----+-----+-----+-----+-----+-----+-----+
      T C I V A A S G G L L Y G Y D L G V S G G V T 53
241 ACGATGGTGCCATTTCTCCAAAAATTTCTTCCAGACATTCTGAGAAAGGCAGCCAGTGCCGAAGTGAATA
-----+-----+-----+-----+-----+-----+-----+
      T M V P F L Q K F F P D I L R K A A S A E V N M 77
351 TGTATTGTGTGTATGATAGTCAAATATTGACACTATTTACGTCTTCTCTTTATCTAGCTGGATTAGTGTCT
-----+-----+-----+-----+-----+-----+-----+
      Y C V Y D S Q I L T L F T S S L Y L A G L V S 100
421 ATCCATTGCAGCTAGCAAAGTCACGGCGGCTTATGGTTCGGAGAAACGTCATCATAATAGGAGGTGCTCTC
-----+-----+-----+-----+-----+-----+-----+
      S I A A S K V T A A Y G R R N V I I I G G A L 123
491 TTCATTGCCGGTGGCGCCATTAATGGTGGTTCGGAAAATATCCCCATGCTCATTTTGGGTCGTGTTCTTC
-----+-----+-----+-----+-----+-----+-----+
      F I A G G A I N G G S E N I P M L I L G R V L L 147
561 TTGGGTTTGGGGTTGGTTTCACTAATCAAGCTGCACCGTTGTACCTATCTGAAACTGCTCCCCAAAATG
-----+-----+-----+-----+-----+-----+-----+
      G F G V G F T N Q A A P L Y L S E T A P P K W 170
631 GCGAGGCACTTTTAACACGGGCTTTTCAGTTCTTCTTGGGAATTGGTGTAGTCGCTGCCGGCTGCATAAAC
-----+-----+-----+-----+-----+-----+-----+
      R G T F N T G F Q F F L G I G V V A A G C I N 193
701 TACGCCACGGCCAAGCACACATGGGGATGGAGACTCTCTCTTGGACTTGCACTGGTTTCTGCAGCTGTGA
-----+-----+-----+-----+-----+-----+-----+
      Y A T A K H T W G W R L S L G L A V V P A A V M 217
771 TGACAATCGGTTCTTCCTCATTACCGATAACCAAACGGCTTGGTAGAACGTGGTAAGATAGAGCAAGC
-----+-----+-----+-----+-----+-----+-----+
      T I G S F L I T D T P N G L V E R G K I E Q A 240
841 CAAACAAGCCTTACGCAAAATTAGAGGATCCTCGGTTGATATTGAACCCGAGTTAGAAGAACTTATCAAG
-----+-----+-----+-----+-----+-----+-----+
      K Q A L R K I R G S S V D I E P E L E E L I K W 263
911 TGGACAGAAATTGCGAAATCAGTGCAACAAGAGCCCTTTAAAACCATATTA AAAAGGGAATATCGACCTC
-----+-----+-----+-----+-----+-----+-----+
      T E I A K S V Q Q E P F K T I L K R E Y R P H 287
981 ACTTGGTGATGGCATTGCAATCCCGTTTTTCCAACAGCTTACAGGGATCAATATTGTAGCCTTTTATTC
-----+-----+-----+-----+-----+-----+-----+
      L V M A F A I P F F Q Q L T G I N I V A F Y S 310

```

```

1051 ACCCAACCTCTTTCACCTCTGTGGGTTTTGGACACGACGGAGCTTTACTTTCCGCCATTATACTTGGATCT
-----+-----+-----+-----+-----+-----+-----+-----+
P N L F H S V G F G H D G A L L S A I I L G S V 333

1121 GTTAGCCTTTTGTCTAACCTTATCTCTGCTGGTATTGTTGATCGAATTGGTCGAAGATTCTTGTTCATAT
-----+-----+-----+-----+-----+-----+-----+-----+
S L L S N L I S A G I V D R I G R R F L F I S 357

1191 CTGGGGGAATTATGATGCTTGTCTGCTTGATTGCTGTGTCCATTGTCCTGGCAGTGGTGACTGGTGTTGA
-----+-----+-----+-----+-----+-----+-----+-----+
G G I M M L V C L I A V S I V L A V V T G V D 380

1261 TGGTACAAAGGACATATCCAAGGGCAATGCAATAGTGGTATTGGTGCTATGTGTTTCTACTCTGCAGGT
-----+-----+-----+-----+-----+-----+-----+-----+
G T K D I S K G N A I V V L V L L C F Y S A G F 403

1331 TTTGGTTGGTCATGGGGTCCATTAACATGGCTTATTCCAAGTGAGATTTTCCAGTAAAAATAAGAACCA
-----+-----+-----+-----+-----+-----+-----+-----+
G W S W G P L T W L I P S E I F P V K I R T T 427

1401 CAGGACAAAGCATAGCTGTTGCTGTGCAATTCATAATAATCTTTGTGTTATCGCAAACATTCTTGACAAT
-----+-----+-----+-----+-----+-----+-----+-----+
G Q S I A V A V Q F I I I F V L S Q T F L T M 450

1471 GTTATGCCACATGAAGTTTGGGGCCTTCGCTTCTATGCTTTTTGGGTTATTGTGATGACTCTGTTTGT
-----+-----+-----+-----+-----+-----+-----+-----+
L C H M K F G A F V F Y A F W V I V M T L F V I 473

1541 ATCTTCTTCTTGCCTGAGACCAAAGGAATTCCTTTGGAGTCAATGTACACTATATGGGGCAGACACTGGT
-----+-----+-----+-----+-----+-----+-----+-----+
F F L P E T K G I P L E S M Y T I W G R H W F 497

1611 TTTGGTCTCGGTATGTTAAAGGACAAGAGGTCCTAGAAAATCTCCCATGAAGTTTTTAACACTTTTTATG
-----+-----+-----+-----+-----+-----+-----+-----+
W S R Y V K G Q E V L E N L P * 512

1681 ATTGATTTATTATTTTTAAAGAAGTCAATGCACATGCATTATATCTTGACAAAATTGTGCAGCATTGGCT
-----+-----+-----+-----+-----+-----+-----+-----+

1751 TCATAAAAATAAATCAATAATAAAAGAAATGTAATCAATAATAACGTCTCAAAAATAATGTATTGATTGT
-----+-----+-----+-----+-----+-----+-----+-----+

1821 TAATGTTAAAAAAGCGGCCGCGGATCCTCGAGAATCACTAGTGAATTC
-----+-----+-----+-----+-----+-----+-----+-----+

```

Figure 3.19. DNA sequence and deduced amino acid sequence of the *M. truncatula* hexose transporter (MtHT). Shaded amino acid sequences represent the membrane-spanning domains predicted by the method of Rost et al. (1995; 1996). Numbers to the right refer to the predicted amino acid sequence of MtHT. Underlining denotes potential phosphorylation consensus sequences. The amino acid sequences that had been used to design the original degenerate oligonucleotide primers are underlined and labelled by bold print.

a cDNA clone from a cDNA library made from RNA of young *Medicago* nodules (MtHTN15; Wabnitz, 1998; Gamas et al., 1996). However, this clone was not full size but started at nucleotide 442 of the full size sequence that was finally obtained in this thesis. Thus, 5' RACEs had to be performed for cDNA. The cDNA sequences available were used for generating primers for 5'-RACEs. The sequences of all primers used are presented in 2.1.3.

For *MtHT* 5'-RACE, reverse transcription was performed with the first gene-specific primer *MtHT 5'race1*. Based on the C-tailed first-strand cDNA (2.10.), two PCRs were performed using for the first PCR the anchor primer *MM1* and primer *MtHT 5'race1* (PCR program was 94 °C 30 s, 35 cycles of 94 °C 30 s, T_{ann}= 61 °C 30 s, 72 °C 90 s, followed by 72 °C for 10 min in the presence of 1.5 mM MgCl₂). For the second PCR the anchor-specific primer *MM2* and second gene-specific primer *MtHT 5'race2* were used (PCR program as described above, except that the T_{ann} was 58 °C). A PCR product of about 500 bp was cloned in pGEM-T Easy and sequenced. The 5'-end sequence was used to design another primer, *MtHT fs*, which in combination with the primer *MM4* was used to amplify the full size cDNA. First strand cDNA was transcribed with primer *MM3* from nodule mRNA, and the full size cDNA was amplified with the following PCR program: 94 °C 5 min, 35 cycles of 94 °C 1 min, 60 °C 1 min, 72 °C 2 min, followed by 72 °C for 10 min. The full size cDNA was cloned in pGEM-T Easy and both strands were sequenced.

The DNA sequence and the deduced amino acid sequence of *M. truncatula* hexose transporter (MtHT) are presented in Figure 3.19. The full size clone comprises 1883 nucleotides, 1536 of which represent an ORF that is predicted to encode a protein of 512 amino acids with an estimated molecular mass of 55.41 kDa. The 5'-untranslated region includes 121 nucleotides, and 3'-untranslated region is composed of 226 nucleotides.

The protein encoded by *MtHT* is predicted to be an extremely hydrophobic integral membrane protein with 12 transmembrane domains according to a hydropathy plot (Figure 3.19; Rost et al., 1995; 1996).

3.4.2. Full size cDNA of the *Datisca glomerata* hexose transporter (DgHT)

At the beginning of this study, only ca. 500 bp of the 3' end of cDNA had been isolated (Wabnitz, 1998; Figure 3.20). The cDNA sequences available were used for generating primers for 5'-RACEs. The sequences of all primers used are presented in 2.1.3.

For *DgHT* 5'-RACE, reverse transcription was performed with a first gene-specific primer *DgHT 5'race1*. Based on the C-tailed first-strand cDNA (2.10.), the first PCR was performed using an anchor primer *MM1* and above-mentioned primer *DgHT 5'race1* (PCR

```

1 GAATTCGATTCCCTTCTCTCTTTATCTCCTTTTCATCACTCCCCTCTTTCTCTCCTCGCAAAAGAAGTCA
-----+-----+-----+-----+-----+-----+-----+-----+
71 GAGATAAAGGACGAAAACATGCCGGCCGTCGGAGGAATCGTTGTTCGGTGGCAGTAAAAGGAGTATCCCG
-----+-----+-----+-----+-----+-----+-----+-----+
      M P A V G G I V V G G S K K E Y P G 18
141 GCAACCTTACTCCTTATGTCACCATAACATGCATTGTTGCCGCTATGGGTGGTCTGATTTTCGGTTACGA
-----+-----+-----+-----+-----+-----+-----+-----+
      N L T P Y V T I T C I V A A M G G L I F G Y D 41
211 TATTGGAATTTAGGTGGGGTGACGTCAATGGATTCATTCTTGAAGAAATCTTCCCGGCGGTTTACCGG
-----+-----+-----+-----+-----+-----+-----+-----+
      I G I S G G V T S M D S F L K K F F P A V Y R 64
241 AAAAAAGAGTTGGATTCGACGACGAACCAGTACTGTCAGTACGACAGTCAGACTCTGACGATGTTACGT
-----+-----+-----+-----+-----+-----+-----+-----+
      K K E L D S T T N Q Y C Q Y D S Q T L T M F T S 88
351 CTTCTCTTTATTTGGCTGCTCTGCTCGCTTCGATAGTGGCTTCCACCATCACCCGTAATTCGGCAGGAG
-----+-----+-----+-----+-----+-----+-----+-----+
      S L Y L A A L L A S I V A S T I T R K F G R R 111
421 ATTATCCATGCTCTTCGGCGGCATTCTGTTCTGTGCCGGTGTATCATCAATGGCTTCGCCAGGCTGTT
-----+-----+-----+-----+-----+-----+-----+-----+
      L S M L F G G I L F C A G A I I N G F A Q A V 134
491 TGGATGCTCATTCTCGGTCGTATGTTTTCTCGGTTTTGGTATTGGGTTTTCCAATCAGTCTGTGCCACTCT
-----+-----+-----+-----+-----+-----+-----+-----+
      W M L I L G R M F L G F G I G F S N Q S V P L Y 158
561 ACCTCTCAGAGATGGCTCCCTACAAGTACAGAGGAGCATTAACATAGGCTTCCAATTATCAATCACAAAT
-----+-----+-----+-----+-----+-----+-----+-----+
      L S E M A P Y K Y R G A L N I G F Q L S I T I 181
631 TGGAATATTGGTAGCAAATGTGTTAAATTACTTCTTTGCCAAGATCAGGGGCGGCTGGGGATGGCGGTTG
-----+-----+-----+-----+-----+-----+-----+-----+
      G I L V A N V L N Y F F A K I R G G W G W R L 204
701 AGCTTAGGTGGCGCAATGGTCCCAGCCCTTATCATCACGGTCGGATCGCTACTCCTTCCCAGACACCCCA
-----+-----+-----+-----+-----+-----+-----+-----+
      S L G G A M V P A L I I T V G S L I L P D T P N 228
771 ACTCATTAATCGAGCGTGGCAACCGAGACGAAGCCCGCAGCAAACCTCAAAGGGTTCGAGGCGTTGATGA
-----+-----+-----+-----+-----+-----+-----+-----+
      S L I E R G N R D E A R S K L Q R V R G V D D 251
841 CGTGGACGAGGAGTTTAAACGATCTGGTGGCGGCAAGTGAAGAGTCAAAGCAAGTGAACATCCTTGGACT
-----+-----+-----+-----+-----+-----+-----+-----+
      V D E E F N D L V A A S E E S K Q V E H P W T 274
911 AACCTGTTGAGGAGGAAGTACAGACCTCATCTTGCAATGGCTATACTAATTCCTTTCTTCCAGCAACTTA
-----+-----+-----+-----+-----+-----+-----+-----+
      N L L R R K Y R P H L A M A I L I P F F Q Q L T 298
981 CCGGCATCAATGTGATTATGTTTTACGCGCCTGTTTTGTTTAAACACCATTGGGTTTGAAGTGATGCTTC
-----+-----+-----+-----+-----+-----+-----+-----+
      G I N V I M F Y A P V L F N T I G F G S D A S 321

```



```

1051 GCTCATGTCGGCTGTGATTACTGGCTGTGTTAATGTCGCTGGGACTTTGGTTTCTATTTATGGGGTTGAT
-----+-----+-----+-----+-----+-----+-----+-----+-----+
L M S A V I T G C V N V A G T L V S I Y G V D 344

1121 AAGTGGGGAAGGAGGTTTCCTTTTCCTTGAGGGTGGATTTCAAATGTTGATTGCCAGGCGGTTGTAGCAG
-----+-----+-----+-----+-----+-----+-----+-----+-----+
K W G R R F L F L E G G F Q M L I C Q A V V A A 368

1191 CTGCAATTGGTGCTAAATTTGGAGTAAATGGAAATCCAGGAGAAGTCCAAAATGGTATGCGATAGTGGT
-----+-----+-----+-----+-----+-----+-----+-----+-----+
A I G A K F G V N G N P G E L P K W Y A I V V 391

1261 GGTGCTGTTCATATGCATATATGTAGCAGGGTCTCTTGGTCATGGGGTCTCTAGGTTGGCTAGTGCCA
-----+-----+-----+-----+-----+-----+-----+-----+-----+
V L F I C I Y V A G F S W S W G P L G W L V P 414

1331 AGTCAAAGTTTCCCCTTAGAAATACGGTCAGCTGCTCAAAGTATCAATGTCTCTGTCAACATGATCTTCA
-----+-----+-----+-----+-----+-----+-----+-----+-----+
S E S F P L E I R S A A Q S I N V S V N M I F T 438

1401 CATTGCTATAGCTCAAATCTTCTTGACAATGCTTTGCCACTTGAAATTCGGTTTATTCATTTCTTCGC
-----+-----+-----+-----+-----+-----+-----+-----+-----+
F A I A Q I F L T M L C H L K F G L F I F F A 461

1471 CTTCTTCGTGGTTGTCATGTCTATCTTCGTCTACTTCTTCTTGCCCGAGACTAAGGGAATCCCGATCGAA
-----+-----+-----+-----+-----+-----+-----+-----+-----+
F F V V V M S I F V Y F F L P E T K G I P I E 484

1541 GAGATGGGCAGAGTATGGAAGTCACATTGGTACTGGTCAAGATTTGTTACTGATGCTGATTACACTATTG
-----+-----+-----+-----+-----+-----+-----+-----+-----+
E M G R V W K S H W Y W S R F V T D A D Y T I G 508

1611 GATCAGGAGTTGAGATGGGAAAGGGAGCGCAGGAGCTTAAGAATATTTAAGTTTAATGTTTGGGGGGAGG
-----+-----+-----+-----+-----+-----+-----+-----+-----+
S G V E M G K G A Q E L K N I * 523

1681 GTTATTTTTAGATTATTTTTTTCTATCTAGTAAATAGAAGTTTGGGTCAATATTAAATTAAGAACATATG
-----+-----+-----+-----+-----+-----+-----+-----+-----+

1751 AATGGGTCAAATTTGATGTATCTGAATCACTAGTGAATTC 1790
-----+-----+-----+-----+-----+

```

Fig. 3.20. DNA sequence and deduced amino acid sequence of the *D. glomerata* hexose transporter (DgHT). Shadowed amino acid sequences represent the membrane-spanning domains predicted by the method of Rost et al. (1995; 1996; see 3.4.3.). Numbers to the right refer to the predicted amino acid sequence of DgHT. Underlining denotes potential phosphorylation consensus sequences. The amino acid sequences that had been used to design the original degenerate oligonucleotide primers are underlined and labeled by bold print.

program was 94 °C 30 s, 35 cycles of 94 °C 30 s, 58 °C 30 s, 72 °C 30 s, followed by 72 °C for 10 min in the presence of 1.5 mM MgCl₂). For the second PCR another anchor-specific primer *MM2* and second gene-specific primer *DgHT 5'race2* were used (PCR program as described above). A 480 bp PCR product was cloned into pGEM-T Easy and sequenced. The 5'-end sequence was used as a template to design primer *DgHT fs5*, which together with the primer from the 3'-end sequence *DgHT fs3* was used to amplify the full size cDNA with the following PCR program: 94 °C 5 min, 35 cycles of 94 °C 1 min, 52 °C 1 min, 72 °C 2 min, followed by 72 °C for 10 min. For this purpose, first strand cDNA was transcribed with primer *dT₂₀* from nodule mRNA. The full size cDNA was cloned in pGEM-T Easy and both strands were sequenced.

The cDNA sequence and the deduced amino acid sequences of the hexose transporter (DgHT) from *Datisca* nodules are shown in Figure 3.20. The full size cDNA clone comprises 1790 nucleotides, 1569 of which represent an ORF encoding a protein of 523 amino acids with an estimated molecular mass of 57.64 kDa. The 5'-untranslated region consists of 88 and the 3'-untranslated region of 133 nucleotides. Like the other members of the hexose transporter protein family, the protein encoded by *DgHT* is predicted to be an extremely hydrophobic integral membrane protein with 12 transmembrane domains (Rost et al., 1995; 1996).

3.4.3. Protein sequence analysis of DgHT and MtHT

The deduced amino sequences of DgHT and MtHT exhibit similarity to known plant hexose transporters, with the highest levels of identity for DgHT to the hexose transporters AtSTP1 from *Arabidopsis* and MtSTP1 from *Medicago* (83.3 and 83.2%, respectively), and for MtHT to AtSTP1 from *Arabidopsis* (55.1%; Table 3.2, Figure 3.21; references see figure legend).

Hydropathy analysis reveals that like the other plant hexose transporters, DgHT and MtHT are extremely hydrophobic and predicted to represent integral membrane proteins with 12 membrane spanning domains (Figures 3.19 and 3.20), a typical feature of transporters belonging to the major facilitator superfamily described by Marger and Saier (1993). The MtHT and DgHT sequences also contain conserved sequence motifs previously identified among sugar transporters, including PETKG at the end of membrane-spanning domain 12 and two potential phosphorylation consensus sequences (Figures 3.19 and 3.20).

```

      *           *           *           *           *
DgHT : MPAVGGIVVGGSKKEYPGNLTTPYVTITCIVAAMGGLIFGYDIGISGGVTSMDSFLK : 56
MtSTP1 : MAGGGIPIGGGNKEYPGNLTTPFVTITCIVAAMGGLIFGYDIGISGGVTSMDPFLK : 55
AtSTP1 : MPAGGFVVGDQKAYPGKLTTPFVLTICVVAAMGGLIFGYDIGISGGVTSMPDFLK : 55
AtSTP4 : MAGGFVSQTPGVRNYNYKLTPKVFVTCFIGAFGGLIFGYDLGISGGVTSMEPFLE : 55
MtHT : MAGGVLVVDSTPVAVTAINIGGKLTLSIIITCIVAASGGLLYGYDLGVSGGVTTMVPFLQ : 60
AtSTP3 : MVAEEARKEAMAKSVSGGKITIFVVASCVMAAMGGVIFGYDIGVSGGVMSMGPFLK : 56
AtSTP2 : MAVGSMNVEEGTKAFPAKLTGQVFLCCVIAAVGGLMFGYDIGISGGVTSMDTFL : 55

      *           *           *           *           *
DgHT : KFFPAVYRKKELD-----STTNQYCYQYDSQTLTMFTSSLYLAALLASIVASTITRKFGRR : 111
MtSTP1 : KFFPAVYRKKNKD-----KSTNQYCYQYDSQTLTMFTSSLYLAALLSSLVASTITRRFGRK : 110
AtSTP1 : RFFPSVYRQQED-----ASTNQYCYQYDSPTLTMFTSSLYLAALLSSLVASTVTRKFGRR : 110
AtSTP4 : EFPFYVYKMKMS-----AHENEYCRFDSQLLTLFTSSLYVAALVSSLFASTITRKFGRK : 109
MtHT : KFFPDILRKAAS-----AEVNYCVYDSQILTLFTSSLYLAGLVSSIAASKVTAAYGR : 114
AtSTP3 : RFFPKVYKLEEDRRRRGNSNNHYCLFNSQLLTSFTSSLYVSGLIATLLASSVTRSWGRK : 116
AtSTP2 : DFFPHVYEKKHR-----VHENNYCKFDDQLLQLFTSSLYLAGIFASFISSVYVSRFGRK : 109

      *           *           *           *           *
DgHT : LSMLFGGILFCAGALNCFQAQVWMLILGRMFLGFGIGFSNQS----- : 154
MtSTP1 : LSMLFGGLLFLVGAALNCFANHVWMLIVGRILLGFGIGFANQP----- : 153
AtSTP1 : LSMLFGGILFCAGALNCFAKHVWMLIVGRILLGFGIGFANQA----- : 153
AtSTP4 : WSMFLGGFTFFIGSAFNCFQNIAMLLIGRILLGFGVGFANQS----- : 152
MtHT : NVILIGGALFIAGGALNCGSENIPMLILGRVLLGFGVGFANQA----- : 157
AtSTP3 : PSIFLGGVSLAGAAFCGSAQNVAMLIARLILGVGVGFANQS----- : 159
AtSTP2 : PTIMLASIFFLVGAILNLSAQELGMLIGRILLGFGIGFNQVSCQTLKTKFFYLSGFLCF : 169

      *           *           *           *           *
DgHT : -----VPLYLSEMAPPYKYRGALNIGFQL : 177
MtSTP1 : -----VPLYLSEMAPPYKYRGALNIGFQL : 176
AtSTP1 : -----VPLYLSEMAPPYKYRGALNIGFQL : 176
AtSTP4 : -----VPVYLSEMAPPNLRGAFNNGFOV : 175
MtHT : -----APLYLSETAPPKWRGTFNIGFQF : 180
AtSTP3 : -----VPLYLSEMAPPYKYRGALNIGFQL : 182
AtSTP2 : HLGFLCFHLGFPLFLCLNSSCFVLFLCLLTLKAILLQTVPLFISEIAPARYRGGLNVMFQF : 229

      *           *           *           *           *
DgHT : SITIGILVANVLNYFFAKIRGGWGWRLSLGGAMVPALIIITVGSLLLPDTPNSLIER-GNR : 236
MtSTP1 : SITIGILVANVLNYFFAKIRGGWGWRLSLGGAMVPALIIITIGSLVLPDTPNSMIER-GDR : 235
AtSTP1 : SITIGILVAEVLNYFFAKIRGGWGWRLSLGGAVVPALIIITIGSLVLPDTPNSMIER-GQH : 235
AtSTP4 : AIIFGIVVATIINYFTAQMKGNIGWRISLGLACVPVMMITGALILPDTPNSLIER-GYT : 234
MtHT : FLIGVVAAGCINYATAKHT--WGWRISLGLAVPAAVMTIGSFLITDTPNGLVER-GKI : 237
AtSTP3 : CIGIGLSANVINYETQNLK--HGWRISLATAAIPASILLGLSFLPETPNSIIQTTGDV : 240
AtSTP2 : LITIGILAASYVNYLSTLKN--GWRYSLGGAAVPALIIITIGSFFIHTETPASLIER-GKD : 286

      *           *           *           *           *
DgHT : DEARSKLQVRVG-VDDVDEEFNDLVAASEESKQVEH-PWTNLLRRKYRPHLAMAILIPFF : 294
MtSTP1 : DGAKAQLKRIRG-IEDVDEEFNDLVAASEASMQVEN-PWRNLLQRKYRQPLTMAVLIIPFF : 293
AtSTP1 : EEAKTKLRRIRG-VDDVDEEFDDLVAASKESQSTEH-PWRNLLRRKYRPHLTMAVMIIPFF : 293
AtSTP4 : EEAKEMLQSRIRG-TNEVDEEFQDLIDASEESKQVKH-PWKNIMLPRYRQPLIMTCFIIPFF : 292
MtHT : EQAKQALRKIRGSSVDIEPELEELIKWTEIAKSVQEPFKTILKREYRPHLVMAFAIPFF : 297
AtSTP3 : HKTEMLLRRVRG-TNDVQDELTDLVEASSGSDTDSN-ATLKLQRKYRPELVMAVLIIPFF : 298
AtSTP2 : EKGKQVLRKIRG-IEDIELEFNEIKYATEVATKVKSPFKELFTKSENRPPLVCGTLLQFF : 345

      *           *           *           *           *
DgHT : QQLTGINVIMFYAPVLENTIGFGSDASLMSAVITGCVNVAGTLVSIYGVDKWGRRFLFLE : 354
MtSTP1 : QQFTGINVIMFYAPVLENSIGFKDDASLMSAVITGVVNVVATCVSIYGVDKWGRRALFLE : 353
AtSTP1 : QQLTGINVIMFYAPVLENTIGFTTASLMSAVVTGCVNVGATLVSIYGVDRWGRRFLFLE : 353
AtSTP4 : QQLTGINVITFYAPVLENTLGFSGKASLLSAMVITGIELLCTFVSVFTVDRFGRRILFLE : 352
MtHT : QQLTGINIVAFYSPNLFHSGVGFHDGALLSAILLGSVSLLSNLISAGIVDRIGRRFLFIS : 357
AtSTP3 : QQVTGINVVAFYAPVLYRTVGFGEGLMSTLVITGIVGTSSLMLLVVDRIGRKTLFLE : 358
AtSTP2 : QQFTGINVVMFYAPVLEQTMGSGDNASLISTVVIINGVNAIATVLSLLVVDFAGRRCFLME : 405

```

```

          *           *           *           *           *           *
DgHT      : GGFQMLICQAVVAAAIGAKFGVNGN-----PGELPKWYAIIVVV : 392
MtSTP1    : GGAQMLICQAVVAAAIGAKFGTSGN-----PGNLPEWYAIIVVV : 391
AtSTP1    : GGTQMLICQAVVAACIGAKFGVDGT-----PGELPKWYAIIVVV : 391
AtSTP4    : GGIQMLVSQLAIGAMIGVKFGVAG-----TGNIKSDANLIV : 389
MtHT      : GGIMMLVCLIAVSVIVLAVVTGVVDG-----TKDISKGNAIIVVL : 394
AtSTP3    : GGLQMLVSOVTIGVIVMVADVHDG-----VIKEGYGYAVV : 393
AtSTP2    : GALQMTATQVSFFFFFFACVTWYTYSYLDNKLTYDNWRHSLSSLEASWSYWPICALIVL : 465

          *           *           *           *           *           *
DgHT      : LFICIYVAGFSSWSWGPLGWLVPSEIFPLEIRSAAQSVNVSVMNLTFTFAIAQIFLTMCLHL : 452
MtSTP1    : LFICIYVAGFAWSWGPLGWLVPSEIFPLEIRSAAQSVNVSVMNLTFTFLVAQVFLIMLCHM : 451
AtSTP1    : TFCIYVAGFAWSWGPLGWLVPSEIFPLEIRSAAQSVITVSVNMTFTFIIAQIFLTMCLHL : 451
AtSTP4    : ALICIYVAGFAWSWGPLGWLVPSEIFPLEIRSAQAIVNVSVMNMTFTFLVAQLFLTMCLHM : 449
MtHT      : VLLCFYSAGFGWSWGPLTWLIPSEIFPVKIRTTGQSIATAVAVQFTIIEVLSQTFLTMLCHM : 454
AtSTP3    : VLVCVYVAGFGWSWGPLGWLVPSEIFPLEIRSAQSVTVAVSEVETFAVAQSAAPPMLCKF : 453
AtSTP2    : ILCVYVSGFAWSWGPLGWLVPSEIYPLEVRNAGYFCAVAMNMVCTFIIGQFFLSALCRF : 525

          *           *           *           *           *           *
DgHT      : KFGLEIFFAFFVVMSIFVYFELPETKGIPIEEMGR-VWKSHPWWSRFVTDADYTIKSGV : 511
MtSTP1    : KFGLELFFFAFFVLVMSIYVFELLPETKGIPIEEMDR-VWKSHPWWSRFVEHGDHGN--GV : 508
AtSTP1    : KFGLELFFFAFFVVMSIFVYIFLPETKGIPIEEMGQ-VWRSHPWWSRFVEDGEYGN--AL : 508
AtSTP4    : KFGLEFFFFAFFVIMTIFVIYMLPETKNVPIEEMNR-VWKAHFWGKFIPEAVNMG-AA : 507
MtHT      : KEGAFVVFYAFWVIVMILEVIFELPETKGIPIESMYT-IWGRHFWFSRYVKGQEVLENLP : 512
AtSTP3    : RAGIFFFFYGGWLVVMTVAVQLELPETKNVPIEKVVG-LWEKHFWFRRMTSKRDIQETTIL : 512
AtSTP2    : RSLLEFFFGIMNIIMGLEVVVFLPETKGVPIEEMAERKWKTHPRWKKYFKD : 576

          *
DgHT      : EMGKGAQELKNI : 523
MtSTP1    : EMGKGAPKNV : 518
AtSTP1    : EMGKNSNQAGTKHV : 522
AtSTP4    : EMQQKSV : 514
AtSTP3    : SH : 514

```

Figure 3.21. Alignment of the deduced amino acid sequences of DgHT and MtHT with amino acid sequences of known monosaccharide transporters from *Arabidopsis* and *Medicago*: AtSTP1 (Sauer et al., 1990), AtSTP2 (GenBank Accession No. AAF79565.1), AtSTP3 (Büttner et al., 2000) and AtSTP4 (Truernit et al., 1996) from *Arabidopsis* and MtSTP1 from *Medicago* roots (Harrison, 1996). – indicates gaps introduced to maximize the homology, inverse print indicates identical amino acids at conserved positions in all proteins. Amino acids conserved in six of the proteins are labelled in dark grey with inverse print, those conserved in four or five proteins are shaded in light grey. Sequence alignment was performed using the program ClustalW from EMBL, Heidelberg (<http://dot.imgen.bcm.tmc.edu:9331/multi-align/Options/clustalw.html>). The alignment was presented using the editor GeneDoc (Nicholas et al., 1997).

Table 3.2. Percentage of identical and similar amino acid residues shared by different hexose transporters. Sequence comparisons were performed using the program bestfit of the GCG program package (Altschul et al., 1990).

		% Identity						
		DgHT	MtHT	MtSTP1	AtSTP1	AtSTP2	AtSTP3	AtSTP4
% Similarity	DgHT		54.7	83.2	83.3	50.5	53.9	63
	MtHT	66.6		52	55.1	46.8	47.4	52.4
	MtSTP1	88.2	63.9		80.7	52.1	55	63.6
	AtSTP1	88	67.5	86.4		50.2	56.3	62.6
	AtSTP2	61.6	59.7	64	60.7		48.3	48.6
	AtSTP3	63.9	61.2	64.1	64.7	58.9		54.5
	AtSTP4	73.1	64	73.4	72.2	59.1	64.2	

3.5. Functional characterization of the hexose transporters by expression in yeast

To demonstrate that *DgHT* and *MtHT* encode functional hexose transporters it was necessary to functionally characterize them in a heterologous expression system that lacked endogenous hexose transporters. For this purpose, the yeast strain *EBY.VW4000* of *Saccharomyces cerevisiae* in which the hexose transporter genes had been deleted was chosen (Wieczorke et al., 1999).

3.5.1. Construction of shuttle vectors for the heterologous expression of *MtHT* and *DgHT* in yeast

For the yeast expression studies, the hexose transporter cDNAs were subcloned into the expression vector pNEV-E (Sauer and Stolz, 1994) under the control of the strong promoter of the yeast plasma membrane H⁺-ATPase (*PMA1*; Serrano et al., 1986).

In order to achieve optimal expression levels, the 5'-untranslated region had to be removed from the hexose transporter cDNA and to be replaced by the sequence 5'-AAGCTTGTAAGAA-3' from the 5'-untranslated region of the sucrose transporter *PmSuc2* from *Plantago major* (N. Sauer, personal communication).

3.5.1.1. Cloning of *MtHT* in pNEV-X

The new sequence was introduced in *MtHT* via a PCR reaction with specific primers. As forward primer, *PmMtHT-for* (5'-CCG **CTC GAG** AAG CTT GTA AAA GAA *ATG GCT GGT GGG GTT TTA CCA GTG-3') was used. This primer contains the *XhoI*-restriction site (bold), the *PmSUC2*-5'-UTR (underlined) and the beginning of an ORF (*). As reverse primer, *PmMtHT-rev* 5'-TTC ACT AGT GAT TCT CGA GGA TCC GC-3' was used which is derived from the 3'-untranslated region of *MtHT*. The product of the reaction was cloned in pGEM-T Easy, where its sequence was confirmed. The insert was excised with *XhoI* using the *XhoI*-restriction site in the primer *PmMtHT-for* at the 5'-end of the recombinant cDNA and the *XhoI*-restriction site at the 3' of the untranslated region of *MtHT*, and cloned in the *XhoI*-site of pNEV-X. The plasmid with *MtHT* in sense orientation was named pX-MNHs; the plasmid with antisense orientation of *MtHT* was named pX-MNHas and used as negative control. The plasmids are shown in Figure 3.22.

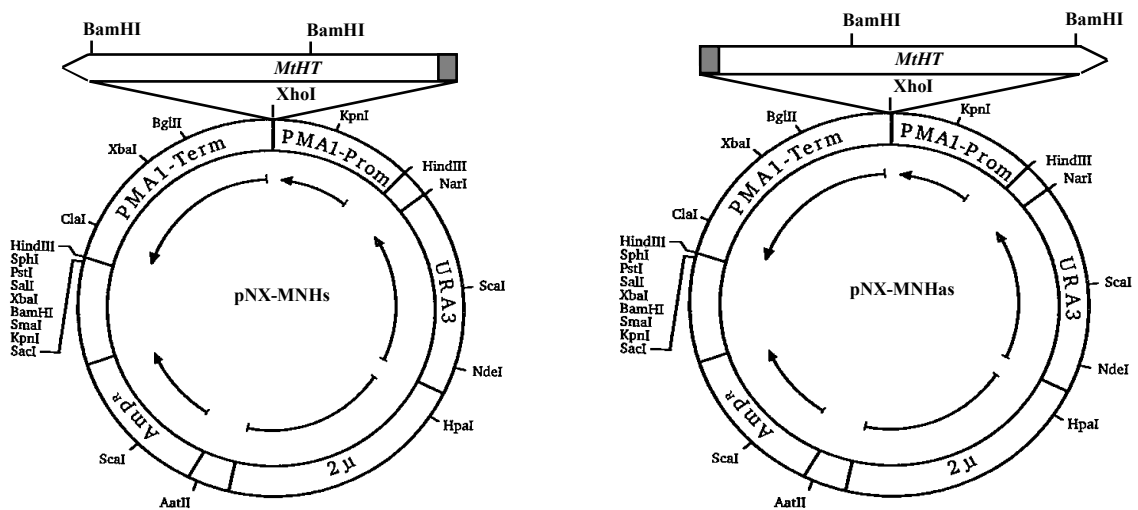


Figure 3.22. *E. coli* / *S. cerevisiae* shuttle vector pNEV-X (Sauer and Stolz, 1994), carrying the *MtHT* cDNA in sense (pNX-MNHs) and antisense orientation (pNX-MNHas), respectively.

3.5.1.2. Cloning of *DgHT* in pNEV-E

The same strategy was used to clone *DgHT* in the yeast expression vector pNEV-E, which is identical to pNEV-X except in that it contains an *EcoRI* instead of an *XhoI* site between promoter and terminator (Sauer and Stolz, 1994). The 5'-untranslated region of

DgHT was substituted by the 5'-untranslated region of *PmSUC2* by PCR with the following primers: PmDgHT-*for* 5'-CCG **GAA TTC** AAG CTT GTA AAA GAA *ATG CCG GCC GTC GGA GG-3' and PmDgHT-*rev* 5'-CTA AAA ATA ACC CTC CCC CCA AAC-3'. The forward primer contains the *EcoRI* restriction site (bold), the *PmSUC2*-5'-UTR (underlined) and the beginning of the ORF of *DgHT* (*), and the reverse primer is derived from the 3'-untranslated region of *DgHT*. The PCR product was cloned in pGEM-T Easy, and after its sequence had been confirmed, it was excised with *EcoRI*, using the *EcoRI* restriction sites in the primer PmDgHT-*for* at the 5'-end of the recombinant cDNA, and the *EcoRI* restriction site in the polylinker of the vector at the 3'-end. The fragment obtained, *PmSUC2*-5'-UTR-*DgHT*, was ligated in the *EcoRI* restriction site between the *PMA1*-promotor and the *PMA1*-terminator of pNEV-E. The plasmid with *DgHT* in sense orientation was named pE-DNHs, and the plasmid with *DgHT* in anti-sense orientation (negative control) was named pE-DNHAs. The plasmids are shown in Figure 3.23.

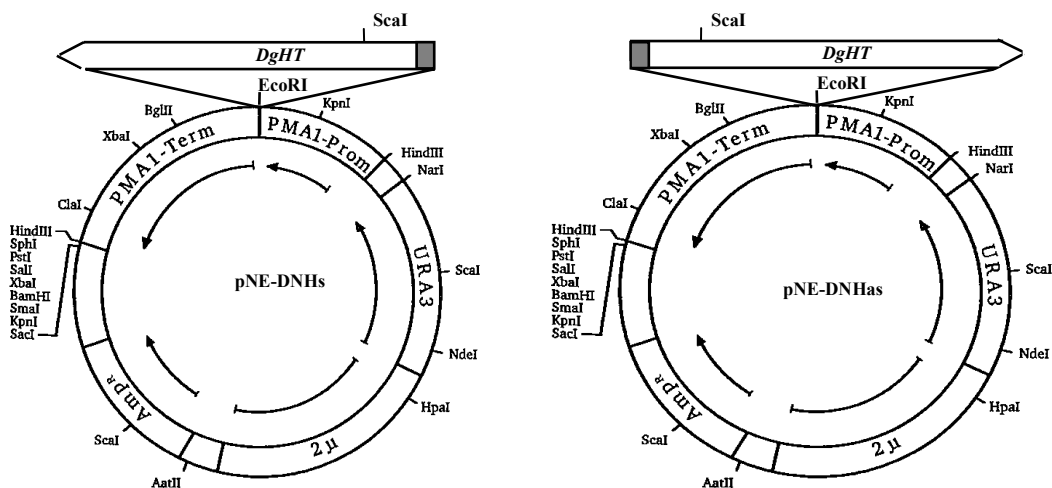


Figure 3.23. *E. coli* / *S. cerevisiae* shuttle vector pNEV-E (Sauer and Stolz, 1994) carrying the *DgHT* cDNA in sense (pNE-DNHs) and antisense orientation (pNE-DNHAs), respectively.

3.5.2. Sugar uptake studies with yeast strains expressing MtHT and *DgHT*

In the *Saccharomyces cerevisiae* strain EBY.VW4000 (Wieczorke et al., 1999), all endogenous hexose transporter genes have been deleted. It can be grown in maltose as carbon source. Therefore, this strain can be used to analyse substrate specificity and other characteristics of heterologous hexose transporters.

3.5.2.1. Functional characterization of MtHT

Hexose uptake studies with EBY.VW4000(pNX-MNHs) and EBY.VW4000(pNX-MNHs) did not reveal any uptake activity of MtHT. Of several monosaccharides tested as potential substrates (D-glucose, 3-O-methylglucose, D-galactose, D-fructose, D-mannose, D-xylose and D-ribose), none were taken up by either EBY.VW4000(pE-MNHs) or EBY.VW4000(pE-MNHs). This may be due to a PCR error in the sequence of MtHT since the original cDNA sequence was derived from a PCR product (3.4.1), the error might have accrued already during the original amplification. It is also possible that MtHT does not in fact represent a hexose transporter. It has been shown that a member of the PTR family of nitrate and oligopeptide transporters transports malate (Jeong et al., submitted). However, a PCR error is the most likely explanation.

3.5.2.2. Functional characterization of DgHT

Hexose uptake studies (see 2.26.) with EBY.VW4000(pNE-DNHs) and EBY.VW4000(pNE-DNHs) showed that DgHT accepts several monosaccharides as substrates (D-glucose \gg D-galactose \geq D-xylose $>$ D-mannose; see Figure 3.24). Under the same conditions no uptake of D-ribose, D-fructose and of the non-metabolizable glucose analogue 3-O-methylglucose (3-OMG) could be detected.

The K_m value of DgHT for glucose was 43 μM (Figure 3.25), which is in the range of K_m values of other plant sugar transporters, such as AtSTP1 in *Arabidopsis* (20 μM ; Stolz et al., 1994), VfSTP1 in *Vicia faba* (30 μM ; Weber et al., 1997), RcHEX3 in *Ricinus communis* (80 μM ; Weig et al., 1994). The V_{max} of DgHT amounts to 2 $\text{nmol } \mu\text{l}^{-1} \text{p.c. h}^{-1}$ (p.c., packed cells; see 2.26).

The energy dependence of monosaccharide transport by DgHT was analysed using D-glucose. No glucose transport was demonstrated in yeast cells expressing DgHT in antisense orientation (Figure 3.26). The results presented in Figure 3.26 show that DgHT catalyzes the uptake of glucose in an energy-dependent manner: (i) uptake rates for glucose increased in the presence of added energy source, namely the 1% ethanol, while (ii) uncouplers of transmembrane proton gradients, namely 50 μM 2,4-dinitro phenol (DNP) or 50 μM carbonyl cyanide-m-chlorophenylhydrazone (CCCP), completely abolished glucose uptake by DgHT.

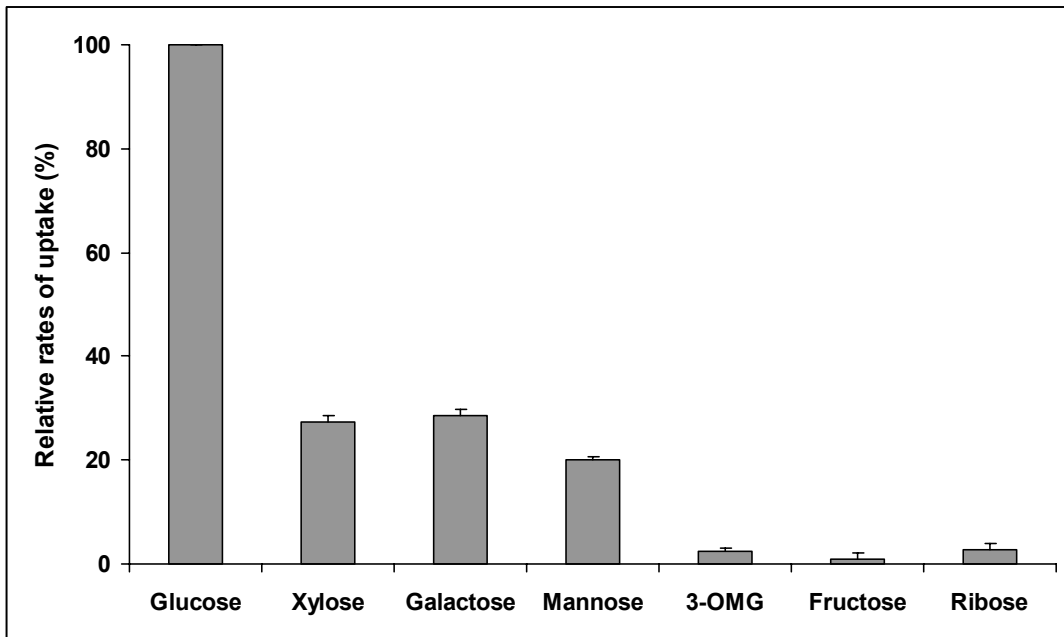


Figure 3.24. Substrate specificity of DgHT in *S. cerevisiae* EBY.VW4000. Uptake rates of varying substrates were compared with the glucose uptake rate, which was taken as 100% value (2.26).

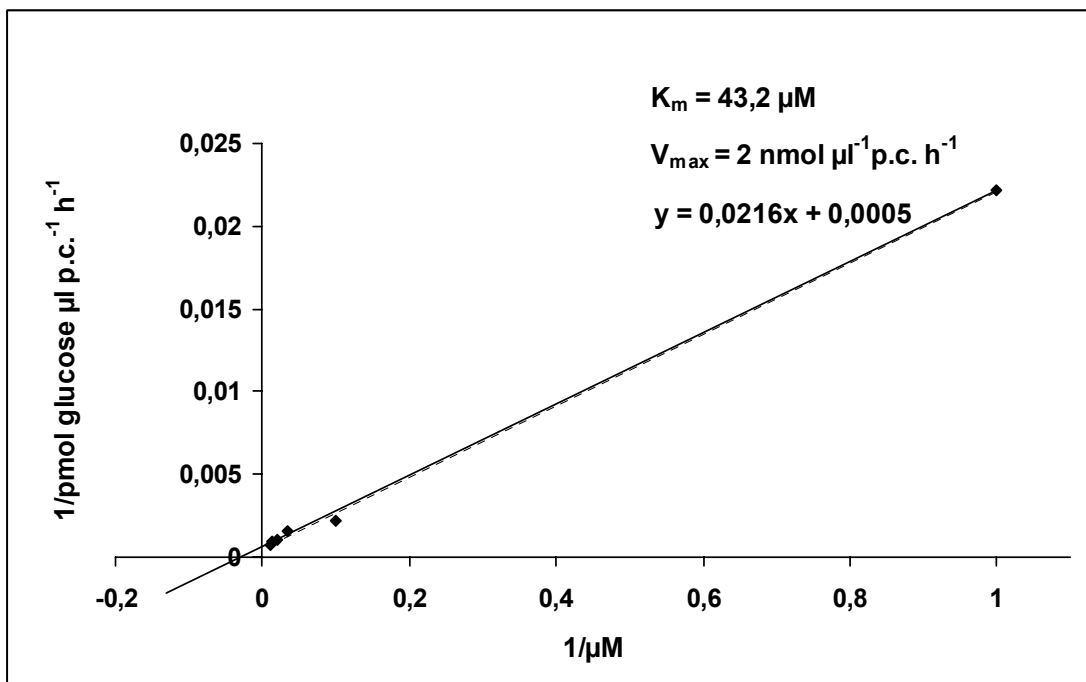


Figure 3.25. The Lineweaver-Burk diagram for determination of K_m and V_{max} of monosaccharide transporter DgHT. p.c., packed cells.

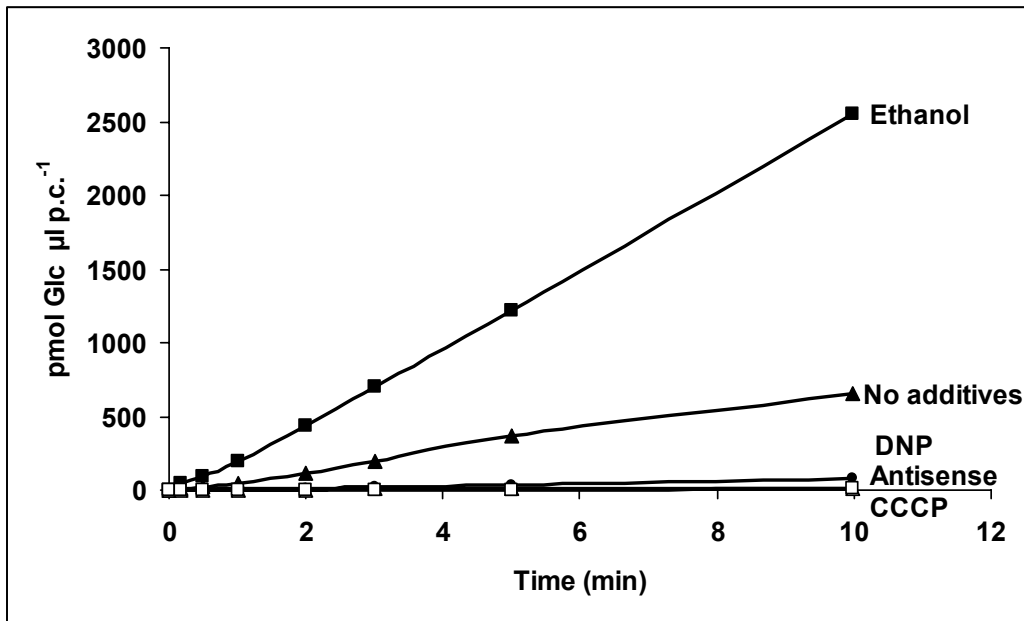


Figure 3.26. Functional characterization of DgHT in *S. cerevisiae* EBY.VW4000. Transport of ^{14}C -glucose was determined in *S. cerevisiae* cells expressing *DgHT* under the control of the *S. cerevisiae* plasmamembrane H^+ -ATPase (*PMA1*) promoter without additives (\blacktriangle), in the presence of 1% ethanol (\blacksquare), 50 μM 2,4-dinitrophenol (DNP, \bullet), or 50 μM carbonyl-cyanid-m-chlorophenylhydrazon (CCCP, \square). Transport of glucose into *S. cerevisiae* cells expressing *DgHT* in antisense orientation (Δ) was determined as negative control. The initial concentration of ^{14}C -D-glucose in the medium was 0.1 mM in all experiments.

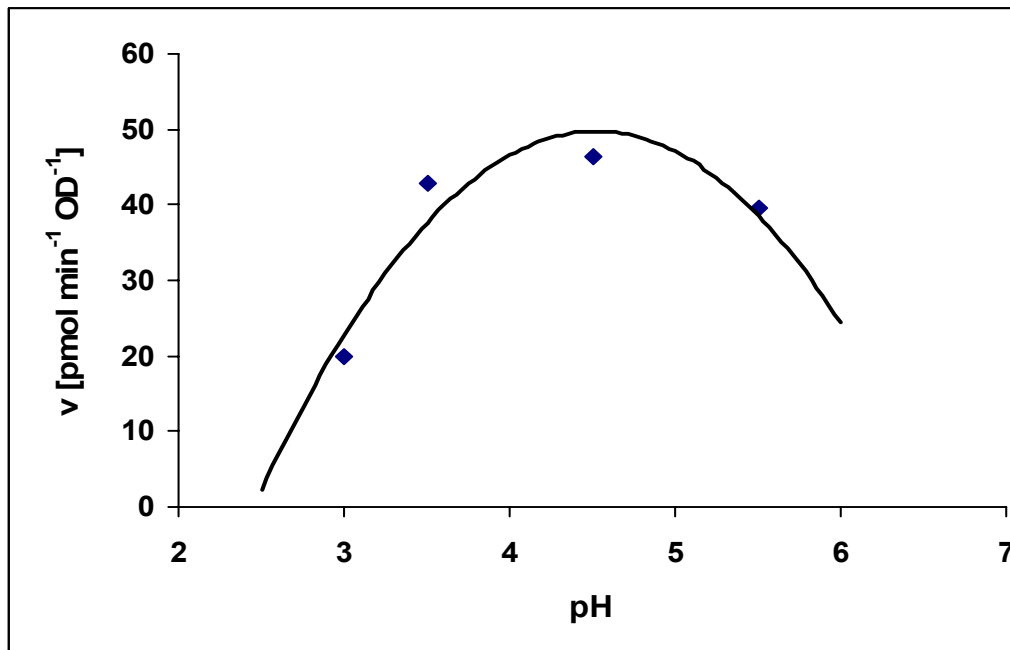


Figure 3.27. Uptake rates of ^{14}C -D-glucose by DgHT in *S. cerevisiae* EBY.VW4000 at different pH values. Two parallel samples were measured for each pH value.

These results show that like all other plant hexose transporters examined thus far, DgHT is a high affinity, energy-dependent monosaccharide transporter, probably a H⁺-symporter, with broad substrate specificity.

Relative rates of D-glucose uptake by DgHT were compared using buffer systems with different pH values (Figure 3.27). The pH optimum of DgHT is about 4.5, whereas the pH optimum of most other plant monosaccharide transporters examined is about 5.5 (M. Büttner, personal communication)

4. Discussion

Carbon partitioning in symbiotic structures is a complex phenomenon that depends on various morphological and biochemical features of both plant and microsymbiont. Three different symbiotic systems, one legume symbiosis (*Medicago truncatula* – *Sinorhizobium meliloti*) and two actinorhizal symbioses from different subclades of actinorhizal plants (Figure 1.4; *Datisca glomerata*, *Casuarina glauca*), were studied in order to understand carbon partitioning mechanisms in nitrogen-fixing root nodules.

There are two possibilities of sucrose unloading from the phloem - symplastically (through plasmodesmata from sieve elements directly into the cells of sink organs) or apoplastically (via specific transporters through membranes into the apoplast and then again by transporters into the next cells; see Figure 1.1). Analysis of expression levels and distribution of hexose and sucrose transporters, as well as of activities of sucrose degrading enzymes (sucrose synthase and invertases) and sugar contents in nitrogen-fixing root nodules was performed in order to understand carbon partitioning.

An important question for the understanding of nodule metabolism is which metabolites are delivered to the microsymbiont as carbon sources. In legumes, these metabolites are known to be dicarboxylic acids (Whitehead et al., 1995). The situation in actinorhizal plants is not yet clear but in analogy to the legume system, dicarboxylic acids have been suggested to be provided to symbiotic *Frankia* (Huss-Danell, 1997). However, in course of the analysis of hexose transporter expression patterns (Wabnitz, 1998) and of invertase activities in *Datisca* nodules in this study, results were obtained that suggested that the carbon sources for the microsymbiont in this plant were in fact hexoses.

4.1. Cytological information on putative mechanism of carbon transport in root nodules

Frequencies of plasmodesmal connections between specific cell types, as well as the presence of cell wall modifications that would block apoplastic transport, can yield information about transport mechanisms. No ultrastructural studies have been performed in this thesis, but literature data will be summarized here.

4.1.1. *Medicago*

Up to now, no comprehensive cytological analysis of *Medicago truncatula* nodules has been performed. Nevertheless, the results of the analysis of other legume nodules may be useful to understand *M. truncatula* nodule structure.

In seven of 27 legume genera examined, including *Medicago*, a special cell type with strongly developed cell wall protuberances, so-called transfer cells, was found in the pericycle of the vascular system (Pate et al., 1969). The inner side of these cells is opposed to the walls of xylem and phloem elements, indicating that apoplastic uptake of sugars from the phloem and/or secretion of nitrogenous compounds, particular amides, into the bundle apoplast, is taking place in these cells (Pate et al., 1969).

In *Vicia faba* nodules, symplastic movement of carbohydrates from the phloem via the vascular endodermis to the inner cortex is most probable, due to the endodermal Casparian band and extensive plasmodesmal connections (Abd-Alla et al., 2000). In the central tissue, plasmodesmata are also numerous at the interfaces of uninfected cells with infected and uninfected cells, but nearly absent between pairs of infected cells, as was shown for determinate nodules of *Glycine max* as well as for indeterminate nodules of *V. faba* (Selker and Newcomb, 1985; Abd-Alla et al., 2000). The extensive interconnection of uninfected cells and their connection to infected cells via plasmodesmata suggests that they play a role in metabolite transport. In contrast to the central tissue of determinate nodules, the low number of uninfected cells in the central tissue of indeterminate *V. faba* nodules suggests an additional apoplastic transport pathway to the infected cells in this plant (Selker and Newcomb, 1985; Abd-Alla et al., 2000).

Therefore, the following model of sugar transport could be proposed for *Medicago* based on cytological observations: sugar unloading from the phloem occurs via the apoplastic pathway and sugars could be transported to the infected cells symplastically using the symplastic network of uninfected cells, or apoplastically when the number of uninfected cells is insufficient.

4.1.2. Cytology of roots and nodules of *Datisca glomerata*

In the lobes of nodules formed on *Datisca* roots, infected cells are organized in a continuous patch that is up to 20 cell layers deep. This would render impossible the supply of nutrients from uninfected cells to infected cells, as it was supposed for *Medicago*. Roots of *Datisca* contain a multilayered pericycle with suberized cell walls (Pawlowski et al., submitted), indicating that post-phloem transport in roots is symplastic.

However, since the vascular system of nodules does not contain cells with suberized walls, both apoplastic and symplastic phloem unloading and post-phloem transport are possible here. However, the presence of fluorescent material, i.e. polyphenolics, in the walls of the endodermis of the nodule vascular system (Figure 4.1) indicates that here, apoplastic transport is blocked, so symplastic transport is needed to cross this cell layer.

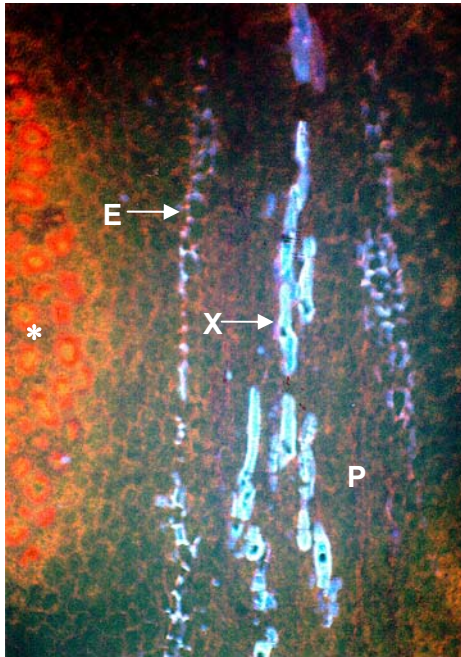


Figure 4.1. Dark field micrograph of a longitudinal section of a *Datisca* nodule lobe photographed under fluorescent light. No fluorescent material can be detected in the walls of the phloem (P) of the nodule vascular bundle, but the cell walls of the endodermis (E) show bright autofluorescence. The photographed region is located next to the fixation zone of the infected cells (*). X – xylem (Courtesy from K. Pawlowski, unpublished).

4.1.3. Cytology of roots and nodules of *Casuarina glauca*

In the cortex of nodules of *Casuarina*, infected and uninfected cells are interspersed. Cells infected by *Frankia* are characterized by strong lignification of their cell walls (Berg and McDowell, 1987b) that together with the low volume of intercellular space in the infection zone (Zeng et al., 1989) restricts oxygen diffusion and therefore protects the oxygen-sensitive bacterial nitrogenase. These morphological features disable apoplastic transport into infected cells. The cell walls of uninfected cells of the nodule cortex and cells of the multilayered pericycle of the nodule vascular system are not lignified (Pawlowski, 2002). No analysis of the distribution of plasmodesmata has been performed for *Casuarina* nodules to date, but the density of infected cells in the cortex is too high to postulate apoplastic sugar transport to the uninfected cells and symplastic transport from there to the infected cells. Altogether, based on current cytological information, symplastic transport of nutrients is expected to take place in the nodule cortex, while both symplastic

and apoplastic pathways are possible for phloem unloading and post-phloem transport to the nodule cortex.

4.2. Expression levels and patterns of hexose transporter genes in roots and nodules

According to the apoplastic model of phloem unloading, this pathway depends on the presence of several types of specific transporters that catalyse the membrane penetration of sugars (Eschrich, 1980; Sauer et al., 1994; Figure 1.1A). Therefore, apoplastic transport activities can be implied from the expression levels and patterns of sugar transporter genes.

4.2.1. *Medicago*

It has been shown in this study that in *Medicago*, apoplastic sugar transport as signified by the expression levels of hexose and sucrose uptake transporter genes (*MtHT* and *MtST*; Figure 3.18) plays a major role in roots. Similarly, M. Harrison (1996) has shown previously that the expression levels of the hexose transporter gene *MtSTP1* which is homologous but not identical with *MtHT*, were higher in roots of *Medicago* than in stems or in young or old leaves. The situation in nodules was different. The sucrose transporter *MtST* was expressed at extremely low levels in nodules, and expression of the hexose transporter *MtHT* in nodules could not be detected by RNA gel blot hybridization (Figure 3.18). In previous experiments, *Medicago* nodules had been grown in hydroponic culture in Fåhraeus medium (Fåhraeus, 1957) where nodules needed two times longer to develop than in aeroponic culture in Lullien's medium (Lullien et al., 1987). These plants had displayed the same high expression levels for *MtHT* and *MtST* in nodules as in roots (Wabnitz, 1998; Schubert et al., submitted). Therefore, while in roots the expression levels of sugar transporter genes seem to be independent of the growth conditions, in nodules this process is regulated, probably by oxygen supply. The data obtained indicate that sugar partitioning mechanisms in *Medicago* change from apoplastic in roots to symplastic in nodules in aeroponic culture. There are only few studies in wheat on the modulation of plasmodesmal-mediated cell-to-cell transport roots under anaerobic stress, that do not give a final answer if the plasmodesmata and assimilate transport become occluded under anaerobic stress conditions. On the one hand, it was shown that the electrical coupling ratio, which is a measure of plasmodesmatal resistance, between cortical cells of wheat

roots was not affected by the low oxygen treatment, suggesting that solute transport through the cytoplasmic annulus of plasmodesmata was not affected (Zhang and Tyerman, 1997). Moreover, the size exclusion limit (SEL) of the plasmodesmata rises under anaerobiosis (Cleland et al., 1994). On the other hand, there is a hypothesis that the transport through the plasmodesmata does not only involve the cytoplasmic compartment, but also the desmotubule which is part of the endoplasmic reticulum (ER) (Gamalei, 1994). In this context, Davies et al. (1987) have observed that the ER condenses into whorls when the energy charge is reduced by hypoxia. This may well account for the observation that there is a significant increase in molecular SEL, described by Cleland et al. (1994).

4.2.2. *Datisca*

Analysis of the expression levels of sugar transporter genes in *Datisca* showed a very strong induction of hexose transporter gene expression in nodules compared to roots (Figure 3.18). *In situ* localization of sugar transporter gene expression had been performed previously by Wabnitz (1998). Expression of the hexose transporter gene *DgHT* was found only in infected cells, while sucrose transporter (*DgST*) gene expression was detected at very low levels in the pericycle of the nodule vascular system adjacent to the senescence zone of infected cells. Expression levels of *DgST* in roots, nodules and leaves were below the detection limit for RNA gel blot hybridization. Hence, the sucrose transporter does not seem to play a major role in the *Datisca* – *Frankia* symbiosis. However, the hexose transporter gene expression pattern seems to indicate that infected cells take up large amount of hexoses from the apoplast.

In roots of *Datisca* low expression levels of sugar transporter genes were found, that indicating that here, sugar transport mostly occurs symplastically, which is consistent with the cytological data (4.1.2.).

4.2.3. *Casuarina*

RNA gel blot hybridization analysis of hexose transporter gene (*CgHT*) expression in *Casuarina* showed that it was somewhat induced in nodules compared to roots, resembling the situation in *Datisca*. However, all attempts to determine the expression pattern of *CgHT in situ* failed. Since the walls of these cells are lignified (Berg and McDowell, 1987b), which would block apoplastic transport, it is extremely unlikely that

hexose transporters are responsible for the uptake of hexose from the apoplast into infected cells in *Casuarina* nodules.

Since up to date, no fragments of *Casuarina* sucrose transporter genes have been amplified, the expression levels of sucrose transporter genes could not be determined in this plant. Thus, it is impossible to propose a model of sugar transport in *Casuarina* nodules based on the expression of sugar transport protein genes.

4.3. Activities and localization of sucrose degrading enzymes in roots and nodules

Utilization of sucrose as a source of carbon and energy depends on its cleavage into hexoses, and in plants this reaction is catalysed either by sucrose synthase (SuSy) or by one of the several isoforms of invertase (cytosolic, apoplastic or vacuolar). In this study the activities of sucrose-cleaving enzymes in roots and nodules of *Medicago*, *Datisca* and *Casuarina* were compared.

4.3.1. Invertases

Different functions have been proposed for the three different types of invertases. Apoplastic invertase is known to participate in phloem unloading by cleaving apoplastic sucrose which allows the subsequent uptake of hexoses into sink cells (Eschrich, 1980). Vacuolar invertase has been proposed to be involved in osmoregulation and cell enlargement and in the control of sugar composition in fruits and storage organs (Sturm and Tang, 1999). The role of cytosolic invertase is unknown, except that it has been proposed to be involved in channelling sucrose into catabolic pathways (Sturm, 1999).

Apoplastic invertase activity is decreased in nodules compared to roots in all three symbiotic systems studied (Figure 3.11). This indicates that in nodules in general, apoplastic sugar transport involving the hydrolysis of sucrose in the apoplast is strongly reduced. Even in *Datisca* and *Casuarina* nodules, where hexose transporter expression was found to be induced compared to roots (Figure 3.18), apoplastic invertase activity was reduced more than ten-fold compared to roots in *Datisca* and almost eight-fold in *Casuarina* (see Table 4.1).

Table 4.1. Invertase activities in roots and nodules (one representative result of three experiments is shown). These data have been presented graphically in Figure 3.11.

Plant species	Plant organ	INVERTASE activity [nmol sucrose cleaved min ⁻¹ mg ⁻¹ protein]			
		apoplastic	cytosolic	vacuolar	sum
<i>Medicago truncatula</i>	Roots	0.992 ± 0.025	0.355 ± 0.017	0.469 ± 0.074	1.816
	Nodules	0.078 ± 0.008	0.532 ± 0.069	0.030 ± 0.006	0.64
<i>Datisca glomerata</i>	Roots	1.549 ± 0.227	1.867 ± 0.367	9.467 ± 0.967	11.489
	Nodules	0.136 ± 0.034	0.133 ± 0.33	0.733 ± 0.067	1.002
<i>Casuarina glauca</i>	Roots	5.326 ± 0.200	4.083 ± 0.04	2.083 ± 0.104	11.447
	Nodules	0.706 ± 0.043	0.571 ± 0.29	2.143 ± 0.202	3.42

Localization of acidic, i.e. apoplastic or vacuolar invertase activity in roots by *in situ* activity staining (Figure 3.13) showed that in *Medicago* roots, acidic invertase activity is present all over the cortex, which is in agreement with the apoplastic and vacuolar invertase activities and high hexose transporter expression levels in *Medicago* roots (Figure 3.18; Table 4.1). Thus, high activities of apoplastic sugar transport involving the hydrolysis of sucrose in the apoplast and the uptake of hexoses are present in the root cortex of *Medicago*.

In *Datisca* roots, however, all acidic, i.e. vacuolar and apoplastic invertase activity was present in the stele, not in the cortex (Figure 3.13). Since uptake of hexoses from the apoplast is required after the apoplastic hydrolysis of sucrose, it can be presumed that in roots, the weak hexose transporter expression is confined to the stele as well. The very high vacuolar invertase activities determined for *Datisca* roots (Table 4.1) have also to be confined to the stele.

Slightly increased cytosolic invertase activities were observed in *Medicago* nodules compared to roots. Elevated cytosolic invertase activities have been found also in potato tubers, where they led to increased carbon flux towards glycolysis and to the accumulation of phosphorylated intermediates (Hajirezaei et al., 2000). In contrast, a strong reduction of cytosolic invertase activities in nodules compared to roots was found in *Datisca* and *Casuarina*. Again, the elevated cytosolic invertase activity in *Medicago* nodules does not exceed the reduced cytosolic invertase activity in *Casuarina* nodules which comprises only about 14 % of the cytosolic invertase activity in *Casuarina* roots.

Vacuolar invertase activity is reduced in *Medicago* and *Datisca* nodules compared to roots, but is similar in roots and nodules of *Casuarina*. It should be pointed out that although vacuolar invertase activity is dramatically reduced in *Datisca* nodules compared to roots, the remaining activity in *Datisca* nodules is still about 20 times higher than in *Medicago* roots (Table 4.1). The high vacuolar invertase activities in *Casuarina* and *Datisca* nodules, compared to nodules of *Medicago* (see Table 4.1) may be related to different requirements for turgor control in actinorhizal versus legume nodules. The mechanism of cell infection is different in actinorhizal nodules than in *Medicago*. In actinorhizal nodules, no complete endocytotic process takes place but the perisymbiont space remains continuous with the apoplast (Mylona et al., 1995). This aspect might necessitate specific mechanisms for turgor control. However, more symbiotic systems have to be examined before such a conclusion can be drawn.

To summarize the data on invertase activities, *Medicago* is characterized by comparatively low activities of all three invertase types – apoplastic, cytosolic and vacuolar – compared to *Datisca* and *Casuarina*. The reduction of total invertase activities in nodules compared to roots, however, is about three times stronger in *Datisca* than in the two other systems. The *in situ* staining results for acidic invertase activity in roots indicate that phloem unloading involves apoplastic transport in *Datisca* (Figure 3.13B). However, post-phloem transport mechanisms in *Medicago* and *Datisca* roots obviously differ, with apoplastic mechanisms dominating in *Medicago*. This is consistent with the results about sugar transporter gene expression levels.

The roots of the two actinorhizal plants differ in respect to their invertase activity distribution among isoforms. In *Datisca* roots, vacuolar invertase plays a major role, whereas in *Casuarina* roots activities of both apoplastic and cytosolic invertases are high, and vacuolar invertase activity is lower (2.1 ± 0.1 nmol sucrose cleaved/min/mg protein (vacuolar) in comparison to 4.1 ± 0.04 (cytosolic) and 5.3 ± 0.2 (apoplastic) activity).

As was mentioned above, the common feature of all systems studied here is a clear reduction of apoplastic invertase activity in nodules compared to roots. This means that the apoplastic transport of sucrose followed by hydrolysis in the apoplast is strongly reduced in nodules compared to roots.

4.3.2. Sucrose synthase (SuSy)

SuSy is recognized as an important enzyme of sucrose utilization in plant sink tissues (Ho et al., 1988). SuSy is a globular protein and thus is generally considered to be soluble in the cytosol. However, some percentage of the enzyme is known to be associated with the plasma membrane, perhaps in a specific complex with glucan synthase, producing

cellulose and/or callose (Amor et al., 1995; Carlson and Chourey, 1996). Part of the soluble fraction of sucrose synthase seems to be associated with the actin cytoskeleton (Winter et al., 1998).

Since in all three types of nodules, invertase activities were reduced in nodules compared to roots, it can be concluded that SuSy has a dominant function in nodule sugar metabolism. This is in agreement with results of Gordon et al. (1999) on a pea mutant with a defect in the SuSy gene expressed in nodules, which caused a dramatic reduction of nitrogenase activity, and thus led to an inefficient symbiosis. SuSy activities are expected to be increased in nodules compared to roots, since a strong increase of sucrose synthase transcription levels in nodules has been reported for the SuSy genes of soybean (Thummler and Verma, 1987), *Medicago* (Hohnjec et al., 1999) and broad bean (Küster et al., 1993). However, in this study, more or less equal SuSy activities were found in nodules and roots of *Medicago* and *Datisca* (see 3.2.2). This is particularly surprising when considering that there is clear transcriptional induction of SuSy in both systems (Figure 3.16) and that in *Datisca*, a corresponding increase of SuSy protein amounts was found in nodules compared to roots (Figure 3.17). However, there was no increase of SuSy protein in *Medicago* nodules compared to roots in spite of the transcriptional induction of the SuSy gene (Figures 3.16 and 3.17). A similar situation has already been described for the SuSy gene *sh1* in maize roots, where the increase of *sh1*-mRNA levels under anaerobic conditions was not reflected to the same degree in SS1 protein amounts which showed no detectable increase (McElfresh and Chourey, 1988; Taliercio and Chourey, 1989). In contrast, the transcription levels of the other maize gene coding for sucrose synthase SS2, *sus1*, decreased during anaerobic stress as indicated by the reduced amounts of *sus1* mRNA in root tissue, while SS2 protein levels actually increased in the root tip (McElfresh and Chourey, 1988). In summary, for maize roots it has been shown that the expression of both SuSy genes is regulated at both the transcriptional and the translational level, and that both levels of regulation may act against each other (McElfresh et al., 1988; Taliercio and Chourey, 1989). Thus, translational regulation of SuSy mRNA could also occur in root nodules, particularly in the infected zone where oxygen-limited conditions are established for nitrogenase function (Vance and Heichel, 1991).

Moreover, recently it was shown that pea contains three different isoforms of sucrose synthase (Sus1, Sus2 and Sus3), and that the genes encoding these different isoforms have distinct patterns of expression in different organs of the plant as well as during organ development (Barratt et al., 2001). The presence of at least two SuSy isoforms was detected immunologically in *Medicago* roots using antibodies raised against SuSy from *Vicia faba* (Ross and Davies, 1992), while only one immunologically active

SuSy isoform was found in nodules (see 3.3.2; Figure 3.17). One of the isoforms detected was somewhat larger than the major isoform. This confirms the results of Hohnjec et al. (1999), who found only one SuSy isoform in nodules of eight different legumes, but two isoforms of SuSy in root and stem extracts of *Medicago*. Studying of the partial cDNA sequences from *Medicago truncatula* at www.tigr.org shows that *Medicago* contains at least five different SuSy genes, with DNA homologies to the *Vicia faba* probe used in this study ranging from 67% to 91% (data not shown). Taking into account the existence of multiple SuSy isoforms, one could also propose that discrepancy between the SuSy expression pattern on the mRNA level and on the level of protein amount and enzyme activity is the consequence of incomplete detection of isoforms in *Medicago* using a cDNA probe from *Vicia faba* (Küster et al., 1993). To date, only a single isoform of SuSy has been characterized from *Vicia faba* (Ross and Davies, 1992), whereas for *Pisum sativum* it has been shown that one of its three SuSy isoforms, Sus2, has less sequence similarity with the two other isoforms than they share among each other (only 70-71 % identity; Barratt et al., 2001). However, Sus3 was found to be only expressed at very low levels. On RNA gel blots containing total RNA, only expression levels in flowers and young testas were high enough for detection, while analysis of Sus3 expression using RNA gel blots with poly(A⁺) RNA revealed that the transcript was also present in nodules, but not in roots (Barratt et al., 2001). Hence, if *Medicago* nodules would contain two larger very homologous SuSy isoforms, while roots contained only one of them, an induction of SuSy expression in nodules compared to roots would be apparent in RNA gel blot hybridizations, but not on the protein level. Furthermore, considering the translational regulation of SuSy (Winter and Huber, 2000), it is possible that only one of the mRNAs for the major isoforms is translated, leading to similar protein levels and enzyme activities of SuSy in *Medicago* roots and nodules in spite of an apparent transcriptional induction.

A study of literature shows that for SuSy a broad analysis of gene expression, protein quantities and presence of isoforms has been performed in different legumes (see e.g. Thummler and Verma, 1987; Buchner et al., 1998; Hohnjec et al., 1999; Küster et al., 1993; Ross and Davies, 1992; Barratt et al., 2001). However, comparisons of SuSy enzyme activities were performed only on nodules grown under different nutrient conditions and stresses, which led to the conclusion that SuSy activity is sufficient for normal nodule function (e.g. González et al., 1995; Gordon et al., 1997). Except for this thesis, SuSy activities in roots and nodules have never been compared so far.

One of the known mechanisms of posttranslational regulation of SuSy activity is the reversible protein phosphorylation (Winter and Huber, 2000). Based on the results for phosphorylation of recombinant SuSy, it has been suggested that phosphorylation specifically activates sucrose cleavage (Nakai et al., 1998). Apart from its effects on SuSy

activity, phosphorylation/dephosphorylation of SuSy seems to play a role in the distribution of the enzyme between cytosol, plasma membrane, and actin cytoskeleton (Winter et al., 1997; Winter et al., 1998). Taking into account that the K_m of non-phosphorylated recombinant SuSy protein for sucrose is several folds higher than that of phosphorylated enzyme, it is possible to explain the lack of increase in SuSy activity in *Datisca* nodules compared to roots by dephosphorylation of part of the total SuSy protein, causing plasma membrane association and a decrease in enzyme activity. It is known that SuSy protein associated with the plasma membrane is involved in cell wall biosynthesis (Amor et al., 1995). The uptake of the microsymbiont into infected cells and its embedding in a polysaccharide-rich cell wall-like matrix necessitates higher activities of synthesis of cell wall-like material in nodules than in roots. Therefore, a change in the distribution of SuSy protein in nodules relative to roots, with an increased fraction of the total SuSy protein being associated with the plasma membrane may reflect the demands of the root nodule symbiosis.

4.4. The *Datisca* nodule paradox: hexose transporter expression in the absence of apoplastic invertase activity. Could hexoses be the carbon sources for symbiotic *Frankia* in *Datisca* nodules?

As mentioned above, in nodules of *Datisca* apoplastic invertase activity was practically absent (Figure 3.11B), indicating that no apoplastic sugar transport occurs that relies on the hydrolysis of sucrose in the apoplast and the uptake of hexoses. However, in spite of the absence of apoplastic invertase activities, a hexose transporter was found to be expressed in nodules at high levels (Figure 3.18), and *in situ* hybridization showed that it was expressed specifically in the infected cortical cells (Wabnitz, 1998). These data could be interpreted to mean that the hexose transporter is working as an exporter to supply endosymbiotic *Frankia* with carbon sources.

In analogy to legume nodules, where the bacteria are supposed to be supplied with dicarboxylic acids by the host plant (see e.g. Streeter, 1995), it has been assumed that dicarboxylic acids might also be the carbon source for symbiotic *Frankia*. While the analysis of enzyme activities in *Frankia* vesicle clusters isolated from nodules of *Alnus* and *Hippophae* yielded results consistent with this hypothesis (Akkermans et al., 1983), experiments on $^{14}\text{CO}_2$ uptake of detached *Alnus* nodules were inconclusive (Huss-Danell, 1990; summarized by Huss-Danell, 1997). Isolated *Frankia* strains have been divided into two genomic groups based on DNA reassociation kinetics (Lechevalier and Lechevalier, 1990). In the free-living state, *Frankia* strains of genomic group A tend to grow fairly on

both sugars and organic acids, while strains of genomic group B grow variably on organic acids and poorly, if at all, on sugars (Lechevalier and Lechevalier, 1990; Benson and Schultz, 1990). The endosymbiont of *Datisca*, however, has not been isolated yet and based on its 16S rRNA and *nifH* gene sequences, does not belong to any group of *Frankia* strains isolated so far (Mirza et al., 1994; Normand et al., 1996; Figure 1.4). Thus, based on the data available, the carbon preferences of the endosymbiont of *Datisca* cannot be determined, and the strains might be able to grow on hexoses as carbon sources.

In summing up, there is no physiological evidence to contradict the hypothesis that this group of strains in particular, or *Frankia* strains in general, are fed hexoses during symbiosis. Based on the results presented in this study and *in situ* hybridisation data of Wabnitz (1998), it is conceivable that in analogy to symbiotic nitrogen-fixing cyanobacteria in *Gunnera* (R. Parsons, personal communication), endosymbiotic *Frankia* is supplied with hexoses in nodules of *Datisca*.

4.5. Hexose transporters from nodules

As described above, an unusual function has been suggested for the hexose transporter from *Datisca* nodules. Preliminary sequence information had also indicated that the hexose transporter from *Medicago* nodules belongs to a different subfamily than all other hexose transporters published thus far (see sequence alignment in Figure 3.21; Table 3.2). Therefore, the full length cDNA sequences of the hexose transporters MtHT and DgHT were amplified from *Medicago* and *Datisca* nodules and sequenced for further analysis.

The amino acid sequences and the predicted secondary structure of DgHT were highly similar to those of other monosaccharide transporters from plants, with the highest homology to AtSTP1 from *Arabidopsis* (Table 3.2; Sauer et al., 1990). The analysis of the full sequence of MtHT confirmed that this hexose transporter belongs indeed to a different subfamily of transporters than AtSTP1, -2, -3 or -4, but its sequence is less dissimilar to those of other hexose transporters than that of *Arabidopsis* AtSTP2. AtSTP2 contains two insertions compared to other known hexose transporters from *Arabidopsis* as well as to MtSTP1, MtHT and DgHT (see sequence alignment in Figure 3.21; Table 3.2).

To analyse the functional characteristics of DgHT, the cDNA was cloned in yeast expression vectors and fused to the strong promoter of the yeast plasmamembrane H⁺-ATPase (*PMA1*; Serrano et al., 1986) and the 5'-UTR of the sucrose transporter *PmSuc2* from *Plantago major* which has been shown to result in high translation activities in yeast

(N. Sauer, personal communication). DgHT was shown to represent a hexose transporter with a broad substrate specificity, with the highest affinity to glucose, but also transporting to a less extent D-galactose, D-xylose and D-mannose. DgHT did not transport fructose or L-rhamnose. Regarding substrate specificity, DgHT has more in common with the hexose transporter AtSTP3 from *Arabidopsis* than with AtSTP1 (Büttner and Sauer, 2000). However, AtSTP3 has a K_m of 2 mM for glucose, while other hexose transporters have K_m values for glucose in the micromolar range, like DgHT with 43 μ M (Figure 3.25). Hence, regarding substrate affinity DgHT does not resemble AtSTP3 at all. Furthermore, AtSTP3 was the first monosaccharide transporter not to be expressed in sink tissues (Büttner et al., 2000), while DgHT is expressed in at least two types of sink organs, namely at high levels in *Datisca* nodules and at low levels in roots, while no *DgHT* transcripts were detected in leaves by RNA gel blot hybridization (Figure 3.18). At any rate, these comparisons show that hexose transporters of the same sequence group can have different substrate specificities.

The most unusual feature of DgHT is its pH optimum which is more acidic (about 4.5; Figure 3.27) than it is known for other monosaccharide transporters with the pH optima lying in the range of 5.5 (M. Büttner, personal communication). It is known that the peribacteroid space in infected cells of legume nodules is more acidic than the apoplast (Blumwald et al., 1985), which is also the case for the periarbuscular space in infected cells of arbuscular mycorrhizal roots (Guttenberger, 2000). In analogy, it can be assumed that the perisymbiont space in infected cells of actinorhizal nodules is also more acidic than the apoplast. A more acidic pH optimum of a transporter specific to the perisymbiont membrane (as implied by its supposed function in feeding the bacteria) would correspond with a location in the perisymbiont membrane. This increased pH gradient between cytosol and perisymbiont space would make the export of sugars in a proton-symport mechanism more difficult, but facilitate the uptake of sugars by the symbiotic bacteria.

Up to now, plant sugar transporters could only be shown to be active in sugar uptake (reviewed by Caspari et al., 1994), although activity in sugar export has been discussed for a sucrose transporter (Truernit and Sauer, 1995) based on its expression pattern and on comparisons of metabolite concentrations in apoplast and cytosol (Lohaus et al., 1995). Interestingly, the only hexose transporter tested *in vivo* and *in vitro* (HUP1 from *Chlorella kessleri*), was found to catalyze strict H⁺-monosaccharide symport (uptake) when expressed in yeast but was facilitating glucose diffusion in both directions when used *in vitro* in artificial vesicles (Caspari et al., 1996). Another example that raises questions about the reliability of transport directions determined in yeast is a recently identified zinc transporter from the peribacteroid membrane of soybean nodules, GmZIP1 (Moreau et al., 2002). When expressed in yeast, it only catalyzes zinc uptake, but this

direction of transport is extremely unlikely in the homologous system where the plant supplies the microsymbiont with micronutrients and not *vice versa*. Thus, the membrane environment seems to be able to influence a transporter's activity, which might allow the hexose transporter of *Datisca* to perform glucose export when present in the perisymbiont membrane of infected nodule cortical cells.

4.6. Nodule and root sugar contents

The steady state levels of soluble sugars in a plant organ can yield information about metabolism. To complete the analysis of sugar partitioning in nodules, soluble sugars were extracted from nodules and roots of the three model plants and analysed by HPLC (Figures 3.1 - 3.3).

4.6.1. Sucrose, glucose and fructose in nodules and roots

A comparison of the amounts of sucrose, glucose and fructose in roots and nodules of the three model plants shows several interesting aspects.

Unusually high sucrose concentrations were found in *Casuarina* nodules (Figure 3.2; Table 4.2). This phenomenon is probably due to the fact that in contrast with *Medicago* and *Datisca* nodules, no starch biosynthesis takes place in *Casuarina* nodules which means that sucrose may serve as carbon storage form. In other systems, sucrose has been shown to be able to serve as long term carbon storage form, e.g. in sugar beet (Reinefeld et al., 1986) or as transient carbon storage form, e.g. in barley leaves (Riens et al., 1994).

The absence of fructose in extracts of *Medicago* nodules and roots (Figure 3.1; Table 4.2) is probably caused by high fructokinase (FK) activities, which are often linked with the operation of sucrose syntase (SuSy). A similar situation has been found in potato tubers, where fructokinase has been suggested to reduce cytosolic fructose contents in order to maintain a high SuSy-catalysed net flux of sucrose to phosphorylated hexoses (Renz and Stitt, 1993; Appeldoorn et al., 1997). Both FK and SuSy genes are expressed in similar fashion during the development of sink tissues and both enzymes are inhibited by elevated fructose concentrations (Schaffer and Petreikov, 1997). Therefore, it is likely to be important to effectively remove fructose to maintain high SuSy activities, which are essential for nitrogen fixation in nodules (Gordon et al., 1999).

In contrast to *Medicago*, both *Datisca* and *Casuarina* nodules contain fructose, but the comparison of the glucose:fructose ratio in roots and nodules reveals differences in the two actinorhizal symbioses. The increase of the glucose:fructose ratio in *Datisca* nodules compared to roots (Table 4.2) could be a result of increased FK activity, as was shown for stolon tips of potato during tuberization (Davies, 1984). In *Casuarina*, the glucose:fructose ratio does not change remarkably between roots and nodules (Table 4.2). This is surprising, since the reduction of invertase activities in *Casuarina* nodules compared to roots, like in *Medicago* and *Datisca*, seems to imply that here, SuSy plays the major role in sucrose hydrolysis. Like in potato tubers, the phosphorylated hexoses produced from sucrose by SuSy in *Medicago* and *Datisca* nodules could be not only used for the synthesis of cell wall-like material and for nodule metabolism, but also for starch biosynthesis. Both *Medicago* and *Datisca* nodules contain large amounts of starch grains while only *Casuarina* nodules are starch-free (*Medicago*: Vasse et al., 1990; *Datisca*: Okubara et al., 1999; *Casuarina*: E. Duhoux, personal communication). Therefore, these facts may be responsible for the difference in sugar ratios.

Table 4.2. Sugar ratios in roots and nodules of *Medicago*, *Datisca* and *Casuarina*

Plant	Sucrose/Hexoses		Glucose/Fructose	
	root	nodule	root	nodule
<i>Medicago</i>	2.1	2.3	no fructose	no fructose
<i>Datisca</i>	0.9	0.4	0.32	0.55
<i>Casuarina</i>	1.2	2.4	0.6	0.63

Absolute hexose concentrations in nodules (glucose and fructose) are higher in actinorhizal nodules (12.5 $\mu\text{mol/g}$ FW and 7.2 $\mu\text{mol/g}$ FW in *Datisca* and *Casuarina*, respectively) than in *Medicago* nodules (4.2 $\mu\text{mol/g}$ FW). These values are also higher in actinorhizal nodules than in the corresponding roots, especially for *Datisca*, where nodule hexose concentrations exceeded concentrations in roots more than six fold (Figure 3.3). In comparison with *Medicago* nodules, increased hexose concentrations in actinorhizal nodules might point at an essential difference between rhizobial and actinorhizal symbioses. This difference cannot be connected to starch metabolism, since here *Casuarina* is different from both *Medicago* and *Datisca*. The hexose concentrations might be dependent solely on invertase activities, regardless of the localization of the isoforms, since the interconnection between futile cycles of sucrose/hexose hydrolysis/synthesis enables the interchange of sugars between apoplast, cytosol and vacuole (Nguyen-Quoc

and Foyer, 2001). The sum of invertase activities is similar in nodules of *Datisca* and *Medicago*, but more than five times higher in *Casuarina* than in *Medicago* nodules (Table 4.1).

As described in 4.3.1 it is possible that the high hexose contents of actinorhizal nodules are required for the osmoregulation that is needed to allow the infection of cells by branching *Frankia* hyphae. In *Medicago*, the uptake of bacteria into infected cells occurs by a complete endocytosis-like process resulting in the formation of symbiosomes. In actinorhizal plants, continuous invagination of the plasma membrane during the infection process requires different turgor control mechanism (Mylona et al., 1995). Interestingly, vacuolar invertase has been implicated in increasing hexose concentrations in source organs during water stress, i.e. particularly in turgor control (Kim et al., 2000). This might be a reason for the high hexose contents of actinorhizal nodules, which contain significantly higher vacuolar invertase activities than *Medicago* (Figure 3.11). Unfortunately, hexose localization in nodules is not possible since *in situ* glucose staining does not work on infected cells (see Figures 3.14A and B as well as 3.2.3.1.).

4.6.2. *Datisca* contains novel non-structural rhamnosyl saccharides

4.6.2.1. Free rutinose and methylrutinose are found in *Datisca* sugar extracts

In extracts of roots and nodules of *Medicago*, *Datisca*, and *Casuarina*, several compounds were present that could not be identified by comparison with the HPLC standards used. The two unknown compounds that were present at high concentrations in *Datisca* nodules were isolated and named M and D. Due to their behaviour in HPLC, M and D were initially assumed to represent a sugar alcohol and a flavone glycoside, respectively. Their structures were determined using NMR, mass spectroscopy, the NMR correlation spectroscopy methods H,H-COSY and C,H-COSY as well as acid and enzyme hydrolysis and HPLC analysis of the hydrolysis products (see 3.1.3.1.). Based on these analyses, M represents a α -L-rhamnopyranosid-(1 \rightarrow 6)-(1-O- β -D-methylglucose (methylrutinose) and D represents α -L-rhamnopyranosid-(1 \rightarrow 6)-glucose (rutinose) (see Figure 3.6).

The isolation and identification allowed the preparation of concentration standards of methylrutinose and rutinose. Based on the real concentrations of these two sugars in *Datisca* extracts could be determined (Figure 3.10). The new results showed that rutinose is the sugar with the highest concentration in roots as well as in nodules with concentrations of about 90 and 200 μ mol/g FW, respectively. Rutinose was also found in leaves of *Datisca*, but in much smaller concentrations (about 11 μ mol/g FW) that are comparable with the concentrations of sucrose in leaves (see 3.1.3.2). Thus, rutinose was not only present in sink organs, but also in source organs. The concentrations of all

sugars in *Datisca* extracts except for rutinose are presented in Figure 4.2 to allow a more precise comparison using a smaller scale than necessitated by the high concentrations of rutinose in Figure 3.10. It can be seen that the concentrations of methylrutinose do not differ dramatically from those of the other sugars in the corresponding plant organs, except that leaves contain more sucrose than methylrutinose and nodules *vice versa* (Figure 3.10).

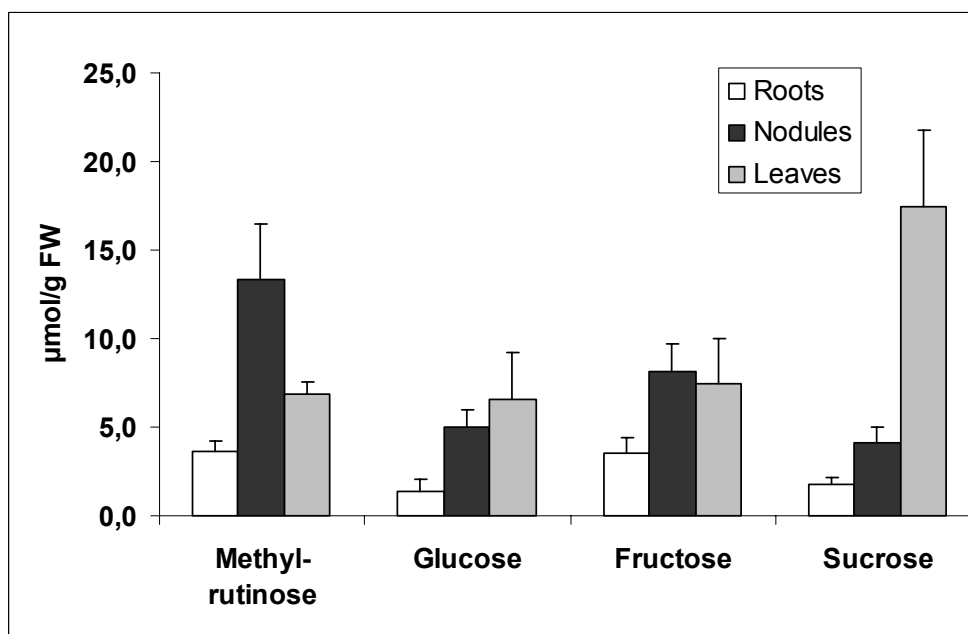


Figure 4.2. Concentrations of methylrutinose, glucose, fructose and sucrose in roots, nodules and leaves of *Datisca*. Data for rutinose are omitted (see Figure 3.10). Average values of three parallel samples are shown.

4.6.2.2. Possible ways of rutinose and methylrutinose synthesis

A study of the literature on plant glycosides showed that rutinose has not been described as free plant sugar, but only as glycoside part of many flavone glycosides, e.g. rutin, galangin, cannabigin, datiscin and datinoside, which have been isolated and characterised from the only other *Datisca* species besides *Datisca glomerata*, *Datisca cannabina* (Zapesochay and Pangarova, 1976). Datiscin represents 5,7,2'-trihydroxyflavone-3-O-rutinose (Zapesochay et al., 1982). Methylrutinose is also not known among free plant metabolites.

Many plant glycosides such as flavonoides, cardenolides, phenols, sterols, coumarins and others, contain a disaccharidyl unit and sometimes even a larger oligosaccharide. The synthesis of these glycosides involves stepwise, sequential transglycosylations from the proper sugar nucleotide donors. The degradation of the glycosides is the sequential removal of the monosaccharides by exoglycosidases.

However, in several cases small amounts of intact disaccharides could be removed from the aglycon by what may be a specific enzymatic "endo"-hydrolysis, catalysed by enzymes called "disaccharidases" or "diglycosidases" (Avigad, 1982). The enzymes degrading a rutinose-containing flavone glycoside, rutin (quercetin-rutinose), were found in seeds of *Fagopyrum* sp. and of *Rhamnus* sp., and two different rutin degrading disaccharidases were purified from tartary buckwheat seeds (*Fagopyrum tataricum*; Yasuda and Nakagawa, 1994; for *Rhamnus* see Charaux, 1925, cited after Zapesochneya and Pangarova, 1976). The roots of *Datisca cannabina* also contain an enzyme hydrolyzing 3-rutinosides of flavones (Favre-Bonvin et al., 1969; cited after Zapesochneya and Pangarova, 1976). However, the localization, activity, and the role of these enzymes have not yet been studied. The levels of free reducing disaccharides of glycoside origin isolated from plants are usually very small (reviewed by Avigad, 1982). Therefore, the high concentrations of rutinose and methylrutinose in extracts do not support an accidental origin from glycosides. It is, however, possible that the synthesis of rutinose in *Datisca* proceeds via consecutive glycosylation of Datiscetin (5,7,2'-trihydroxyflavone) and subsequent removal of the rutinose units by a disaccharidase. Nevertheless, it is still unusual to find such high concentrations of a reducing sugar like rutinose. Possibly, the methylation of rutinose to methylrutinose is applied to eliminate this disadvantage. Preliminary results suggest that *Datisca* seems to contain highly active rutinose demethylases, since a short incubation of ground roots in H₂O precludes the isolation of methylrutinose, but not of rutinose (data not shown).

4.6.2.3. Are rutinose and methylrutinose carbon storage or transport forms?

Literature studies reveal that all unusual non-structural plant carbohydrates studied thus far represent either polyols or galactosides. The best analysed galactosides are the raffinose oligosaccharides that serve as transport carbohydrates and as carbon storage compounds in leaves, roots and tubers of Cucurbitaceae, Lamiaceae and other plant families (Keller and Pharr, 1996). There is also a biochemical link between the metabolism of raffinose oligosaccharides and that of galactosyl cyclitols (Hoch et al., 1999) which are found in the seeds of many legumes.

As mentioned above, rutinose represents a reducing sugar, and for storage and/or transport purposes the methylation of the anomeric carbon atom might be essential. The following models could be proposed for sugar metabolism in *Datisca*:

1. Rutinose is an intermediate carbon storage form, additional to transient starch. It accumulates in vacuoles and in case of metabolic demand is introduced into metabolism

by the action of an α -rhamnosidase. Unfortunately, since no plant α -rhamnosidases have been cloned yet, it is not possible to analyse their expression pattern and localization.

2. Rutinose is a carbon transport form. Rutinose and sucrose are synthesised in leaves, and rutinose is methylated to methylrutinose. Sucrose and methylrutinose are transported in the phloem to sink organs, where phloem unloading is drawn by immediate demethylation of methylrutinose and hydrolysis of sucrose. At times of carbon excess, rutinose accumulates in sink organs in vacuoles. This assumption begs the question why rutinose and not the non-reducing methylrutinose accumulates in vacuoles, since the rutinose content of roots and nodules is far higher than the methylrutinose content (Figure 3.10). However, storage of reducing sugars has been already reported. For example, tomato fruits are characterized by an accumulation of reducing sugars as the predominant fruit soluble carbohydrates (Garvey and Hewitt, 1991). Glucose was found to accumulate in the fruits of sea buckthorn (Tang, 2002) and of several Rosaceae (e.g. peach; Lo Bianco and Rieger, 2002).

To examine whether rutinose and/or methylrutinose represent carbon transport forms in *Datisca*, phloem sap samples or exudates from leaf petioles have to be examined. Preliminary results of HPLC analysis of petiole exudates showed the presence of rutinose in high concentrations, whereas methylrutinose levels were low (data not shown). However, instead of high sucrose concentrations, higher levels of glucose and fructose were found, although hexoses are no transport sugars (Heineke et al., 1992). This could be explained by contamination of the petiole exudates with invertase. Similar results have been obtained for transgenic potato plants expressing yeast apoplastic invertase under control of the CaMV 35S-promoter. Petiole exudates of these plants contained sucrose, glucose and fructose (Günther, 1991), while phloem sap won from the same plants by the laser aphid stylet technique as well as petiole exudates of wild type plants contained sucrose, but neither glucose nor fructose (Günther, 1991; Heineke et al., 1992). Thus, it is possible that demethylases as well as invertase were present in the petiole exudates. In analogy to the transgenic potato plants, the demethylases of *Datisca* should be located in the apoplast. Assuming that the hexoses were hydrolysis products of sucrose, the petiole exudates contained almost 10 times more rutinose/methylrutinose than sucrose. To address the question whether methylrutinose or rutinose is transported, i.e. to avoid the contamination of phloem exudates with sugar-modifying enzymes, it will be necessary to analyse pure phloem sap directly, i.e. to analyse phloem sap isolated using the laser aphid-stylet technique (Barlow and McCully, 1972; Fisher and Frame, 1984).

Since comparisons of petiole exudates and phloem sap are not available from many plants, it is still possible that the invertase/putative demethylase activity in *Datisca*

petiole exudates does not come from the apoplast. Rutinose is present in nodules in relatively high concentrations (Figure 3.10), indicating that it is likely to accumulate in vacuoles. That would mean that demethylases could be present in either vacuoles or cytosol, or in both.

In another preliminary experiment, the diurnal rhythm of the concentrations of sucrose, rutinose and methylrutinose was examined in leaves and roots. The concentration changes of both rhamnosyl disaccharides paralleled those of sucrose (data not shown). So, it is possibly to propose that rutinose and/or methylrutinose represent carbon transport forms alternative to sucrose. In principle, the transport of unusual carbohydrates in the phloem is a marker of symplastic phloem loaders which were analysed only on presence of sugar alcohols and raffinose family of oligosaccharides (Zimmermann and Ziegler, 1975). However, symplastic phloem loaders are also characterised by the fact that they transport a variety of carbon compounds in general, while apoplastic phloem loaders have one dominant carbon transport form (Gamalei, 1984). The phloem loading mode of *Datisca* has not yet been examined. Based on the phylogenetic position of the Datisceae, which are closely related to Begoniaceae, *Datisca* would be expected to represent a primitive apoplastic phloem loader (O. Voitsekhovskaja and Yu. Gamalei, personal communication). It will be very interesting to examine the companion cell differentiation in *Datisca* leaves in order to find out whether symplastic or apoplastic loading is used for rutinose/methylrutinose. If *Datisca* were indeed an apoplastic phloem loader, as the presence of about 90% rutinose/methylrutinose in the petiole exudate and the putative apoplastic location of demethylases (see above) would support, this would imply that either special plasmamembrane rutinose transporters are present in this plant, or, more likely, that the sucrose transporter of *Datisca* also can transport rutinose/methylrutinose. Plant disaccharide transporters analysed thus far are not strictly specific for sucrose, but also accept, for example, vitamin H (biotin) as substrate (Ludwig et al., 2000). Of course, rutinose or methylrutinose are not commercially available and therefore were never tested as substrates of disaccharide transporters. Hence, it would be possible that (a) all disaccharide transporters accept rutinose and/or methylrutinose as substrates, or (b) that disaccharide transporters in primitive apoplastic phloem loaders have a broader substrate specificity than those of highly evolved apoplastic phloem loaders. Furthermore, the possibility exists that since rutinose is a reducing sugar, it is recognized by hexose transporters. At least, it has been shown that some transporters of the reducing disaccharide maltose also accept hexoses as substrates (Wieczorke et al., 1999). In this case, membrane penetration of methylrutinose and rutinose could be catalyzed by

different transporters. Summing up, the identification of novel sugars in *Datisca* opens very interesting new perspectives on plant carbon partitioning mechanisms in general.

4.6.2.4. The implications of the discovery of rutinose (methylrutinose) as major carbohydrate for nodule carbon partitioning in *Datisca*

Since the rutinose concentration in nodules is much higher than that of sucrose, it is very important that the analysis of carbon partitioning mechanisms in *Datisca* involves also the analysis of rutinose-hydrolysing enzymes, namely, α -rhamnosidases. Unfortunately, the localization of these enzymes is not possible to examine, since no plant α -rhamnosidase has been cloned yet. However, the conclusions on sugar metabolism in *Datisca* roots and nodules that were based on the assumption that sucrose represents the main transport sugar have to be reconsidered with care. For instance, regarding chapter 4.5. it is possible that rutinose is hydrolysed in the apoplast, followed by the uptake of rhamnose by the microsymbiont *Frankia*, while glucose is imported into the cytoplasm of host cells via the hexose transporter that is specifically expressed in infected cells. This would mean that *Frankia* bacteria are fed hexoses in *Datisca* nodules, but that the hexose transporter is not working as an exporter.

Moreover, the decrease of sucrose synthase activity and strong reduction of invertase activities in nodules compared to roots is no more surprising. Since rutinose and not sucrose is the main transitory storage sugar in *Datisca* nodules, while both are present at similar concentrations in roots, the higher metabolic activity of nodules should be reflected by the induction of α -rhamnosidase and not sucrose synthase expression or activity.

For the future, the identification of rutinose (methylrutinose) as the major sugar in *Datisca* nodules necessitates the analysis of α -rhamnosidase and methylrutinose demethylase activities in roots and nodules of this plant, preferentially including the cloning of the corresponding cDNAs. Furthermore, the presence of rhamnosyl disaccharides in other actinorhizal plants should be examined, considering that the Rhamnaceae, named after their high content of rhamnose-containing flavone glycosides, are one of the eight actinorhizal plant families. There might actually be a link between the presence of rhamnosyl glycosides in a plant species, and the ability to enter a symbiosis with a *Frankia* strain of clade III (Figure 1.4).

5. Summary

In this thesis sucrose-cleaving enzymes and sugar transport proteins were studied to determine the way of sugar transport and their role in the function of nitrogen-fixing root nodules. Soluble sugar metabolite profile was analysed to reveal dominating sugars, which could be important for the symbiotic function of root nodules. To find out a possible common feature of root nodule symbioses, different model systems, one legume symbiosis (*Medicago truncatula* – *Sinorhizobium meliloti*) and two actinorhizal symbioses from different *Frankia* subclades, *Datisca glomerata* and *Casuarina glauca* were chosen. In order to reveal whether sugar partitioning mechanisms represent system-specific adaptations, i.e. resemble sugar partitioning mechanisms established in roots or are common to all nitrogen-fixing root nodules, all experiments included comparisons between roots and nodules.

The main results obtained can be summarized as follows:

- Legume and actinorhizal symbioses differ with respect to sugar transporter (HT) expression: induction of HT expression was found in nodules of actinorhizal plants *Datisca* and *Casuarina*, but expression levels of HT in *Medicago* nodules were strongly reduced.
- Full-size cDNA sequences for hexose transporters were isolated from *Medicago* (*MtHT*) and *Datisca* (*DgHT*) nodules. Based on their amino acid sequence, the encoded proteins belonged to different classes of sugar transporters. The functional characterization of DgHT in a heterologous system (yeast) demonstrated that DgHT is a high affinity, energy-dependent monosaccharide transporter, probably a H⁺-symporter, with broad substrate specificity.
- Expression levels of sucrose transporter (ST) in *Medicago* nodules were strongly reduced compared to roots.
- The total (sum of apoplastic, cytosolic and vacuolar) invertase activity is strongly reduced in nodules compared to roots of all three symbiotic systems studied.
- Different localizations of acid invertase activity suggest that sugar transport in *Medicago* roots occurs apoplastically, whereas in *Datisca* roots it takes place symplastically. There may be apoplastic transport in vascular parenchyma of *Datisca* roots.
- The major sucrose-cleaving activity in *Medicago* and *Datisca* roots and nodules is represented by sucrose synthase (SuSy). *Datisca* and *Casuarina* possess a

single immunoreactive protein for SuSy of about 92 kDa, *Medicago* contains an additional, somewhat larger SuSy protein in roots, but not in nodules. SuSy activities were similar in the soluble protein fractions in both roots and nodules of *Medicago*. In *Datisca* nodules they were lower compared to roots.

- Two unknown sugars were isolated from *Datisca* and identified using biochemical methods, NMR and mass spectroscopy. They were shown to represent rutinose (α -L-rhamnopyranosyl-(1 \rightarrow 6)-D-glucose) and methylrutinose (α -L-rhamnopyranosyl-(1 \rightarrow 6)-1-O-methyl- β -D-glucose). Both of them were present in large amounts in roots, nodules and leaves of *Datisca*.
- Sucrose is the principal sugar of *Medicago* and *Casuarina* nodules. The major sugar of *Datisca* root and nodule extract is rutinose.

The data presented in this thesis show significant differences between carbon partitioning mechanisms in the three symbiotic systems examined. However, some common features were also noted.

In all systems studied there was a decrease of total invertase activity, determined mostly by apoplastic invertase, in nodules compared to roots that could be an evidence for symplastic transport of sugars in nodules. In *Medicago*, this was underlined by the strong reduction of sugar transporter expression. This implies a shift toward symplastic transport mechanisms in nodules, which is likely to represent a symbiosis-specific adaptation in that symplastic transport allows the plant to control the microsymbiont's access to carbon sources.

Both actinorhizal symbioses showed strong induction of hexose transporter expression in nodules combined with a considerable reduction of apoplastic invertase activity which would be needed to provide these transporters with substrates. The last circumstance allows to propose a special role of the hexose transporter in supplying the microsymbiont with carbon sources in nodules.

6. Abbreviations

Amp	ampicillin
Amp ^R	ampicillin resistance
ATP	adenosine 5' triphosphate
bp	base pairs
BSA	bovine serum albumin
CAA	casamino acids
CC	companion cell
CCCP	carbonyl cyanide-m-chlorophenylhydrazone
cDNA	complementary DNA
CgHT	<i>Casuarina glauca</i> hexose transporter
CW	cell wall
DAB	diaminobenzidine
dCTP	deoxycytosine 5' triphosphate
dd H ₂ O	double distilled water
DgHT	<i>Datisca glomerata</i> hexose transporter
DMF	dimethylformamide
DMSO	dimethylsulfoxide
DNA	deoxyribonucleic acid
DNase	deoxyribonuclease
DNP	2,4-dinitrophenol
dNTP	deoxynucleotide triphosphate
dNTPs	deoxyribonucleotides
DTT	dithiothreitol
ECL	enhanced chemiluminescence
EDTA	Ethylenediamine tetraacetic acid
EGTA	Ethyleneglycole-bis-(2'-aminoester)-N,N,N',N'-tetraacetate
EtOH	ethanol
FW	fresh weight
G-6-PDH	glucose-6-phosphate dehydrogenase
GWDG	Gessellschaft für wissenschaftliche Datenverarbeitung Göttingen
HEPES	hydroxyethyl-piperazinethane sulfonic acid
HPLC	high performance liquid chromatography
IPTG	isopropyl-β-D-thiogalactopyranoside
kb	kilobase pairs

kDa	kilodalton
Km	kanamycin
K_m	Michaelis-Menten constant
Km^R	kanamycin resistance
MEN	MOPS-sodium acetate-EDTA
MOPS	morpholinopropane sulfonic acid
MtHT	<i>Medicago truncatula</i> hexose transporter
MtST	<i>Medicago truncatula</i> sucrose transporter
NAD	nicotine adenine dinucleotide (oxidized)
NADH	nicotine adenine dinucleotide (reduced)
NADP	nicotine adenine dinucleotide phosphate (oxydized)
NADPH	nicotine adenine dinucleotide phosphate (reduced)
NMR	nuclear magnetic resonance
OD	optical density
ORF	open reading frame
p.c.	packed cells
PAGE	polyacrylamide-gel electrophoresis
PCR	polymerase chain reaction
PEG	polyethylenglycol
PMSF	phenylmethylsulfonylfluoride
PVP	polyvinylpyrrolidone
PVPP	polyvinylpolypyrrolidone
RACE	rapid amplification of cDNA ends
RNA	ribonucleic acid
RNase	ribonuclease
rpm	rounds per minute
RT	reverse transcriptase
SDS	sodium dodecylsulfate
SE	sieve element
SE-CC complex	sieve element-companion cell complex
ST	sucrose transporter
STEL	sucrose-Triton-X-100-Tris-EDTA-lysozyme buffer
SuSy	sucrose synthase
T_{ann}	annealing temperature
<i>Taq</i>	<i>Thermus aquqticus</i>
TdT	terminal deoxynucleotidyl transferase
TEA	triethanolamine

TEMED	N,N,N',N'-tetramethylene diamine
T _m	melting temperature
Tris	tris-(hydroxymethyl)-aminomethane
U	enzyme activity unit (1 unit corresponds to the conversion of 1 μmol substrate min ⁻¹)
UDP	uridine 5' diphosphate
UDPG- DH	uridine diphosphate glucose dehydrogenase
UDP-glucose	uridine diphosphate glucose
UTP	uridine 5' triphosphate
UV	ultraviolet light
v/v	volume/volume
w/v	weight/volume
X-Gal	5-bromo-4-chloro-3-indolyl-β-D-galactopyranoside
YNB	yeast nitrogen base

7. References

- Abd-Alla MH, Koyro H-W, Schubert S, Peiter E** (2000) Functional structure of the indeterminate *Vicia faba* L. root nodules: implications for metabolite transport. *J Plant Physiol* 157: 335-343.
- Akkermans ADL, Roelofsen W, Blom J, Huss-Danell K, Harkink R** (1983) Utilization of carbon and nitrogen compounds by *Frankia* in synthetic media and in root nodules of *Alnus glutinosa*, *Hippophae rhamnoides*, and *Datisca cannabina*. *Can J Bot* 61: 2793-2800.
- Altschul SF, Gish W, Miller W, Myers EW, Lipman DJ** (1990) Basic local alignment search tool. *J Mol Biol* 215: 403-410.
- Amor Y, Haigler CH, Jonson S, Wainscott M, Delmer DP** (1995) A membrane-associated form of sucrose synthase and its potential role in synthesis of cellulose and callose in plants. *Proc Natl Acad Sci USA* 92: 9353-9357.
- Angelini R, Manes F, Federico R** (1990) Spatial and functional correlation between diamine-oxydase and peroxidase activities and their dependence upon deetiolation and wounding in chickpea stems. *Planta* 182: 89-96.
- Anthon GE, Emmerich DW** (1990) Developmental regulation of enzymes of sucrose and hexose metabolism in effective and ineffective soybean nodules. *Plant Physiol* 92: 346-351.
- Appeldoorn NJG, de Bruijn SM, Koot-Gronsveld EAM, Visser RGF, Vreugdenhil D, van der Plas LHW** (1997) Developmental changes of enzymes involved in conversion of sucrose to hexose-phosphate during early tuberisation of potato. *Planta* 202: 220-226.
- Appleby CA** (1984) Leghemoglobin and rhizobial respiration. *Annu Rev Plant Physiol* 35: 443-478.
- Arai M, Mori H, Imaseki H** (1992) Expression of the gene for sucrose synthase during growth of mung bean seedlings. *Plant Cell Physiol* 33: 503-506.
- Avigad G** (1982) Sucrose and disaccharides. In: *Encyclopedia of Plant Physiology*, Lowus FA and Tanner W, eds. (Berlin: Springer Verlag), pp 217-347.
- Ayres PG, Press MC, Spencer-Phillips PTN** (1996) Effects of pathogens and parasitic plants on source-sink relationships. In: *Photoassimilate Distribution in Plants and Crops*, E Zamski and AA Schaffner, eds. (New-York: Marcel Dekker), pp 479-499.
- Barker DG, Bianchi S, Blondon F, Datté Y, Duc G, Flament P, Gallusci P, Génier P, Guy P, Muel X, Tourneur J, Dénarié J, Huguet T** (1990) *Medicago truncatula*, a model plant for studying the molecular genetics of the *Rhizobium*-legume symbiosis. *Plant Mol Biol Rep* 8:40-49.
- Barlow CA, Mc Cully ME** (1972) The ruby laser as an instrument for cutting the stylets of feeding aphids. *Can J Zool* 50: 1497-1498.
- Barratt DHP, Barber L, Kruger NJ, Smith AM, Wang TL, Martin C** (2001) Multiple, distinct isoforms of sucrose synthase in pea. *Plant Physiol* 127: 655-664.
- Basset B, Goodman RN, Novacky A** (1977) Ultrastructure of soybean nodules. I. Release of rhizobia from the infection thread. *Can J Microbiol* 23: 573-582.
- Batut J, Boistard P** (1994) Oxygen control in *Rhizobium*. *Anthonie Van Leeuwenhoek* 66: 129-150.

- Benson DR, Clawson ML** (2000) Evolution of the actinorhizal plant symbiosis. In: Prokaryotic Nitrogen Fixation: A Model System for Analysis of a Biological Process (Symondham: Horizon Scientific Press), pp 207-224.
- Benson DR, Schultz NA** (1990) Physiology and biology of *Frankia* in culture. In: The Biology of *Frankia* and Actinorhizal Plants, Schwintzer CR and Tjepkema JD, eds. (San Diego: Academic Press), pp 107-127.
- Benson DR, Silvester WB** (1993) Biology of *Frankia* strains, actinomycete symbionts of actinorhizal plants. Microbiol Rev 57: 293-319.
- Berg RH, McDowell L** (1987a) Endophyte differentiation in *Casuarina* actinorrhizae. Protoplasma 136: 104-117.
- Berg RH, McDowell L** (1987b) Cytochemistry of the wall of infected cells in *Casuarina* actinorrhizae. Can J Bot 66: 2038-2047.
- Berry AM, Harriot OT, Moreau RA, Osman SF, Benson DR, Jones AD** (1993) Hopanoid lipids compose the *Frankia* vesicle envelope, presumptive barrier of oxygen diffusion to nitrogenase. Proc Natl Acad Sci USA 90: 6091-6094.
- Blauenfeldt J, Joshi PA, Gresshoff PM, Caetano-Anollés G** (1994) Nodulation of white clover (*Trifolium repens*) in the absence of *Rhizobium*. Protoplasma 179: 106-110.
- Blumwald E, Fortin MG, Rea PA, Verma DPS, Poole R** (1985) Presence of host-plasma membrane type H⁺-ATPase in the membrane envelope enclosing the bacteroids in soybean root nodules. Plant Physiol 78: 665-672.
- Bradford MM** (1976) A rapid and sensitive method for the determination of microgram quantities of protein utilizing the principle of protein-dye binding. Anal Biochem 72:248-254.
- Buchner P, Poret M, Rochat C** (1998) Cloning and characterization of a cDNA (Accession No. AJ001071) encoding a second sucrose synthase gene in pea (*Pisum sativum* L.). Plant Physiol 117: 719.
- Burgos RC, Chiang VL, Zhang X-H, Campbell ER, Podila GK, Champbell WH** (1995) RNA isolation from plant tissues resistant to extraction in guanidine. Bio Techniques 19: 734-737.
- Bush DR** (1993) Proton-coupled sugar and amino acid transporters in plants. Annu Rev Physiol Plant Mol Biol 44: 513-542.
- Büttner M, Sauer N** (2000) Monosaccharide transporters in plants: structure, function and physiology. Biochim Biophys Acta 1465: 263-274.
- Büttner M, Truernit E, Baier K, Scholz-Starke J, Sontheim M, Lauterbach C, Huss VAR, Sauer N** (2000) AtSTP3, a green leaf-specific, low affinity monosaccharide-H⁺ symporter of *Arabidopsis thaliana*. Plant Cell 23: 175-184.
- Carlson SJ, Chourey PS** (1996) Evidence for plasma membrane-associated forms of sucrose synthase in maize. Mol Gen Genet 252:303-310.
- Caspari T, Robl I, Stolz J, Tanner W** (1996) Purification of the *Chlorella* HUP1 hexose-proton symporter to homogeneity and its reconstitution *in vitro*. Plant J 10: 1045-1053.
- Caspari T, Will A, Opekarova M, Sauer N, Tanner W** (1994) Hexose/H⁺ symporters in lower and higher plants. J Exp Biol 196: 483-491.
- Chandler MR, Date RA, Roughley RJ** (1982) Infection and root nodule development in *Stilosanthes* species by *Rhizobium*. J Exp Bot 33: 47-57.
- Cleland RE, Fujiwara T, Lucas WJ** (1994) Plasmodesmal-mediated cell-to-cell transport in wheat roots is modulated by anaerobic stress. Protoplasma 178: 81-85.

- Davies DD, Kenworthy P, Mocquot D, Roberts K** (1987) The effects of anoxia on the ultrastructure of pea roots. In: *Plant Life in Aquatic and Amphibious Habitats*, Crawford RMM, ed (Oxford: Blackwell Scientific Publication), pp 265-277.
- Davies HV** (1984) Sugar metabolism in stolon tips during early tuberization. *Z Pflanzenphysiol* 113: 377-381.
- Day DA, Kaiser BN, Thomson R, Udvardi MK, Moreau S, Puppo A** (2001) Nutrient transport across symbiotic membranes from legume nodules. *Aust J Plant Physiol* 28: 667-674.
- Delmer DP, Amor Y** (1995) Cellulose biosynthesis. *Plant Cell* 7: 987-1000.
- Denison RF, Layzell DB** (1991) Measurement of legume nodule respiration and O₂ permeability by noninvasive spectrophotometry of leghemoglobin. *Plant Physiol* 96: 137-143.
- Doyle JJ** (1994) Phylogeny of the legume family: an approach to understanding the origins of nodulation. *Annu Rev Ecol Syst* 25: 325-349.
- Doyle JJ, Doyle JL, Ballenger JA, Dickson EE, Kajita T, Ohashi H** (1997) A phylogeny of the chloroplast gene *rbcL* in the Leguminosae – taxonomic correlations and insights into the evolution of nodulation. *Amer J Bot* 84: 541-554, 1997.
- Ehneß R, Roitsch T** (1997) Co-ordinated induction of mRNAs for extracellular invertase and glucose transporter in *Chenopodium rubrum* by cytokinins. *Plant J* 11: 539-548.
- Eschrich W** (1980) Free space invertase, its possible role in phloem unloading. *Ber Dtsch Bot Ges* 93: 363-378.
- Fåhraeus G** (1957) The infection of clover root hairs by nodule bacteria studied by simple glass technique. *J Gen Microbiol* 16: 374-381.
- Fisher DB, Frame JM** (1984) A guide to the use of the exuding-stylet technique in phloem physiology. *Planta* 161: 385-393.
- Fleming AI, Wittenberg JB, Wittenberg BA, Dudman WF, Appleby CA** (1987) The purification, characterization and ligand-binding kinetics of hemoglobins from root nodules of the non-leguminous *Casuarina glauca* – *Frankia* symbiosis. *Biochim Biophys Acta* 911: 209-220.
- Fontaine MS, Young PH, Torrey JG** (1986) Effect of long-term preservation of *Frankia* strains on infectivity, effectivity and *in vitro* nitrogenase activity. *Appl Environ Microbiol* 51: 694-698.
- Frohman MA, Dush MK, Martin GR** (1988) Rapid production of full-length cDNAs from rare transcripts: Amplification using a single gene-specific oligonucleotide primer. *Proc Natl Acad Sci USA* 85: 8998-9002.
- Gahrtz M, Schmelzer E, Stolz J, Sauer N** (1996) Expression of the PmSUC1 sucrose carrier gene from *Plantago major* L. is induced during seed development. *Plant J* 9: 93-100.
- Gamalei YV** (1984) The structure of leaf minor veins and the types of translocated carbohydrates. *Dokl Akad Nauk (in Russ)* 277: 1513-1516.
- Gamalei YV** (1994) The endoplasmic reticulum of plants: its origin, structure and functions. BIN RAN, St-Petersburg.
- Gamas P, de Carvalho Niebel F, Lescure N, Cullimore JV** (1996) Use of a subtractive hybridization approach to identify new *Medicago truncatula* genes induced during root nodule development. *Mol Plant-Microbe Interact* 9: 233-242.

- Garvey TC, Hewitt JD** (1991) Starch and sugar accumulation in two accessions of *Lycopersicon cheesmanii*. *J Am Soc Hortic Sci* 116:77-79.
- Geigenberger P, Langerberger S, Wilke I, Heineke D, Heldt H and Stitt M** (1993) Sucrose is metabolised by sucrose synthase and glycolysis within phloem complex of *Ricinus communis* L. seedlings. *Planta* 190:446-453.
- Geigenberger P, Lerchl J, Stitt M, Sonnewald U** (1996) Phloem-specific expression of pyrophosphatase inhibits long distance transport of carbohydrates and amino acids in tobacco plants. *Plant Cell Environ* 19: 43-45.
- Girgis ZMG, Ishac ZI, El-Haddad M, Saleh AE, Diem HG, Dommergues RY** (1990) First report on isolation and culture of effective *Casuarina*- compatible strain of *Frankia* from Egypt. In: *Advance in Casuarina Research and Utilisation*, El-Lakany HM, Turnbull WJ and Brewbaker JL, eds. (Kairo: Desert Development Center, A.U.C.), pp156-164.
- Godt DE, Roitsch T** (1997) Regulation and tissue-specific distribution of mRNAs for three extracellular invertase isoenzymes of tomato suggest an important function in establishing and maintaining sink metabolism. *Plant Physiol* 115: 273-282.
- González EM, Gordon AJ, James CL, Arrese-Igor C** (1995) The role of sucrose synthase in the response of soybean nodules to drought. *J Exp Bot*, 46: 1515-1523.
- Gordon AJ** (1991) Enzyme distribution between the cortex and the infected region of soybean nodules. *J Exp Bot* 42: 961-967.
- Gordon AJ, Minchin FR, James CL, Komina O** (1999) Sucrose synthase is essential for nitrogen fixation. *Plant Physiol* 120: 867-877.
- Gordon AJ, Minchin FR, Skøt L, James CL** (1997) Stress-induced declines in soybean N₂ fixation are related to nodule sucrose synthase activity. *Plant Physiol* 114: 937-946.
- Greiner S, Rausch T, Sonnewald U, Herbers K** (1999) Ectopic expression of a tobacco invertase inhibitor homolog prevents cold-induced sweetening of potato tubers. *Nat Biotechnol* 17: 708-711.
- Greutert H, Keller F** (1993) Further evidence for stachyose and sucrose/H⁺ antiporters on the tonoplast of Japanese artichoke (*Stachys sieboldii*) tubers. *Plant Physiol* 101: 1317-1322.
- Günther G** (1991) Vergleichende Untersuchungen von Stoffwechselintermediaten in Blättern von transgenen Kartoffelpflanzen. Diplomarbeit, Universität Göttingen.
- Guttenberger M** (2000) Arbuscules of vesicular-arbuscular mycorrhizal fungi inhabit an acidic compartment within plant roots. *Planta* 211: 299-304.
- Hafeez F, Akkermans ADL, Chaudhary AH** (1984) Observations on the ultrastructure of *Frankia* sp. in root nodules of *Datisca cannabina* L. *Plant Soil* 79: 383-402.
- Hajirezaei M-R, Takahata Y, Trethewey RN, Willmitzer L, Sonnewald U** (2000) Impact of elevated cytosolic and apoplastic invertase activity on carbon metabolism during potato tuber development. *J Exp Bot* 51: 439-445.
- Harrison MJ** (1996) A sugar transporter from *Medicago truncatula*: altered expression pattern in roots during vesicular-arbuscular (VA) mycorrhizal associations. *Plant J* 9: 491-503.
- Heim U, Weber H, Bäumlein H, Wobus U** (1993) A sucrose-synthase gene of *Vicia faba* L.: Expression pattern in developing seeds in relation to starch synthesis and metabolic regulation. *Planta* 191: 394-401.

- Heineke D, Sonnewald U, Büssis D, Günther G, Leidreiter K, Wilke I, Raschke K, Willmitzer L, Heldt HW** (1992) Apoplastic expression of yeast-derived invertase in potato: effects on photosynthesis, leaf solute composition, water relations, and tuber composition. *Plant Physiol* 100: 301-308.
- Hirsch AM, LaRue TA** (1997) Is the legume nodule a modified root or stem or an organ *sui generis*? *CRC Crit Rev Plant Sci* 16: 361-392.
- Ho LC** (1988) Metabolism and compartmentation of imported sugars in sink organs in relation to sink strength. *Annu Rev Plant Physiol Plant Mol Biol* 39: 355-378.
- Hoagland DR, Arnon DT** (1938) The water-culture method for growing plants without soil. California Agriculture Experiment Station Circular 347.
- Hoch G, Peterbauer T, Richter A** (1999) Purification and characterization of stachiose synthase from lentil (*Lens culunaris*) seeds. Galactopinitol and stachyose synthesis. *Arch Biochem Biophys* 366:75-81.
- Hohnjec N, Becker JD, Pühler A, Perlick AM, Küster H** (1999) Genomic organization and expression properties of the *MtSucS1* gene, which encodes a nodule-enhanced sucrose synthase in the model legume *Medicago truncatula*. *Mol Gen Genet* 261: 514-522.
- Huber SC, Huber JL, Liao P-C, Gage DA, McMichael RW, Chourey PS, Hannah LD, Koch K** (1996) Phosphorylation of serine-15 of maize leaf sucrose synthase. Occurrence *in vivo* and possible regulatory significance. *Plant Physiol* 112: 793-802.
- Huss-Danell K** (1990) The physiology of actinorhizal nodules. In: The biology of *Frankia* and actinorhizal plants, Schwintzer CR, Tjepkema JD, eds. (San Diego: Acad Press), pp 129-156.
- Huss-Danell K** (1997) Tansley Review No. 93. Actinorhizal symbioses and their N₂ fixation. *New Phytol* 136, 375-405.
- Inoue H, Nojima H, Okayama H** (1990) High efficiency transformation of *Escherichia coli* with plasmids. *Gene* 96: 23-28.
- James EK, Sprent JI, Sutherland JM, McInroy SG, Minchin FR** (1992) The structure of nitrogen fixing root nodules on the aquatic mimosoid legume *Neptunia plena*. *Ann Bot (Lond)* 69: 173-180.
- Jeong J, Suh SJ, Guan C, Tsay Y-F, Moran N, Pawlowski K, Lee Y** (2002) A nodule-specific dicarboxylate transporter from *Alnus glutinosa*. *Proc Natl Acad Sci USA*, submitted.
- Joshi PA, Caetano-Anollés G, Graham ET, Gresshoff PM** (1993) Ultrastructure of transfer cells in spontaneous nodules of alfalfa (*Medicago sativa*). *Protoplasma* 172: 64-76.
- Keller F, Pharr DM** (1996) Metabolism of carbohydrates in sinks and sources: galactosyl-sucrose oligosaccharides. In: Photoassimilate distribution in plants and crops, Zamski E and Schaffer AA, eds. (New York: Marcel Dekker), pp 115-184.
- Kijne JW** (1992) The *Rhizobium* infection process. In: Biological Nitrogen Fixation, G Stacey, RH Burris, and HJ Evans, eds. (New York: Chapman and Hall), pp 349-398.
- Kim J-Y, Mahe A, Brangeon J, Prioul J-L** (2000) A maize vacuolar invertase, IVR2, is induced by water stress. Organ/tissue specificity and diurnal modulation of expression. *Plant Physiol* 124: 71-84.
- King SP, Lunn JE, Furbank RT** (1997) Carbohydrate content and enzyme metabolism in developing canola siliques. *Plant Physiol* 114: 153-160.

- Kouchi H, Katsuhiko F, Katagiri H, Minamisawa K, Tajima S** (1988) Isolation and enzymological characterization of infected and uninfected cell protoplasts from root nodules of *Glycine max*. *Physiol Plant* 73: 327-334.
- Krausgrill S, Greiner S, Kröger U, Vogel R, Rausch T** (1998) In transformed tobacco cells the apoplasmic invertase inhibitor operates as a regulatory switch of cell wall invertase. *Plant J* 13: 275-280.
- Kühn C, Franceschi VR, Schulz A, Lemoine R, Frommer WB** (1997) Macromolecular trafficking indicated by localization and turnover of sucrose transporters in enucleate sieve elements. *Science* 275: 1298-1300.
- Küster H, Frühling M, Perlick AM, Pühler A** (1993) The sucrose synthase gene is predominantly expressed in the root nodule tissue of *Vicia faba*. *Mol Plant-Microbe Interact* 6: 507-514.
- Kutschera U, Heiderich A** (2002) Sucrose metabolism and cellulose biosynthesis in sunflower hypocotyls. *Physiol Plant* 114: 372-379.
- Laemmli UK** (1970) Cleavage of structural proteins during assembly of the head of bacteriophage T4. *Nature* 227: 680-685.
- Laplaze L, Duhoux E, Franche C, Frutz T, Svistoonoff S, Bisseling T, Bogusz D, Pawlowski K** (2000) *Casuarina glauca* preodule cells display the same differentiation as the corresponding nodule cells. *Mol Plant Microbe Interact* 13:107-112.
- Lechevalier MP, Lechevalier HA** (1990) Systematics, isolation, culture of *Frankia*. In: *The Biology of Frankia and Actinorhizal Plants*, Schwintzer CR and Tjepkema JD, eds. (San Diego: Academic Press), pp 35-60.
- Lerchl J, Geigenberger P, Stitt M, Sonnewald U** (1995) Impaired photoassimilate partitioning caused by phloem-specific removal of pyrophosphate can be complemented by a phloem-specific cytosolic yeast-derived invertase in transgenic plants. *Plant Cell* 7: 259-270.
- Liu Q, and Berry AM** (1991) Localization and characterization of pectic polysaccharides in roots and root nodules of *Ceanothus* spp. during intercellular infection by *Frankia*. *Protoplasma* 164: 93-101.
- Lo Bianco R, Rieger M** (2002) Partitioning of sorbitol and sucrose catabolism within peach fruit. *J Amer Soc Hortic Sci* 127:115-121.
- Ludwig A, Stolz J, Sauer N** (2000) Plant sucrose-H⁺ symporters mediate the transport of vitamin H. *Plant J* 24: 503-509.
- Lullien V, Barker DG, Lajudie P, Huguet T** (1987) Plant gene expression in effective and ineffective root nodules of alfalfa (*Medicago sativa*). *Plant Mol Biol* 9: 469-478.
- Marger MD, Saier MH Jr** (1993) A major superfamily of transmembrane facilitators that catalyze uniport, symport and antiport. *Trends Biochem Sci* 18: 13-20.
- McElfresh KC, Chourey PS** (1988) Anaerobiosis induces transcription but not translation of sucrose synthase in maize. *Plant Physiol* 87: 542-546.
- Meade HM, Long SR, Ruvkun GB, Brown SE, Ansubel FM** (1982) Physical and genetic characterization of symbiotic and auxotrophic mutants of *Rhizobium meliloti* induced by transposon Tn5 mutagenesis. *J Bacteriol* 149:114-122.
- Meesters TM, Genesen ST, Akkermans ADL** (1985) Growth, acetylene reduction activity and localization of nitrogenase in relation to vesicle formation in *Frankia* strains Cc1.17 and Cp1.2. *Arch Microbiol* 143: 137-142.
- Miller IM, Baker DD** (1985) The initiation, development and structure of root nodules in *Elaeagnus angustifolia* L. (Elaeagnaceae). *Protoplasma* 128: 107-119.

- Minchin FR** (1997) Regulation of oxygen diffusion in legume nodules. *Soil Biol Biochem* 29: 881-888.
- Mirza MS, Hahn D, Dobritsa SV, Akkermans ADL** (1994) Phylogenetic studies on uncultured *Frankia* populations in nodules of *Datisca cannabina*. *Can J Microbiol* 40: 315-318.
- Mullis KB, Faloona FA** (1987) Specific synthesis of DNA *in vitro* via a polymerase-catalysed chain reaction. *Methods Enzymol* 155: 335-350.
- Murry MA, Zhongze Z, Torrey JG** (1985) Effect of O₂ on vesicle formation, acetylene reduction, and O₂-uptake kinetics in *Frankia* sp. HFPCc13 isolated from *Casuarina cunninghamiana*. *Can J Microbiol* 31: 804-809.
- Mylona P, Pawlowski K, Bisseling T** (1995) Symbiotic nitrogen fixation. *Plant Cell* 7: 869-885.
- Nakai T, Konishi T, Zhang X-Q, Chollet R, Tonouchi N, Tsuchida T, Yoshinaga F, Mori H, Sakai F, Hayashi T** (1998) An increase in apparent affinity for sucrose of mung bean sucrose synthase is caused by *in vitro* phosphorylation or directed mutagenesis of Ser¹¹. *Plant Cell Physiol* 39: 1337-1341.
- Newcomb W** (1981) Nodule morphogenesis and differentiation. *Int Rev Cytol Suppl* 13: S247-S297.
- Newcomb W, Wood SM** (1987) Morphogenesis and fine structure of *Frankia* (Actinomycetales): The microsymbiont of nitrogen-fixing actinorhizal root nodules. *Int Rev Cytol* 109: 1-88.
- Nguyen-Quoc B, Foyer CH** (2001) A role of "futile cycles" involving invertase and sucrose synthase in sucrose metabolism of tomato fruit. *J Exp Bot* 52: 881-889.
- Nguyen-Quoc B, Krivitzky M, Huber SC, Lecharyn A** (1990) Sucrose synthase in developing maize leaves. Regulation of activity by protein level during the import to export transition. *Plant Physiol* 94: 516-523.
- Nicholas KB, Nicholas HB Jr, Deerfield DW** (1997) GeneDoc: Analysis and Visualization of Genetic Variation. *EMBnet.NEWS* 4: 14.
- Nolte KD, Koch KE** (1993) Companion-cell specific localization of sucrose synthase in zones of phloem loading and unloading. *Plant Physiol* 101: 899-905.
- Normand P, Orso S, Cournoyer B, Jeannin P, Chapelon J, Dawson J, Evtushenko L, Misra AK** (1996) Molecular phylogeny of the genus *Frankia* and related genera and emendation of the family Frankiaceae. *Int J Syst Bacteriol* 46: 1-9.
- N'tchobo H, Dali N, Nguyen-Quoc B, Foyer CH, Yelle S** (1999) Starch synthesis in tomato remains constant throughout fruit development and is dependent on sucrose supply and sucrose activity. *J Exp Bot* 50: 1457-1463.
- Okubara PA, Pawlowski K, Murphy TM, Berry AM** (1999) Symbiotic root nodules of the actinorhizal plant *Datisca glomerata* express Rubisco activase mRNA. *Plant Physiol* 120: 411-420.
- Parsons R, Silvester WB, Harris S, Gruijters WTM, Bullivant S** (1987) *Frankia* vesicles provide inducible and absolute protection for nitrogenase. *Plant Physiol* 83: 728-731.
- Pate JS, Gunning BES, Briarty LG** (1969) Ultrastructure and functioning of the transport system of the leguminous root nodule. *Planta* 85: 11-34.
- Patrick JW** (1997) Phloem unloading: sieve element unloading and post-sieve element transport. *Annu Rev Plant Physiol Plant Mol Biol* 48: 191-222.

- Patrick JW, Zhang W, Tyerman SD, Offler CE, Walker NA** (2001) Role of membrane transport in phloem translocation of assimilates and water. *Aust J Plant Physiol* 28: 695-707.
- Pawlowski K** (2002) Actinorhizal symbioses. In: Nitrogen Fixation at the Millenium; Leigh GJ (ed), Elsevier Science, Pergamon Press, Amsterdam, in press.
- Pawlowski K, Bisseling T** (1996) Rhizobial and actinorhizal symbioses: What are the shared features? *Plant Cell* 8: 1899-1913.
- Pawlowski K, Swensen SM, Guan C, Hadri A-E, Berry AM, Bisseling T** (2002) Distinct patterns of symbiosis-related gene expression and metabolic specialization in actinorhizal nodules from different plant families. *Mol Plant-Microbe Interact*, submitted.
- Pharr DM, Hendrix DL, Robbins NS, Gross KC and Sox HN** (1987) Isolation of galactinol from leaves of *Cucumis sativus*. *Plant Sci* 50:21-26.
- Pradel KS, Ullrich CI, Santa Cruz S, Oparka KJ** (1999) Symplastic continuity in *Agrobacterium tumefaciens*-induced tumors. *J Exp Bot* 50: 183-192.
- Pueppke SG, Broughton WJ** (1999) *Rhizobium* sp. strain NGR234 and *R. fredii* USDA257 share exceptionally broad, nested host ranges. *Mol Plant Microbe Interact* 12: 293-318.
- Racette S, Torrey JG** (1989) Root nodule initiation in *Gymnostoma* (Casuarinaceae) and *Shepherdia* (Elaeagnaceae) induced by *Frankia* strain HFPGpl1 *Can J Bot* 67: 2873-2879.
- Reinefeld E, Emmerich A, Burba M, Possiel M** (1986) Evaluation of sugarbeet quality in terms of corrected sugar content, particularly for evaluation of the importance of classes of involved substances. *Zuckerindustrie*, 111, 730-738.
- Renz A, Stitt M** (1993) Substrate specificity and product inhibition of different forms of fructokinases and hexokinases in developing potato tubers. *Planta* 190: 166-175.
- Ribeiro A, Akkermans ADL, van Kammen A, Bisseling T, Pawlowski K** (1995) A nodule-specific gene encoding a subtilisin-like protease is expressed in early stages of actinorhizal nodule development. *Plant Cell* 7: 785-794.
- Riens B, Lohaus G, Winter H, Heldt WH** (1994) Production and diurnal utilization in leaves of spinach (*Spinacia oleracea* L.) and barley (*Hordeum vulgare* L.). *Planta* 192: 497-501.
- Riesmeier JW, Willmitzer L, Frommer WB** (1992) Isolation and characterization of a sucrose carrier cDNA from spinach by functional expression in yeast. *EMBO J* 11: 4705-4713.
- Roitsch T, Bittner M, Godt DE** (1995) Induction of apoplastic invertase of *Chenopodium rubrum* by D-glucose and a glucose analog and tissue-specific expression suggest a role in sink-source regulation. *J Plant Physiol* 108: 285-294.
- Roitsch T, Tanner W** (1994) Expression of a sugar transporter gene family in a photoautotrophic suspension culture of *Chenopodium rubrum* L. *Planta* 193: 365-371.
- Romanov VI, Gordon AJ, Minchin FR, Witty JF, Skøt L, James CL, Borisov AY, Tikhonovich IA** (1995) Anatomy, physiology and biochemistry of Sprint-2 Fix⁻, a symbiotically defective mutant of pea (*Pisum sativum* L.) *J Exp Bot* 46: 1809-1816.
- Ross HA, Davies HV** (1992) Purification and characterization of sucrose synthase from the cotyledons of *Vicia faba* L. *Plant Physiol* 100: 1008-1013.
- Rost B, Casadio R, Fariselli P, Sander C** (1995) Transmembrane helices predicted at 95% accuracy. *Protein Sci* 4: 521-533.

- Rost B, Fariselli P, Casaido R** (1996) Topology prediction for helical transmembrane proteins at 86% accuracy. *Protein Science*, 5:1704-1718.
- Roth LF, Stacey G** (1989) Bacterium release into host cells of nitrogen-fixing soybean nodules: the symbiosome membrane comes from three sources. *Eur J Cell Biol* 49: 13-23.
- Rouhier H, Usuda H** (2001) Spatial and temporal distribution of sucrose synthase in the radish hypocotyls in relation to thickening growth. *Plant Cell Physiol* 42: 583-593.
- Roychoudhury R, Jay E, Wu, R** (1976) Terminal labelling and addition of homopolymer tracts to duplex DNA fragments by terminal deoxynucleotidyl transferase. *Nucleic Acids Res* 3: 863-877.
- Rozenkranz H, Vogel R, Greiner S, Rausch T** (2001) In wounded sugar beet (*Beta vulgaris* L.) tap-root, hexose accumulation correlates with the induction of a vacuolar invertase isoform. *J Exp Bot* 52: 2381-2385.
- Ruan Y-L, Chourey PS, Delmer DP, Perez-Grau L** (1997) The differential expression of sucrose synthase in relation to diverse patterns of carbon partitioning in developing cotton seed. *Plant Physiol* 115: 375-385.
- Ruan Y-L, Patrick JW** (1995) The cellular pathway of post-phloem sugar transport in developing tomato fruit. *Planta* 196: 434-444.
- Saftner RA, Daie J, Wyse RE** (1983) Sucrose uptake and compartmentation in sugar beet taproot tissue. *Plant Physiol* 72: 1-6.
- Sambrook J, Fritsch EF, Maniatis T** (1989) *Molecular cloning: A laboratory manual*. Second edition (New York: Cold Spring Harbor).
- Sander A, Krausgrill S, Greiner S, Weil M, Rausch T** (1996) Sucrose protects cell wall invertase but not vacuolar invertase against proteinaceous inhibitors. *FEBS Lett* 385: 171-175.
- Sauer N, Baier K, Gahrtz M, Stadler R, Stolz J, Truernit E** (1994) Sugar transport across the plasma membranes of higher plants. *Plant Mol Biol* 26: 1671-1679.
- Sauer N, Friedländer K, Gräml-Wicke U** (1990) Primary structure, genomic organization and heterologous expression of a glucose transporter from *Arabidopsis thaliana*. *EMBO J* 9: 3045-3050.
- Sauer N, Stadler R** (1993) A sink-specific H⁺/monosaccharide co-transporter from *Nicotiana tabacum*: cloning and heterologous expression in baker's yeast. *Plant J* 4: 601-610.
- Sauer N, Stolz J** (1994) SUC1 and SUC2: two sucrose transporters from *Arabidopsis thaliana*; expression and characterization in baker's yeast and identification of the histidine-tagged protein. *Plant J* 6: 67-77.
- Sauer N, Stolz J** (2000) Expression of foreign transport protein in yeast. In: *Membrane transport. A practical approach* (Oxford: Oxford University Press), 79-105.
- Sauer N, Tanner W** (1989) The hexose carrier from *Chlorella*. cDNA cloning of a eucariotic H⁺ cotransporter. *FEBS Lett* 258: 43-36.
- Sauer N, Tanner W** (1993) Molecular biology of sugar transporters in plants. *Bot Acta* 106: 277-286.
- Schaffer AA, Petreikov M** (1997) Inhibition of fructokinase and sucrose synthase by cytological levels of fructose in young tomato fruit undergoing transient accumulation of starch. *Physiol Plant* 101: 800-806.
- Selker JML, Newcomb EH** (1985) Spatial relationships between uninfected and infected cells in root nodules of soybean. *Planta* 165: 446-454.

- Senser M, Kandler O** (1967) Vorkommen und verbreitung von galactinol in blättern höherer pflanzen. *Phytochemistry* 7: 1533-1540.
- Serrano R, Kielland-Brandt MC, Fink GR** (1986) Yeast plasma membrane ATPase is essential for growth and has homology with (Na⁺ + K⁺), K⁺- and Ca²⁺-ATPases. *Nature* 319: 689-693.
- Shakya R, Sturm A** (1997) Characterization of source and sink specific sucrose/H⁺ symporters from carrot. *Plant Physiol* 118: 1473-1480.
- Shaw VK, Brill WJ** (1977) Isolation of an iron-molybdenum cofactor from nitrogenase. *Proc Natl Acad Sci USA* 74: 1493-1497.
- Silvester WB, Langenstein B, Berg RH** (1999) Do mitochondria provide the oxygen diffusion barrier in root nodules of *Coriaria* and *Datisca*? *Can J Bot* 77: 1358-1366.
- Skøt L, Egsgaard H** (1984) Identification of ononitol and O-methyl-scylllo-inositol in pea root nodules. *Planta* 161: 32-36.
- Smith AE, Phillips DV** (1980) Occurrence of pinitol in foliage of several forage legume species. *Crop Sci* 20: 75-77.
- Smith SE, Dickson S, Smith FA** (2001) Nutrient transfer in arbuscular mycorrhizas: how are fungal and plant processes integrated? *Aust J Plant Physiol* 28: 685-696.
- Soltis DE, Soltis PS, Morgan DR, Swensen SM, Mullin BC, Dowd JM, Martin PG** (1995) Chloroplast gene sequence data suggest a single origin of the predisposition for symbiotic nitrogen fixations in angiosperms. *Proc Natl Acad Sci USA* 92: 2647-2651.
- Sonnewald U, Willmitzer L** (1992) Molecular approaches to sink-source interactions. *Plant Physiol* 99: 1267-1270.
- Stadler R, Brandner J, Schulz A, Gahrtz M, Sauer N** (1995) Phloem loading by the PmSUC2 sucrose carrier from *Plantago major* occurs into companion cells. *Plant Cell* 7: 1545-1554.
- Stitt M, Sonnewald U** (1995) Regulation of metabolism in transgenic plants. *Annu Rev Plant Physiol Plant Mol Biol* 46: 341-368.
- Stolz J, Stadler R, Opekarová M, Sauer N** (1994) Functional reconstitution of the solubilized *Arabidopsis thaliana* STP1 monosaccharide-H⁺ symporter in lipid vesicles and purification of the histidine tagged protein from transgenic *Saccharomyces cerevisiae*. *Plant Journal* 6: 225-233.
- Streeter JG** (1995) Recent developments in carbon transport and metabolism in symbiotic systems. *Symbiosis* 19: 175-196.
- Sturm A** (1996) Molecular characterization and functional analysis of sucrose cleaving enzymes in carrot (*Daucus carota* L.). *J Exp Bot* 47: 1187-1192.
- Sturm A** (1999) Invertases. Primary structures, functions, and roles in plant development and sucrose partitioning. *Plant Physiol* 121: 1-7.
- Sturm A, Chrispeels MJ** (1990) cDNA cloning of carrot extracellular β -fructosidase and its expression in response to wounding and bacterial infection. *Plant Cell* 2: 1107-1119.
- Sturm A, Šebková V, Lorenz K, Hardegger M, Lienhard S, Unger C** (1995) Development- and organ-specific expression of the β -fructofuranosidase in carrot. *Planta* 195: 601-610.
- Sturm A, Tang GQ** (1999) The sucrose-cleaving enzymes of plants are crucial for development, growth and carbon partitioning. *Trends in Plant Science* 4: 401-407.

- Sung S-JS, Xu D-P, Black CC** (1989) Identification of actively filling sucrose sinks. *Plant Physiol* 89: 1117-1121.
- Swensen S** (1996) The evolution of actinorhizal symbioses: Evidence for multiple origins of the symbiotic association. *Am J Bot* 83: 1503-1512.
- Taliercio EW, Chourey PS** (1989) Posttranscriptional control of sucrose synthase expression in anaerobic seedlings of maize. *Plant Physiol* 90:1359-1364.
- Tang XR** (2002) Intrinsic change of physical and chemical properties of sea buckthorn (*Hippophae rhamnoides*) and implications for berry maturity and quality. *J Hortic Sci Biotech* 77:177-185.
- Tartof KD, Hobbs CA** (1987) Improved media for growing plasmid and cosmid clones. *Bethesda Res Lab Focus* 9: 12.
- Thummler F, Verma DPS** (1987) Nodulin-100 of soybean is the subunit of sucrose synthase regulated by the availability of free heme in nodules. *J Biol Chem* 262: 14730-14736.
- Topfer R, Maas C, Horicke-Grandpierre C, Schell J, Steinbiss HH** (1993) Expression vectors for high-level gene expression in dicotyledonous and monocotyledonous plants. *Methods Enzymol* 217:67-78.
- Torrey JG** (1976) Initiation and development of root nodules of *Casuarina* (Casuarinaceae). *Amer J Bot* 63: 335-344.
- Truchet G, Barker DG, Calmut S, de Billy F, Vasse J, Huguet T** (1989) Alfalfa nodulation in the absence of *Rhizobium*. *Mol Gen Genet* 219: 65-68.
- Truernit E, Sauer N** (1995) The promoter of the *Arabidopsis thaliana* SUC2 sucrose-H⁺ symporter gene directs expression of β -glucuronidase to the phloem: Evidence for phloem loading and unloading by SUC2. *Planta* 196: 564-570.
- Truernit E, Schmid J, Epple P, Illig J, Sauer N** (1996) The sink-specific and stress-regulated *Arabidopsis* *STP4* gene: enhanced expression of a gene encoding a monosaccharide transporter by wounding, elicitors, and pathogen challenge. *Plant Cell* 8: 2169-2182.
- Truernit E, Stadler R, Baier K, Sauer N** (1999) A male gametophyte-specific monosaccharide transporter in *Arabidopsis*. *Plant J* 17: 191-201.
- Tymowska-Lalanne Z, Kreis M** (1998) Expression of the *Arabidopsis thaliana* invertase gene family. *Planta* 207: 259-265.
- Van Larebeke N, Genetello C, Hernalsteen J, De Picker A, Zaenen I, Messens E, Van Montagu M, Schell J** (1977) Transfer of Ti plasmids between *Agrobacterium* strains by mobilisation with conjugative plasmid RP4. *Mol Gen Genet* 152: 119-124.
- Vance CP, Heichel GH** (1991) Carbon in N₂ fixation: limitation or exquisite adaptation. *Annual Review of Plant Physiology & Plant Molecular Biology* 42: 329-392.
- Vasse J, de Billy F, Camut S, Truchet G** (1990) Correlation between ultrastructural differentiation of bacteroids and nitrogen fixation in alfalfa nodules. *J Bacteriol* 172: 4295-4306.
- Verma DPS, Hong ZL** (2001) Plant callose synthase complexes. *Plant Mol Biol* 47: 693-701.
- Viola R, Roberts AG, Haupt S, Gazzani S, Hancock RD, Marmioli N, Machray GC, Oparka KJ** (2001) Tuberization in potato involves a switch from apoplastic to symplastic phloem unloading. *The Plant Cell* 13: 385-398.

- Wabnitz P** (1998) Untersuchung über die Verteilung von Zuckern in Stickstoff-fixierenden Wurzelknöllchen. Diploma thesis. Georg-August-University, Göttingen, Germany.
- Walker NA, Patric JW, Zhang W, Fieuw S** (1995) Identification and characterization of a phloem-specific β -amylase. *Plant Physiol* 109: 743-750.
- Wall LG** (2000) The actinorhizal symbiosis. *J Plant Growth Regul* 19: 167-182.
- Weber H, Borisjuk L, Wobus U** (1996) Controlling seed development and seed size in *Vicia faba*: A role for seed coat-associate invertases and carbohydrate state. *Plant J* 10: 101-112.
- Weber H, Borisjuk L, Heim U, Sauer N, Wobus U** (1997) A role for sugar transporters during seed development: molecular characterization of a hexose transporter and a sucrose carrier in *Vicia faba*. *Plant Cell* 9: 895-908.
- Weig A, Franz J, Sauer N, Komor E** (1994) Isolation of a family of cDNA clones from *Ricinus communis* L. with close homology to the hexose carriers. *J Plant Physiol* 143: 178-183.
- Weil M, Krausgrill S, Schuster A, Rausch T** (1994) A 17-kDa *Nicotiana tabacum* cell-wall peptide acts as an *in-vitro* inhibitor of the cell wall isoform of acid invertase. *Planta* 193: 438-445.
- Whitehead LF, Tyermann SD, Salom CL, Day DA** (1995) Transport of fixed nitrogen across symbiotic membranes of legume nodules. *Symbiosis* 19: 141-154.
- Wieczorke R, Krampe S, Weierstall T, Freidel K, Hollenberg CP, Boles E** (1999) Concurrent knock-out of at least 20 transporter genes is required to block uptake of hexoses in *Saccharomyces cerevisiae*. *FEBS Lett* 464:123-128.
- Wieczorke R, Krampe S, Weierstall T, Freidel K, Hollenberg CP, Boles E** (1999) Concurrent knock-out of at least 20 transporter genes is required to block uptake of hexoses in *Saccharomyces cerevisiae*. *FEBS Lett* 464: 123-128.
- Williams LE, Lemoine R, Sauer N** (2000) Sugar transporters in higher plants – a diversity of roles and complex regulation. *Trends Plant Sci* 5: 283-290.
- Winter H, Huber JL, Huber SC** (1997) Membrane association of sucrose synthase: changes during the graviresponse and possible control by protein phosphorylation. *FEBS Lett* 420:151-155.
- Winter H, Huber JL, Huber SC** (1998) Identification of sucrose synthase as an actin-binding protein. *FEBS Lett* 430: 205-208.
- Winter H, Huber SC** (2000) Regulation of sucrose metabolism in higher plants: Localization and regulation of activity of key enzymes. *Crit Rev Plant Sci* 19: 31-67.
- Wisniewski J-P, Rathbun EA, Knox JP, Brewin NJ** (2000) Involvement of diamine oxydase and peroxidase in insolubilization of the extracellular matrix: implications for pea nodule initiation by *Rhizobium leguminosarum*. *Mol Plant-Microbe Interact* 13: 413-420.
- Woodcock DM, Crowther PJ, Doherty J, Jefferson S, Decruz E, Noyer C, Weidner M, Smith SS, Michael MZ, Graham MW** (1989) Quantitative evaluation of *Escherichia coli* host strains for tolerance to cytosine methylation in plasmid and phage recombinants. *Nucleic Acids Res* 17: 3469-3478.
- Xu D-P, Sung S-J, Loboda T, Komarnik PP, Black CC** (1989) Characterization of sucrolysis via the uridine diphosphate and pyrophosphate-dependent sucrose synthase pathway. *Plant Physiol* 90: 635-642.

- Xu J, Avigne WT, McCarty DR, Koch K** (1996) A similar dichotomy of sugar modulation and developmental expression affects both path of sucrose metabolism: evidence from a maize invertase gene family. *Plant Cell* 8: 1209-1220.
- Yasuda T, Nakagawa H** (1994) Purification and characterization of the rutin-degrading enzymes in tartary buckwheat seeds. *Phytochemistry* 37: 133-136.
- Zamski E, Schaffner AA** (1996) Photoassimilates distribution in plants and crops: source-sink relationships (New York: Marcel Decker).
- Zapesochnaya GG and Pangarova TT** (1976) Structure of flavonoids from *Datisca cannabina* L. *Rastitelnye Resursy* (in Russ) 12: 237-241.
- Zeng S, Tjepkema JD, Berg RH** (1989) Gas diffusion pathway in nodules of *Casuarina cunninghamiana*. *Plant Soil* 118: 119-123.
- Zhang WH, Tyerman SD** (1997) Effect of low oxygen concentration on the electrical properties of cortical cells of wheat roots. *J Plant Physiol* 150: 567-572.
- Zimmermann MH, Ziegler H** (1975) List of sugars and sugar alcohols in sieve-tube exudates. In: *Transport in Plants, Encyclopedia of Plant Physiology, New Series Vol.1 I. Phloem Transport*, MH Zimmermann and JA Milburn, eds. (New York: Springer-Verlag), pp 245-271.

Danksagung

Frau Dr. Katharina Pawlowski danke ich, dass ich dieses spannende Projekt übernehmen konnte und sie mich bei meiner Dissertation stets unterstützte. Dabei halfen mir ihre umfangreichen praktischen und theoretischen Erfahrungen, meine wissenschaftlichen Kenntnisse zu erweitern.

Prof. Dr. Hans-Walter Heldt danke ich für die Möglichkeit, die Arbeit in seiner Abteilung durchführen zu können und für seine kritischen Kommentare.

Bei Frau PD Dr. Gertrud Lohaus bedanke ich mich für die Unterstützung bei allen HPLC-Analysen.

Frau Prof. Renate Scheibe, Dr. Heike Winter und Daniela Holtgräwe von der Universität Osnabrück bin ich sehr dankbar für die Einführung in die Saccharosesynthese-Aktivitätsmessungen.

Prof. Dr. Norbert Sauer und Dr. Michael Büttner danke ich für die Möglichkeit, die Hexosen-Aufnahmetests an der Universität Erlangen durchführen zu können, und ihre Unterstützung bei den Experimenten.

Prof. Dr. Lutz Tietze und Dr. Rocco Fortte vom Institut für Organische Chemie in Göttingen möchte ich danken für die NMR-Analyse und Strukturaufklärung von bis dahin unbekanntem Zuckern aus *Datisca*.

Frau Prof. Dr. Christiane Gatz bin ich sehr dankbar für die Übernahme des Korreferates sowie dafür, dass ich jederzeit die Geräte ihrer Abteilung benutzen durfte. Den Mitarbeitern der Abteilung Gatz danke ich für ihre Hilfsbereitschaft.

Prof. Dr. Dieter Heineke, Frau Dr. Sigrun Reumann, Dr. Christian Knop und Jens Tilsner danke ich für die guten praktischen Ratschläge bei der täglichen Laborarbeit und die kritische Durchsicht meiner Dissertation.

Allen Kollegen aus der Abteilung Biochemie der Pflanze, besonders Anne Brandeck, Andrea Nickel, Monika Raabe, Melanie Hußmann, Dr. Michaela Strauß, Dr. Olga Voitsekhovskaja, Dr. Kirill Demchenko, Dr. Anke Sirrenberg und Anita Stottmeister möchte ich danken für ihre große Hilfsbereitschaft bei allen meinen Fragen und für das angenehme Arbeitsklima.

Herrn Uwe Wedemeyer danke ich für die sorgfältige Betreuung meiner Pflanzen und Herrn Gerd Mader für die Hilfe bei allen technischen Problemen.

Meinen Eltern möchte ich herzlich danken für ihre große Unterstützung meiner Promotion in Deutschland.

Meinem Mann Marcel danke ich von ganzem Herzen für seine Geduld und für sein freundliches Warten auf den Abschluss meiner Promotion sowie sein Verständnis und seinen Trost in schwierigen Situationen.

Lebenslauf

- 09.01.1975 geboren in Leningrad (Russland),
Staatsangehörigkeit: russisch
- 1982-1992 Mittelschule Nr. 98 St. Petersburg
- Juni 1992 Abschlußzeugnis
- 1992-1996 Biologiestudium an der Universität St. Petersburg
- Juni 1996 Qualifikationsgrad: Bakkalaureus der Biologie mit der
Qualifikationsabschlussarbeit zum Thema:
„Benutzung von Baitan für die Selektion von
Tomatenpflanzen mit verändertem
Isoprenoidmetabolismus“ unter Anleitung von
Dr. L.T. Khodjajova
- Juni 1996-November 1998 Biologiestudium (Hauptfach: Genetik, Aufbaustudium für
Magister-Grad) an der Universität St. Petersburg
Magisterarbeit über: „Erzeugung einer Form von Tomaten
(*Lycopersicon esculentum* L.) mit unspezifischer
Resistenz gegen den Phitopthoroseerreger *Phytophthora
infestans*“ in der Arbeitsgruppe von Prof. Dr. L.A. Lutova
- November 1998 Akademischer Grad: Magister der Biologie
- Januar-April 1999 Promotionsstudium an der Universität St. Petersburg
(Fortsetzung des Themas der Magisterarbeit)
- Ab Juni 1999 Promotionsstudium an der Universität Göttingen
Abteilung Prof. Dr. H.-W. Heldt, in der Arbeitsgruppe von
Dr. K.Pawlowski, Projekt „Zuckerverteilung in Stickstoff-
fixierenden Wurzelknöllchen“